LA-UR-14-23352
Approved for public release; distribution is unlimited.

Title: Validation of MCNP6.1 for Criticality Safety of Pu-Metal, -Solution, and -Oxide Systems

Author(s): Kiedrowski, Brian C.
Conlin, Jeremy Lloyd
Favorite, Jeffrey A.
Kahler, Albert C. III
Kersting, Alyssa R.
Parsons, Donald K.
Walker, Jessie L.

Intended for: Report

Issued: 2014-05-13

# Validation of MCNP6.1 for Criticality Safety of Pu-Metal, -Solution, and -Oxide Systems

**Brian C. Kiedrowski, Jeremy L. Conlin, Jeffrey A. Favorite, Albert C. Kahler, Alyssa R. Kersting, D. Kent Parsons, Jessie L. Walker**

**ABSTRACT**

Guidance is offered to the Los Alamos National Laboratory Nuclear Criticality Safety division towards developing an Upper Subcritical Limit (USL) for MCNP6.1 calculations with ENDF/B-VII.1 nuclear data for three classes of problems: Pu-metal, -solution, and -oxide systems. A benchmark suite containing 1,086 benchmarks is prepared, and a sensitivity/uncertainty (S/U) method with a generalized linear least squares (GLLS) data adjustment is used to reject outliers, bringing the total to 959 usable benchmarks. For each class of problem, S/U methods are used to select relevant experimental benchmarks, and the calculational margin is computed using extreme value theory. A portion of the margin of subcriticality is defined considering both a detection limit for errors in codes and data and uncertainty/variability in the nuclear data library. The latter employs S/U methods with a GLLS data adjustment to find representative nuclear data covariances constrained by integral experiments, which are then used to compute uncertainties in $k_{eff}$ from nuclear data. The USLs for the classes of problems are as follows: Pu metal, 0.980; Pu solutions, 0.973; dry Pu oxides, 0.978; dilute Pu oxide-water mixes, 0.970; and intermediate-spectrum Pu oxide-water mixes, 0.953.

## 1. Introduction

This document offers guidance to determine an Upper Subcritical Limit (USL) for three classes of problems: Pu-metal, Pu-solution, and Pu-oxide systems. This document is in accordance with ANSI/ANS-8.24 [1], "Validation of Neutron Transport Methods for Nuclear Criticality Safety Calculations," and is meant to be used by the Los Alamos National Laboratory (LANL) Nuclear Criticality Safety (NCS) division.

A description of the computer platform, code version, and nuclear data is given. The verification done for the computer code system is documented and the change control is detailed.

Next, the comprehensive NCS benchmark suite containing 1,086 critical experiment benchmarks is described. The validation suite covers a wide range of fissionable materials and forms as well as spectra, configurations, etc. Sensitivity/uncertainty (S/U) methods are used with a generalized linear least squares (GLLS) nuclear data adjustment to perform rejection of outlier benchmarks; this methodology is described. Next, the S/U-based method of selecting relevant benchmarks from the comprehensive suite minus the rejected outliers is discussed.

The area of applicability (AOA) is detailed for each class of problem through parametric studies using process models, which are described herein. The calculational margin for the three classes of problems is computed using extreme value theory (EVT). The approaches are described along with the results for each class of problem.

Guidance is offered for developing the margin of subcriticality. Three factors are considered herein. The first considers the quality of the transport code and the data libraries and the possibility of errors (i.e., bugs) having escaped notice. The second considers the effect of uncertainties and variations from nuclear data libraries. The uncertainties from nuclear data libraries are quantified using a GLLS nuclear data adjustment along with standard S/U error propagation techniques. The third discusses how sensitivities to parameters must be considered in the

context of the validation, and how modeled systems must fall within the AOA of this validation. Actual numbers are given for the first two factors, and determining an appropriate margin of subcriticality for the third is left to the analyst as it is inexorably linked to the model being analyzed.

### 1.1. Responsibilities of NCS Analysts

This document should be viewed as a **starting point** for the NCS analyst. It is the responsibility of the analyst to ensure that the computational model being analyzed resides within the defined AOA of this validation. If this is so, the analyst may use the calculational margins derived herein. If the computational model is not within the defined AOA, the NCS analyst must either expand the AOA using validation, or explain any potential effect of using unvalidated nuclear data, and apply any adjustments to the model and/or control deemed appropriate.

It is still up to the analyst to develop a reasonable margin of subcriticality to ensure that the process is subcritical. This document gives a portion of the margin of subcriticality that is related to the code and data but does not address issues related to the specific processes and whether they are within the AOA. The analyst should consider using the guidance herein as a starting point, but it is ultimately up to the analyst to provide any additions to the margin of subcriticality.

**In any case, it is never acceptable to simply use the numbers in this document without further analysis.**

### 1.2. Definitions

The definitions in this validation are consistent with those specified in the ANS-8.24 standard. In the case of bias, the sign is arbitrary. For this validation report, the sign of the bias is taken such that a positive bias is nonconservative, i.e., a positive bias implies that the code predicts $k_{eff}$ lower than what the benchmark experiments would indicate. In other words,

$$\text{Bias} = \text{Benchmark } k_{eff} - \text{Calculated } k_{eff} .$$

This choice was made so that each quantity for determining the USL has a positive sign.

## 2. Verification of the Computer Code System

ANS-8.24 defines the computer code system as, “A calculational method, computer hardware, and computer software (including the operating system).” The computer platform is the Moonlight cluster at LANL hosted and maintained by the High-Performance Computing (HPC) division. The hardware consists of nodes having two Eight-Core Intel Xeon model E5-2670 processor chips at 2.6 GHz. The operating system is Clustered High Availability Operating System (CHAOS). CHAOS is a Livermore-modified version of RedHat Linux.

The transport software (calculational method) used is MCNP6.1 [2], a mature, widely-used, production, continuous-energy and -angle Monte Carlo package. While many changes to core coding have occurred between MCNP5 and MCNP6, the software development process ensured that results for criticality problems did not change between the two versions. The executables themselves may give slightly different answers because of numerical roundoff as a consequence of using more modern versions of the Intel compiler; but, when the same compiler is used, the results match exactly. Any changes in results because of compiler version are not statistically significant and are therefore judged to be, statistically speaking, the same [3].

The nuclear data are from the ENDF/B-VII.1 library [4]. The data were processed by NJOY99.393 [5] into the ACE format that MCNP can read; the formatted data libraries are maintained by the LANL Nuclear Data Team.

ANS-8.24 Sec. 4.1 states, "Verification of the computer code system shall be completed prior to validation. Correct installation and operation of the computer code system should be documented." The verification of the installation on Moonlight is checked by ensuring the MCNP6.1 Regression and Keff Verification test suites give expected answers. The Regression suite is a set of 157 short test problems that run a broad portion of the MCNP6.1 coding, including nuclear criticality (KCODE) calculations. The Keff Verification suite contains 10 selected analytic test problems from Ref. 6 to check if MCNP6.1 is solving the $k_{eff}$ eigenvalue problem correctly.

These two suites were run. The Regression suite shows zero differences from the defined reference results, indicating the installation of MCNP6.1 on Moonlight was successful. Table I documents the results of the Keff Verification suite. All agree within 2σ of the analytic value, which confirms that the algorithms in MCNP6.1 are computing $k_{eff}$ correctly.

Local copies of the MCNP6.1 executable and nuclear data are placed in a separate space, and the NCS division is responsible for maintaining these copies. ANS-8.24 Sec. 4.2 states, "The computer code system to be validated shall be placed under an appropriate configuration control program. Any change to the computer code system shall be evaluated to determine its effect on the validation." The configuration control program is enforced by UNIX permission groups. Only the owner of the files, a single individual, has the ability to modify the executables and nuclear data. This could, in principle, be overridden by the HPC system administrators, but their doing so accidentally and remaining undetected is not credible. The MCNP6.1 executable itself is linked statically where possible during compilation and build; this makes it not credible that changes could be made to a professionally maintained, high-traffic computing cluster, such as Moonlight, that somehow affect the executable in such a way to influence calculations and have those changes go unnoticed.

Note that this validation exclusively covers criticality (KCODE) calculations. No fixed-source (SDEF) calculations are included. Tallies are not part of the validation. The problems do not use any variance reduction techniques beyond those that are on by default, nor are periodic and white boundary conditions exercised, etc., and while using these features should be fine, this would be non-compliant with the ANS 8.24 standard. When in doubt, NCS analysts should contact the MCNP Development Team.

**Table I. Analytic $k_{eff}$ Verification Results**

| Case | Name | Analytic $k_{eff}$ | MCNP $k_{eff}$ | Unc. |
|---|---|---|---|---|
| prob11 | Ua-1-0-IN | 2.25000 | 2.25000 | 0.00000 |
| prob14 | Ua-1-0-SP | 1.00000 | 1.00006 | 0.00010 |
| prob18 | Uc-H2O(2)-1-0-SP | 1.00000 | 1.00005 | 0.00011 |
| prob23 | UD2O-1-0-CY | 1.00000 | 1.00000 | 0.00006 |
| prob32 | PUa-1-1-SL | 1.00000 | 0.99995 | 0.00011 |
| prob41 | UD2Ob-1-1-SP | 1.00000 | 1.00003 | 0.00007 |
| prob44 | PU-2-0-IN | 2.68377 | 2.68377 | 0.00003 |
| prob54 | URRa-2-0-SL | 1.00000 | 1.00007 | 0.00013 |
| prob63 | URRd-H2Ob(1)-2-0-ISLC | 1.00000 | 0.99993 | 0.00006 |
| prob75 | URR-6-0-IN | 1.60000 | 1.59999 | 0.00001 |

### 3. Validation Benchmarks

Benchmarks were obtained from the International Criticality Safety Benchmark Evaluation Project (ICSBEP) Handbook [7]. The ICSBEP Handbook separates benchmark experiments by dominant fissile isotope (and enrichment if uranium), fissile form, and spectrum. For this work, a suite of 1,086 benchmarks was obtained from the previous NCS validation suite [8], the Mosteller Expanded Criticality Suite for MCNP validation [9], the Kahler validation suite for ENDF/B-VII.1 [10], and, when needed and unavailable elsewhere, benchmark models were prepared by the NCS division and independently reviewed as part of this validation. A summary of benchmarks by

their ICSBEP Handbook identifiers is given in Table II. A full listing is given in Appendix A along with their benchmark and MCNP6.1 (with ENDF/B-VII.1) calculated $k_{eff}$ and $k_{eff}$ uncertainties.

The benchmark suite was created to be comprehensive for a large set of possible applications. The S/U methods to be discussed select the relevant benchmarks for a particular application.

The geometric configurations of the various benchmarks cover a range of slab, spherical, and cylindrical geometries. Some have a single unit, while others have multiple interacting units or are in lattice configurations. The configurations are bare or reflected, and, in some cases, have interstitial materials. For a Monte Carlo code like MCNP6.1, the surfaces are defined analytically and ray-tracing routines to track neutrons through the geometry are robust. Unlike deterministic methods, there are no problems associated with quadrature sets, mesh spacing, homogenization, etc. Therefore when using MCNP6.1, geometry not being covered in the validation is not as significant a concern as coverage of materials and spectra.

Review of the experiments used as benchmarks show that they were drawn from a number of experimental series, conducted by different critical facilities, by different experimenters, over a range of chronological time periods. This helps minimize any systemic issues relating to a particular facility, experimenter, or approach.

The benchmarks were obtained from various sources and some were prepared by the NCS division. In all cases, the benchmarks were independently reviewed for accuracy at some point. While this does not preclude mistakes, it does significantly reduce the chance of errors because of faulty input. Also, the rejection scheme discussed in Sec. 3.1 should reject any inputs with gross errors that produce results inconsistent with similar benchmarks.

In five cases (HEU-MET-FAST-004-001 and the four cases of IEU-MET-FAST-001), the benchmark uncertainties are not provided by the ICSBEP Handbook. In this case, a weighted average of the variances (of those benchmarks with a quantified uncertainty) is used to determine representative benchmark uncertainties. The weighting factors in the averaging are the similarity factors discussed in Sec. 3.2. This method is consistent with Ref. 11, which states, "Where no documentation is located to substantiate an experimental uncertainty, engineering judgement [sic] should be used, based upon factors such as the **typical uncertainties of similar experiments**. Although this appears artificial, it is **a more realistic assumption than assuming that there is no error associated with the measurements** in the critical experiments" (emphasis added).

In cases where two one-sided (i.e., asymmetric) benchmark uncertainties are given, the larger of the two is assumed for conservatism.

**Table II. Summary of Benchmark Suite**

| ICSBEP Identifier | # Included | # After Rejection |
|---|---|---|
| heu-met-fast | 251 | 218 |
| heu-met-inter | 4 | 2 |
| heu-met-therm | 4 | 2 |
| heu-met-mixed | 8 | 7 |
| heu-comp-inter | 1 | 1 |
| heu-comp-therm | 25 | 17 |
| heu-sol-therm | 93 | 91 |
| ieu-met-fast | 12 | 12 |
| ieu-comp-therm | 1 | 1 |
| leu-comp-therm | 182 | 178 |
| leu-sol-therm | 27 | 25 |
| mix-met-fast | 33 | 32 |
| mix-met-mixed | 1 | 1 |
| mix-comp-fast | 2 | 2 |
| mix-comp-inter | 1 | 1 |

| | | |
|---|---|---|
| mix-comp-therm | 15 | 15 |
| mix-sol-therm | 21 | 11 |
| pu-met-fast | 53 | 49 |
| pu-comp-fast | 1 | 1 |
| pu-comp-inter | 1 | 1 |
| pu-comp-mixed | 34 | 17 |
| pu-sol-therm | 158 | 141 |
| u233-met-fast | 10 | 8 |
| u233-comp-therm | 9 | 9 |
| u233-sol-inter | 33 | 23 |
| u233-sol-therm | 106 | 94 |
| **Total** | **1086** | **959** |

### 3.1. Rejection of Inconsistent Benchmarks

Before selecting benchmarks, a subset of the benchmarks is rejected as outliers. This is determined by a chi-squared data adjustment process using nuclear data sensitivities and covariance data.

Possible sources of computational bias include: poor experimental results, inadequacy of the benchmark description, errors in the quoted benchmark $k_{eff}$ and uncertainty, errors in the input files, and uncertainties in the nuclear data. It is typically assumed that the dominant source of the computational discrepancy from experiment is a result of the latter, uncertainties in the nuclear data. Testing this assumption can be done by adjusting the nuclear data within their covariances to minimize the computational bias. Benchmarks where the bias cannot be reduced through a consistent adjustment of the nuclear data with the rest of the suite likely have other problems associated with them and are rejected.

The nuclear data adjustment uses a generalized linear least squares (GLLS) method [12]. The GLLS method adjusts the nuclear data to minimize the chi-squared statistic. A more detailed discussion of the chi-squared statistic and how it is minimized may be found in Ref. 13.

The GLLS method is used to find the minimum chi-squared. The value of chi-squared per degree of freedom (number of benchmark experiments in the set) should be unity for a perfect regression model post adjustment. In practice, the chi-squared statistic is significantly higher, indicating the presence of inconsistent benchmarks. Benchmarks are rejected using the iterative diagonal chi-squared method until the chi-squared is below 1.2. During this process 127 of the benchmarks (about 12%) are rejected. The number remaining for each ICSBEP class of benchmark is given in Table II, and the rejected benchmarks are denoted in red in Appendix A.

The sensitivity coefficients [14] are generated with continuous-energy physics in MCNP6 on the energy grid provided by the 44-group covariance library from ORNL [15]. The nuclear data considered are elastic scattering, inelastic scattering, fission, capture [(n,2n), (n,γ), (n,p), (n,d), (n,t), (n,$^3$He), (n,α)], fission total ν, and fission χ, which are the ones available in the ORNL covariance library. In cases where covariance data are unavailable, a uniform uncorrelated (diagonal) uncertainty of 10% is assumed; this value is typically bounding of nuclear data uncertainties in the energy regime of interest to criticality, i.e., several MeV or less. All the validation runs used 100,000 neutrons per cycle, 100 skip cycles, and 600 total cycles, except for the LEU-COMP-THERM-60 cases, which used 300 total cycles because their high level of geometric detail led to very long run times. Source convergence was checked for all benchmarks.

The experimental benchmark correlation data from the ICSBEP Handbook (via DICE, the Database for ICSBEP that is available both on DVD and online [16]) are used where numerical values are provided. Unfortunately, this data is rather sparse, and currently none of the Pu-metal or -solution benchmarks have their correlations quantified. Since assigning meaningful correlation values to the set of benchmarks would require extensive studies taking years of effort, these benchmarks are currently assumed to be uncorrelated. This is of course not true as many benchmarks

used similar equipment, were in the same facility, or had common experimenters. Using a 99% confidence interval on the calculational margin and for setting a portion of the margin of subcriticality should provide enough conservatism to account for this approximation.

### 3.2. Selection of Relevant Benchmarks

Of the 959 remaining benchmarks following the rejection process, only a much smaller subset is going to be relevant for a particular application. Selecting which benchmarks are relevant to validating a specific application by hand can be a time-consuming and error-prone procedure. S/U methods are used to help automate this process based upon quantitative measures of neutronic similarity.

Recall from Sec. 3.1 that the dominant source of computational bias is typically from uncertainties in the nuclear data. The GLLS rejection method, which uses a nuclear data adjustment, retains over 88% of the benchmarks, supporting this assertion about the source of computational bias. If this is true, a correlation coefficient $c_k$ has been shown to adequately select benchmarks with similar sources of computational bias [12]. The $c_k$ parameter applies the sensitivity coefficients to nuclear data (generated with continuous-energy physics in MCNP6.1) and the nuclear data covariances. A $c_k$ of unity implies that the two systems being compared are neutronically identical and therefore have identical sources of bias. A $c_k$ of zero implies that the two systems are completely dissimilar. Positive values of $c_k$ quantify the degree of similarity. Negative values of $c_k$ indicate antisimilarity of benchmarks, but this rarely occurs in practice.

Generating the $c_k$ uses the same energy grid for the sensitivity profiles and the same covariance data as used for the GLLS nuclear data adjustment for the rejection of benchmarks.

A set of process models for the Pu metals, solutions, and oxides are prepared and the $c_k$ are generated for those application models with respect to all the benchmarks. The $c_k$ are sorted and the largest $c_k$ is found. This value determines how many benchmarks are required for the validation – as to be discussed in Sec. 5, adding more benchmarks for the method for computing the calculational margin only increases it. A larger maximum $c_k$ indicates that there exists a benchmark that is more similar to the application being analyzed than had the maximum $c_k$ been smaller. It therefore makes more sense to require a greater number of benchmarks so long as adding more benchmarks does not cause the calculational margin to become less conservative; it does not for the method employed in this validation [13].

The details of the criteria that are used to select the benchmarks are given in Ref. 13. More precisely, the selected benchmarks are assigned a weighting factor based upon their relative similarities to the application being analyzed. Reference 13 gives the criteria for which benchmarks are used for validating a specific application. The criteria are based upon a ranking of $c_k$, and the total sum of benchmark weighting factors is determined by the maximum $c_k$ from the benchmark suite. The equation in Ref. 13 giving the criteria has two parameters: $A$, representing the minimum number of perfect benchmarks, and $B$, representing a penalty factor for a lower maximum $c_k$ than unity. The values were chosen empirically based on standard statistical "rules of thumb" about sample sizes and to ensure desired behavior where benchmark coverage is lacking. The values are $A = 25$ and $B = 100$. To illustrate the impact of the choice of these parameters, in practice these values enforce the use of about 50 benchmarks for metals, about 45 benchmarks for solution concentrations with much benchmark data available and about 75 where there is less data, and about 100 benchmarks for oxides where the benchmark availability is poor.

Weighting the benchmarks with the similarity factors is consistent with ANS-8.24 Sec. 6.3.1. The standard specifies that "Data may be weighted to account for benchmark uncertainties or other indications of benchmark quality (e.g., degree of characterization or **degree of applicability**)" (emphasis added).

### 3.3. Characterization of Benchmarks

The process to select benchmarks is automated via the S/U techniques. The assumption with this automation is that there is a sufficiently large number of benchmarks in the suite. The $c_k$ parameter by itself, while useful, does not state which physical parameters are useful for trending the calculational margin and how to interpret the bias results. This section studies various physical parameters for the metals, solutions, and oxides. Any trends are identified and their impact on the calculational margin is given.

If trending is performed on the calculational margin or USL, then the NCS analyst must understand the behavior of the bias as a function of those parameters.

#### 3.3.1. Pu Metals

There are 53 PU-MET-FAST (PMF) benchmarks in the suite, which are typically the most relevant benchmarks for this class of problems (Pu metals). The GLLS rejection algorithm identified four of the benchmarks as inconsistent, leaving 49 PMF benchmarks for the validation. Energy of Average Lethargy causing Fission (EALF) and Pu-isotopic fractions (both Pu-240 and Pu-241) are parameters that are considered to characterize these benchmarks.

The spectra of the PMF benchmarks cover a range of EALF between 7.3 keV and 1.26 MeV. There are no obvious gaps in the energy spectral coverage. Pu-240 atomic fractions (relative to all Pu) of the PMF benchmarks range from 0% (according to the benchmark specifications of PMF-045, where the actual amount of Pu-240 is unknown and its impact on $k_{eff}$ was factored into the benchmark uncertainty using a sensitivity study) to about 10%. There is one data point with about 20% Pu-240 (PMF-002-001) and none in between. Caution should be used if Pu-240 atomic fractions of greater than 10% are present in the application space, and additional margin may be appropriate. The Pu-241 concentrations of the benchmarks vary from 0% (presumably where it was unknown and factored into the benchmark uncertainty) to about 1.7%; PMF-002-001 is a notable different case with a Pu-241 concentration of 3.1%. Likewise, similar caution should be applied if the Pu-241 concentration is greater than 1.7%.

Figures 1-3 give the bias in $k_{eff}$ as a function of EALF, Pu-240 composition, and Pu-241 composition. In regard to EALF, there is a visible and known (conservative) bias for the PMF benchmarks with softer, but still fast, spectra [9]. There is no statistically significant trend in $k_{eff}$ for either Pu-240 or Pu-241 concentration of the PMF benchmarks, indicating that extrapolation to pure Pu-239 should not introduce additional uncertainty. The calculational margin computed in Sec. 5 is also displayed on these figures.

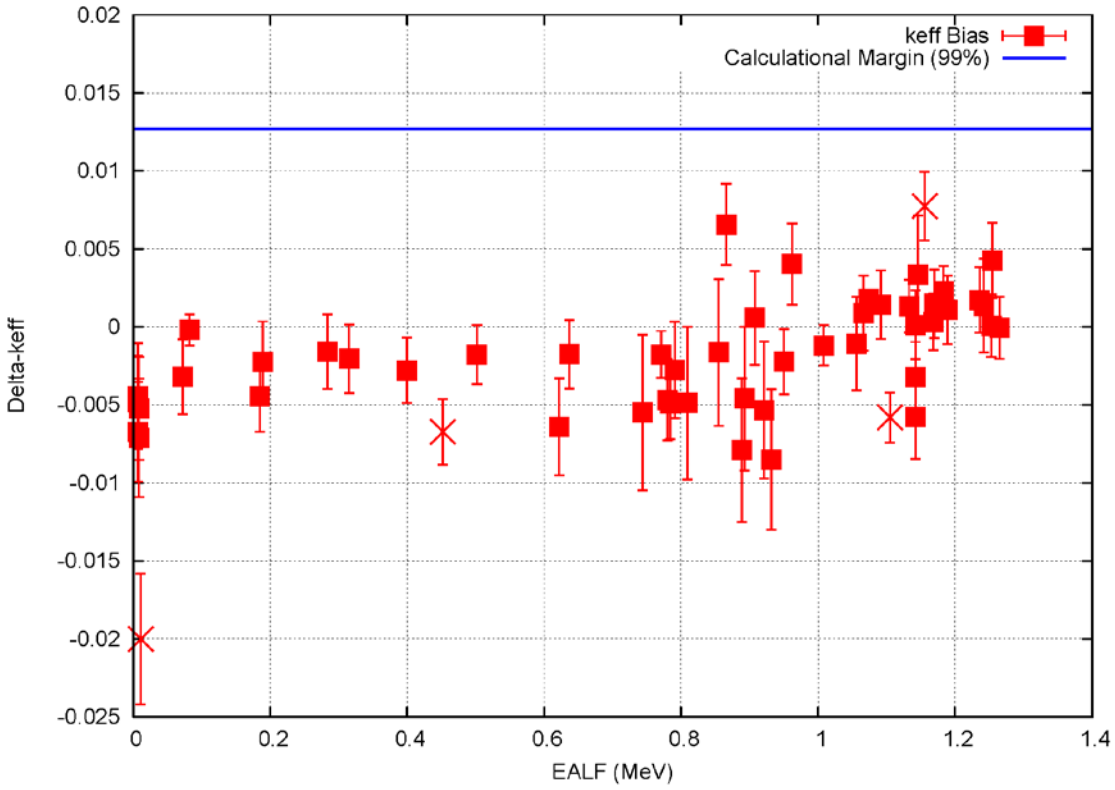


**Fig. 1. $\Delta k_{eff}$ or bias in $k_{eff}$ (Bias = Benchmark $k_{eff}$ – Calculated $k_{eff}$; positive bias is nonconservative) and calculational margin at the 99% confidence level for Pu-metal systems as a function of Energy of Average Lethargy causing Fission (EALF). Error bars (1σ) are the combination of benchmark and calculational uncertainty. Data points marked with an "×" were those rejected by the generalized linear least squares method.**

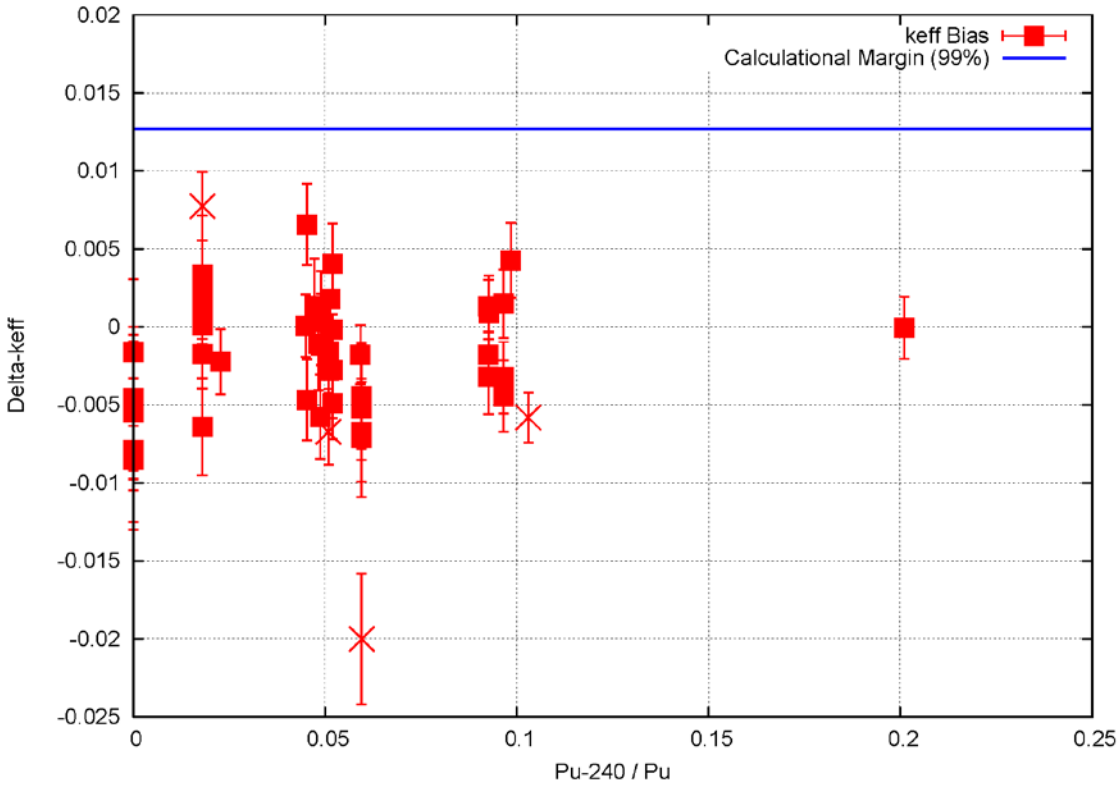


**Fig. 2. $\Delta k_{eff}$ or bias in $k_{eff}$ (Bias = Benchmark $k_{eff}$ – Calculated $k_{eff}$; positive bias is nonconservative) and calculational margin at the 99% confidence level for Pu-metal systems as a function of $^{240}$Pu atom fraction. Error bars (1σ) are the combination of benchmark and calculational uncertainty. Data points marked with an "×" were those rejected by the generalized linear least squares method.**

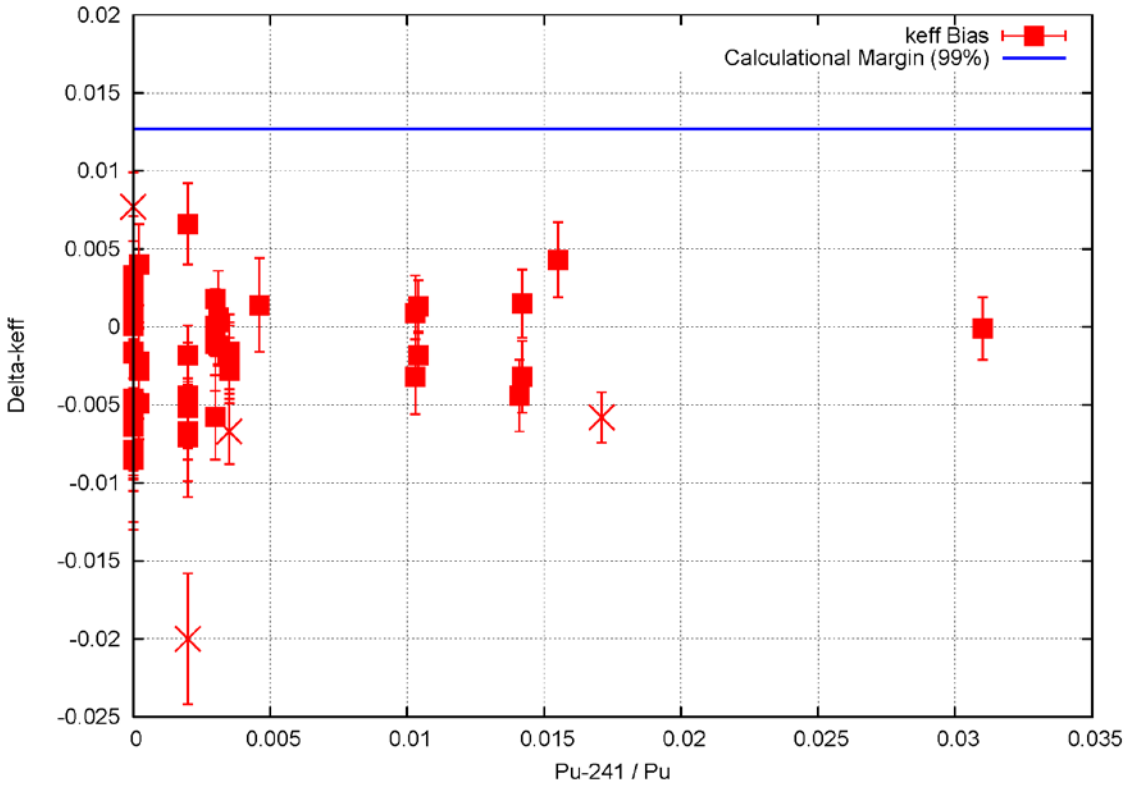


**Fig. 3. $\Delta k_{eff}$ or bias in $k_{eff}$ (Bias = Benchmark $k_{eff}$ – Calculated $k_{eff}$; positive bias is nonconservative) and calculational margin at the 99% confidence level for Pu-metal systems as a function of $^{241}$Pu atom fraction. Error bars (1σ) are the combination of benchmark and calculational uncertainty. Data points marked with an "×" were those rejected by the generalized linear least squares method.**

### 3.3.2. Pu Solutions

There are 158 PU-SOL-THERM (PST) benchmarks, which are the most relevant for the benchmarking of Pu solutions or metal-water mixes. The GLLS rejection algorithm identified 17 of the benchmarks as inconsistent, leaving 141 PST benchmarks for the validation.

The trending parameters that appear to make the most sense for the Pu solutions or metal-water mixes are Pu concentration and EALF. Figures 4 and 5 display the bias in the benchmarks as a function of those two respective parameters. The calculational margin computed in Sec. 5.2 is also displayed as a function of both of those parameters; the calculational margin only extends over a portion of the range in the plot, and this is shown explicitly in the figures.

Figures 6 and 7 give the calculational bias as a function of Pu-240 and Pu-241 atomic fractions. No trending is performed on these parameters since the NCS models typically use pure Pu-239.

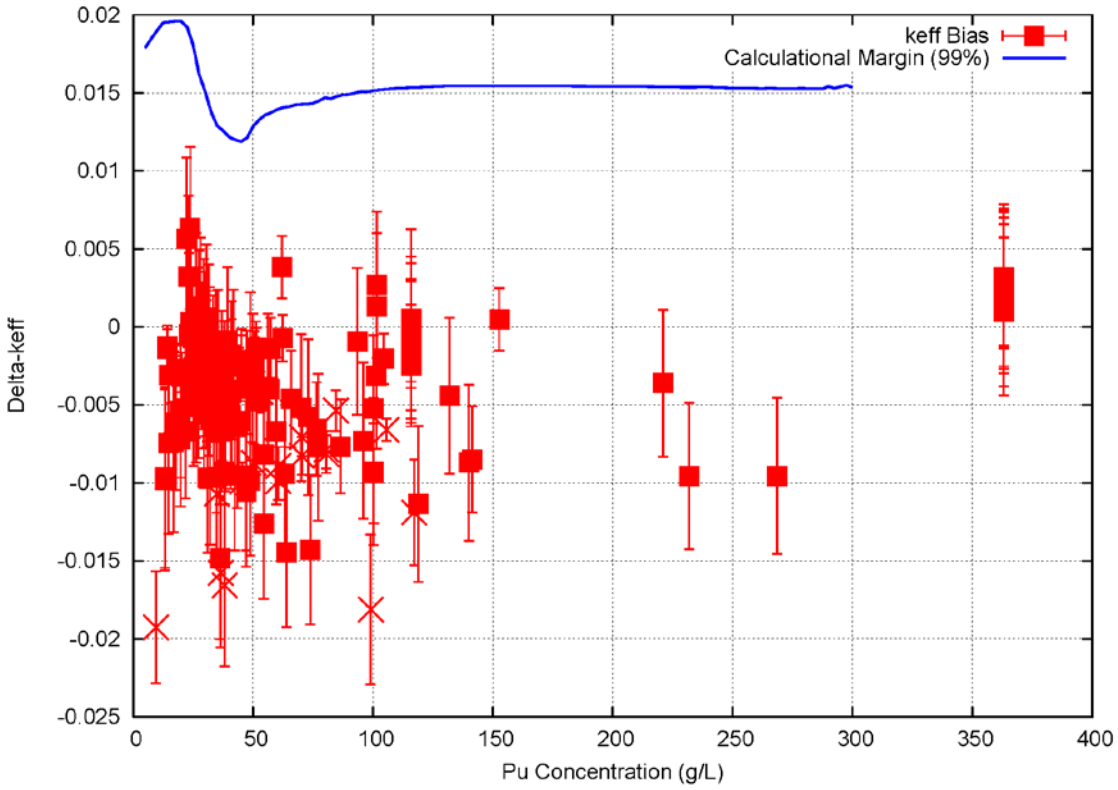


**Fig. 4. $\Delta k_{eff}$ or bias in $k_{eff}$ (Bias = Benchmark $k_{eff}$ – Calculated $k_{eff}$; positive bias is nonconservative) and calculational margin at the 99% confidence level for Pu solution/metal-water mix systems as a function of Pu solution concentration in g/L. Error bars (1σ) are the combination of benchmark and calculational uncertainty. Data points marked with an "×" were those rejected by the generalized linear least squares method.**

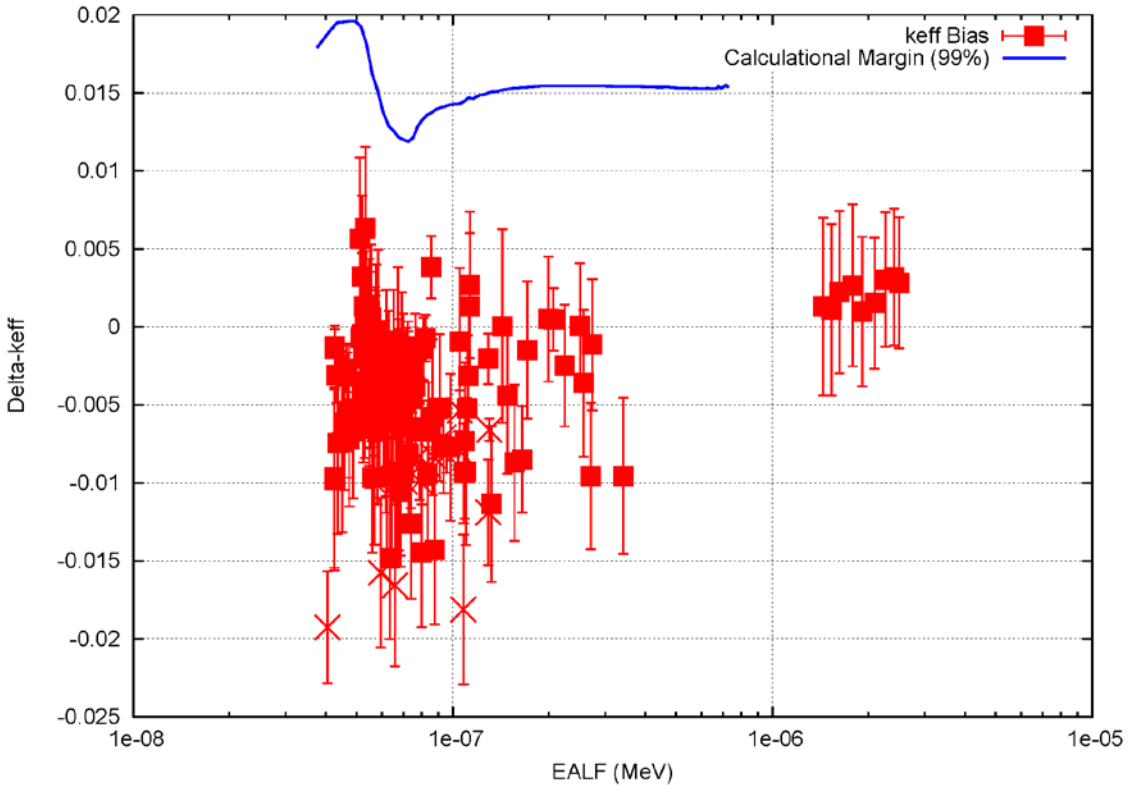


**Fig. 5. $\Delta k_{eff}$ or bias in $k_{eff}$ (Bias = Benchmark $k_{eff}$ – Calculated $k_{eff}$; positive bias is nonconservative) and calculational margin at the 99% confidence level for Pu solution/metal-water mix systems as a function of Energy of Average Lethargy causing Fission (EALF). Error bars (1σ) are the combination of benchmark and calculational uncertainty. Data points marked with an "×" were those rejected by the generalized linear least squares method.**

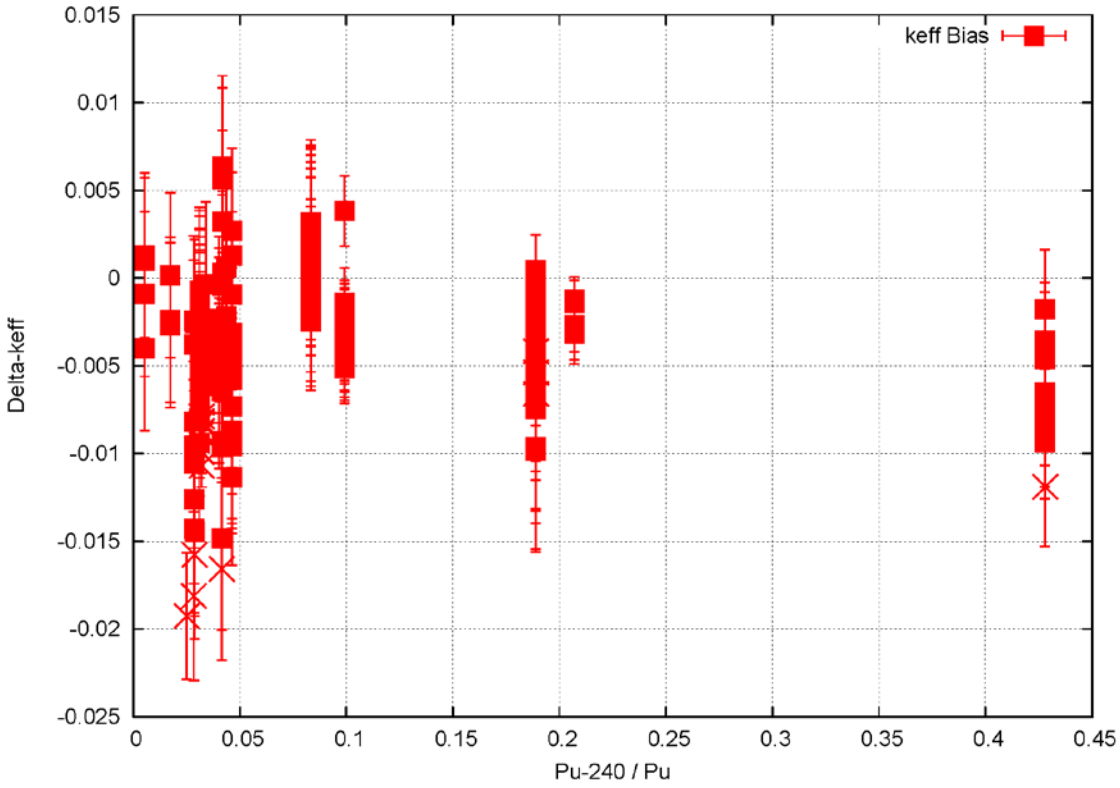


**Fig. 6. $\Delta k_{eff}$ or bias in $k_{eff}$ (Bias = Benchmark $k_{eff}$ – Calculated $k_{eff}$; positive bias is nonconservative) for Pu solution/metal-water mix systems as a function of $^{240}$Pu atom fraction. Error bars (1σ) are the combination of benchmark and calculational uncertainty. Data points marked with an "×" were those rejected by the generalized linear least squares method.**

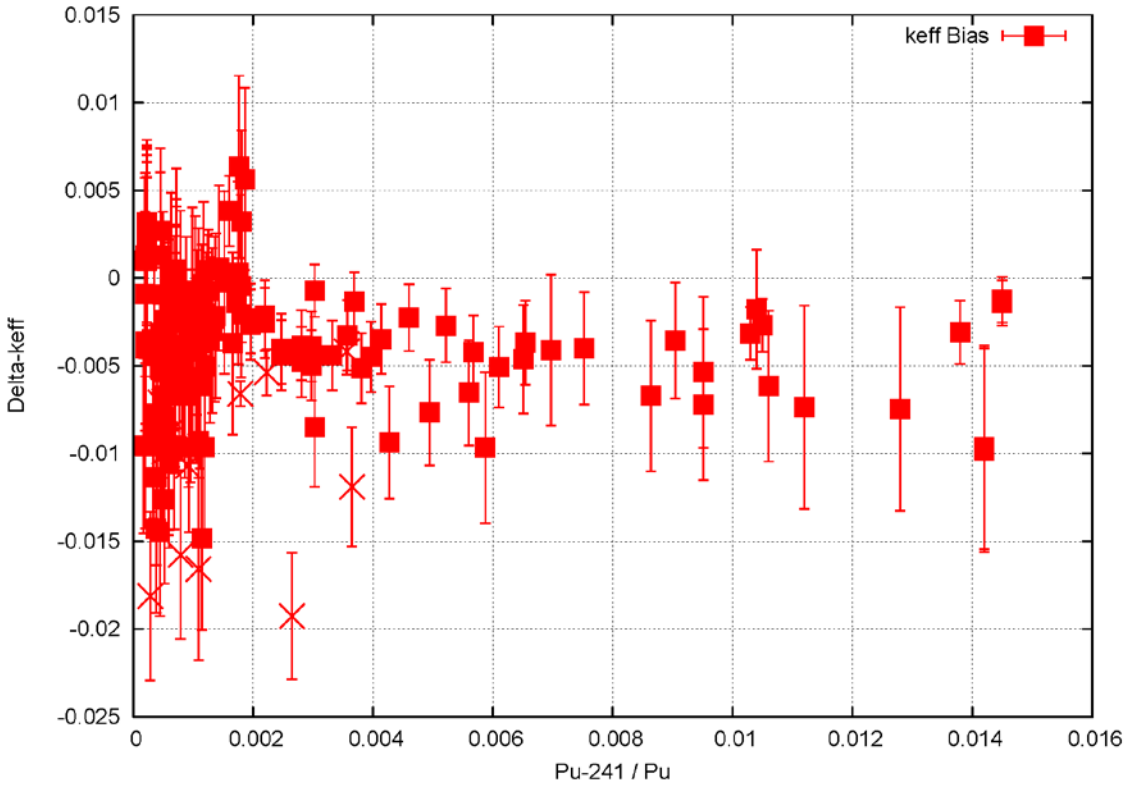


**Fig. 7. $\Delta k_{eff}$ or bias in $k_{eff}$ (Bias = Benchmark $k_{eff}$ – Calculated $k_{eff}$; positive bias is nonconservative) for Pu solution/metal-water mix systems as a function of $^{241}$Pu atom fraction. Error bars (1σ) are the combination of benchmark and calculational uncertainty. Data points marked with an "×" were those rejected by the generalized linear least squares method.**

### 3.3.3. Pu Oxides

The benchmark database for Pu-oxide systems is very sparse compared to the metals and solutions. These consist of the PU-COMP-MIXED (PCM) series, PU-COMP-FAST-004 (PCF-004), and PU-COMP-INTER-001 (PCI-001). The PCM benchmarks are $PuO_2$-polystyrene($C_8H_8$) compacts in various configurations. Unfortunately, these benchmarks, while still acceptable for the ICSBEP Handbook, are anecdotally considered to be of marginal quality. PCF-004 is the ZPR-3 assembly reflected by nickel. PCI-001 is a $k_\infty$ experiment with graphite moderation.

Overall there are 36 benchmark cases. The GLLS rejection algorithm identified 17 of the benchmarks as inconsistent (all from the PCM series, supporting the assertion that these experiments are marginal), leaving only 19 benchmarks for the validation.

It also turns out that for dry Pu-oxide systems, which have a softer spectrum than bare Pu-metal systems, Pu-metal systems reflected by low-Z materials (e.g., water, polyethylene, beryllium) tend to act as reasonable surrogates because those reflectors soften the spectrum to a similar degree as in dry Pu-oxide systems. For dilute Pu oxide-water mixtures, the Pu-solution benchmarks are good surrogates because they have similar neutronically important

isotopes (Pu, hydrogen, and oxygen), but in slightly different proportions. In the dry and dilute regimes, the analysis in Secs. 3.3.1 and 3.3.2 should apply.

Because of the wide range of energy spectra and the need for metal and solution benchmarks, EALF is the only trending parameter used for the Pu oxides. Figure 8 shows the bias for all three classes of Pu benchmarks (oxides, solutions, and metals) along with the trendline in the calculational margin for the oxides (as computed in Sec. 5.3). As confirmed by Fig. 8, the Pu benchmark data in the intermediate range is scant. The large increase in the calculational margin is because of a single benchmark, PCM-001-005, that could not be rejected by the GLLS method.

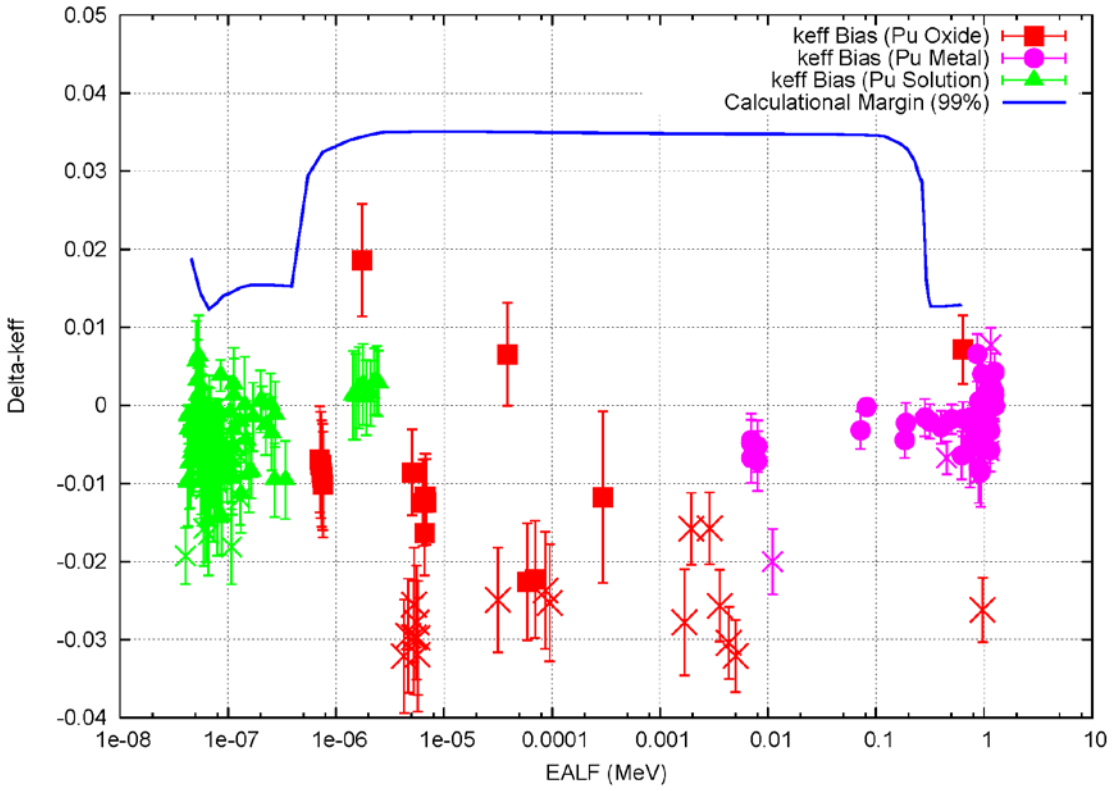


**Fig. 8. $\Delta k_{eff}$ or bias in $k_{eff}$ (Bias = Benchmark $k_{eff}$ – Calculated $k_{eff}$; positive bias is nonconservative) and calculational margin at the 99% confidence level for Pu oxide/oxide-water mix systems as a function of Energy of Average Lethargy causing Fission (EALF). Error bars (1σ) are the combination of benchmark and calculational uncertainty. Data points marked with an "×" were those rejected by the generalized linear least squares method.**

### 4. Area of Applicability and Representative Process Models

To perform the validation and define the area of applicability (AOA), representative process models were prepared for each class of problem. These computational models represent bounding cases of processes and are similar to those used by the NCS division as part of their workflow.

The AOA of this validation is defined by these process models. The models are taken to be representative of typical NCS calculations, and the validation results should apply for similar models. It is the responsibility of the analyst to show that their computational analysis models have similar characteristics based upon relevant physical parameters (e.g., materials, spectra, etc.) for this validation to apply.

### 4.1. Pu Metals

There are two sets of process models for the Pu-metal systems. The first consists of Pu-metal cylinders with water reflection and on a stainless steel floor, and the second is a set of Pu-metal spheres with various reflectors.

The first set of process models for Pu metal consists of three Pu-metal cylinders on a steel (SS-304) floor reflected by water to represent hands. The bare case is not explicitly analyzed, but the selection of benchmarks will apply to bare Pu metal as well. The three identical cylinders are placed touching each other in a triangular pattern with their bases sitting on the SS-304 floor (density of 7.92 g/cm$^3$), which is 0.5 in. thick. The reflection of hands is treated as a 1-in. thick cylindrical jacket surrounding one of the cylinders (the Pu from the other cylinders displace the "hands") consisting of pure water at 1.0 g/cm$^3$. The Pu is modeled as pure Pu-239 at the theoretical density of 19.85 g/cm$^3$.

Various cylinder masses and height-to-diameter (H/D) ratios were considered. The (single) cylinder masses are 2300, 2500, 3000, 3300, 3500, 4000, and 4500 g. The H/D ratios vary between 1.0 and 2.2 in increments of 0.1. All possible combinations of these were run, resulting in 91 different cases. The EALF of the process models have EALF values ranging from 790 keV to about 1 MeV.

A calculational margin is computed for each of the 91 parametric cases using the methodology to be discussed in Sec. 5. The resulting calculational margin does not change by more than 0.0002 over the entire range of process conditions considered, demonstrating the stability of the similarity parameter for this type of process. Because of the insensitivity to process conditions, a single case with a mass of 3500 g and H/D of 1.6 was selected as the basis for selecting benchmarks for determining the calculational margin.

The second set of process models is a 4-cm radius sphere consisting of pure Pu-239 at theoretical density with 50 different reflector materials with varied thickness. Table III lists the reflector materials and densities. The reflector thicknesses are 1, 2, 3, 4, 5, 6, 8, 10, 12, 15, 20, 25, and 30 cm.

**Table III. List of Pu-Metal Sphere Reflector Materials and Mass Densities (g/cm$^3$)**

| Reflector Material | Mass Density |
|---|---|
| Water (H2O) | 1.00 |
| Heavy Water (D2O) | 1.11 |
| Polyethylene | 0.95 |
| Borated Polyethylene | 0.95 |
| Lucite | 1.18 |
| PVDF (Kynar) | 1.76 |
| Mock HE | 1.67 |
| BISCO | 1.16 |
| Fire-Rated BISCO | 1.86 |
| PVC | 1.41 |
| Bromobenzene | 1.50 |
| LiH | 0.78 |
| Be Metal | 1.85 |
| BeO | 3.02 |
| B4C | 2.54 |
| Graphite | 2.23 |
| PF-5050 | 1.60 |

| | |
|---|---|
| SiO2 | 2.65 |
| Borosilicate Glass | 2.24 |
| Vermiculite | 2.70 |
| VAF | 2.73 |
| Foray | 2.70 |
| Los Alamos Concrete | 2.25 |
| NaCl | 2.17 |
| NaHCO3 | 2.20 |
| MgO2 | 3.58 |
| Al Metal | 2.70 |
| Alumina (Al2O3) | 4.10 |
| SS-304 | 8.00 |
| Carbon Steel | 7.82 |
| Inconel | 8.30 |
| Pewter | 7.26 |
| Copper | 8.96 |
| Titanium | 4.51 |
| Molybdenum | 10.28 |
| Zirconium | 6.52 |
| Zirconium Hydride (ZrH) | 5.90 |
| Cadmium | 8.65 |
| Zinc | 7.13 |
| Vanadium | 6.00 |
| Tantalum | 16.69 |
| Lead | 11.34 |
| Bismuth | 9.74 |
| Tungsten | 19.25 |
| Tungsten Carbide (WC) | 15.63 |
| Thorium Metal | 11.70 |
| Natural Uranium Metal | 19.10 |
| LEU (3%) Metal | 19.10 |
| HEU (93.1%) Metal | 19.10 |
| U233 Metal | 19.10 |

### 4.2. Pu Solutions

The Pu-solution model consists of two cylinders of Pu metal-water mix that are touching and sitting on a 0.5-in. SS-304 (density of 7.92 g/cm$^3$) stainless steel floor. The reflection of hands (modeled as pure water at 1.0 g/cm$^3$) is modeled by a 0.5-in. cylindrical annulus surrounding one of the Pu metal-water mixture cylinders. The H/D of the cylinders is varied from 0.5 to 2.0 in increments of 0.25. For each H/D the Pu-239 concentration is varied from 5 to 300 g/L (the density of the metal-water mix is a linear combination of Pu metal at 19.84 g/cm$^3$ and water at 1.0 g/cm$^3$) in various intervals to resolve the behavior of the calculational margin.

The calculational margin is relatively insensitive to varying H/D, but it is sensitive to the Pu-239 concentration. To simplify the analysis so that it is based upon a single parameter, the H/D is fixed at 1.0 and the trends are observed. The EALF varies from 0.04 eV at the concentration of 5 g/L to 0.72 eV at 300 g/L.

### 4.3. Pu Oxides

The Pu-oxide model is very similar geometrically to the one used for the metals except that now oxide-water ($PuO_2$-$H_2O$) mixtures are investigated to simulate damp powders. Like the Pu metals and solutions, the oxides are insensitive to H/D, and a fixed H/D of 1.6 is used as the validation application model. The mass of the $PuO_2$-$H_20$ mix is fixed at 3500 g. The oxide-water mix has a varied water atomic fraction from 1.e–6 (effectively zero for a dry powder) to 0.999 (which looks like a solution) with sufficient resolution to resolve the calculational margin behavior. This corresponds to varying the concentration of Pu-239 from 1014.2 to 1.32 g/L. The density of the oxide-water mix is a linear combination of the theoretical oxide density of 11.5 g/cm$^3$ and water at 1.0 g/cm$^3$.

The range of EALF for the models is from 600 keV for the dry case to 0.05 eV for the diluted case with a water fraction of 0.999.

**5. Calculational Margin**

The calculational margin is defined by ANS-8.24 to be "an allowance for the bias and bias uncertainty plus considerations of uncertainties related to interpolation, extrapolation, and trending." The bias measures the "systematic difference between calculated results and experimental data." The sign of the bias is arbitrary; in this document, a positive bias is defined to be non-conservative, i.e., benchmark $k_{eff}$ minus calculated $k_{eff}$. The bias uncertainty is "the uncertainty that accounts for the combined effects of uncertainties in the benchmarks, the calculational models of the benchmarks, and the calculational method."

In computing the calculational margin, the benchmark $k_{eff}$ and $k_{eff}$ uncertainties quoted in the ICSBEP are used. It is assumed that the benchmark uncertainties are normally distributed. MCNP6.1 is used to calculate values of $k_{eff}$ with an estimate of the statistical uncertainty that is assumed to be normal (MCNP6.1 conducts normality tests on $k_{eff}$). Except where otherwise noted, the calculations for the benchmarks and application models used 100,000 neutrons per cycle, 100 skip cycles, and 600 active cycles for a total of 50 million active histories. The convergence of the fission source is verified via the Shannon entropy test and relevant statistical checks on $k_{eff}$ pass.

The bias in $k_{eff}$ for an individual benchmark is computed by taking the difference of the benchmark $k_{eff}$ and the calculated $k_{eff}$ (this is consistent with the definition of positive bias being nonconservative) and the uncertainty in the bias of an individual benchmark is the square root of the sum of the squares of the uncertainty of the benchmark and calculated $k_{eff}$; in all cases the statistical uncertainty in the $k_{eff}$ calculation is negligible.

The bias in $k_{eff}$ for each benchmark is assumed to be normally distributed and therefore symmetric about its mean. Given this assumption, it is possible using extreme value theory (EVT) for a given set of benchmarks with weight functions to compute the probability that a certain value bounds the worst case of the biases in $k_{eff}$. The cumulative density function (CDF) of the worst-case bias in $k_{eff}$ is the product of the CDFs for each individual case. The calculational margin is the value where the CDF for the worst-case bias becomes greater than 0.99. This value is a 99% confidence interval stating that there is a 99% chance that the worst-case bias in $k_{eff}$ is less than the quoted value.

The details of how the EVT calculational margin is computed with the weighting functions are given in Ref. 13, but a few properties are given here. An attractive property of the EVT calculational margin is that it never decreases because of the addition of more benchmarks. Given that $c_k$ is a parameter that quantifies sources of computational bias, benchmarks can be added until a sufficient sample size has been achieved. The $c_k$ values are used as weights for the EVT calculational margin, so the size of this sample is adaptive, requiring more benchmarks for those that have smaller $c_k$ and that are therefore less similar. The net effect is that having fewer similar benchmarks leads to a more conservative calculational margin.

Note that the benchmarks were assumed to be uncorrelated, which is not correct. Because the maximum value of the calculational margin is taken, this, non-intuitively, leads to a conservative result. Why this is can be understood by thinking of sampling the EVT calculational margin via Monte Carlo: The bias for each benchmark is randomly sampled from each normal distribution and the worst bias found is taken. This process is repeated many times and the distribution of worst-case bias in $k_{eff}$ is used to form a confidence interval. The uncorrelated assumption is more conservative because each independent sampling of the benchmark's bias gives another independent chance for having that benchmark be the maximum and therefore decide the calculational margin for that random trial.

The calculational margin for each class of problems is discussed individually.

### 5.1. Pu Metals

For the process model considered for Pu-metal cylinders on a stainless steel floor and with water reflection, the computed calculational margin is quite stable, being around 0.0126. The maximum $c_k$ ranges from 0.98 to 0.99, indicating the presence of a benchmark with a high degree of similarity. The benchmarks used for the validation of the case with 3500 g and H/D of 1.6 are given in Table IV. Also given are the $c_k$ values and the weighting factors used.

Because of the insensitivity to process conditions for the Pu-metal case, no trending is performed and a single bounding value of 0.0127 is assigned as the calculational margin. This is shown in Figs. 1-3.

As a confirmation that the results are reasonable, a 99% calculational margin computed with the methodology in Ref. 17 gives a value of 0.0112 for the same benchmark data, showing the calculational margin obtained from the methodology described in this report, 0.0127, is slightly more conservative. The difference arises because the methodology developed in this report uses a different definition of calculational margin that bounds, to some probability, the occurrence of the worst-case bias in $k_{eff}$. Reference 17 uses different definitions and statistical techniques while testing the underlying normality assumptions, which are shown to be satisfied for the benchmarks considered in this validation, and reaches similar results. In no way should this methodology and its definitions be viewed as superior to the techniques in Ref. 17; both are valid approaches.

For the second set of Pu-metal models, the Pu sphere with different reflectors of varying thickness, the calculational margin for reflector thickness of 2, 5, 10, 20, and 30 cm are given in Table V.

**Table IV. Benchmarks Used, Correlation Coefficients, and Weighting Factors for the Validation of Pu Metal on a Stainless Steel Floor and with Water Reflection**

| Benchmark | ck | weight |
|---|---|---|
| pu-met-fast-021-001.i | 0.9884 | 1.0000 |
| pu-met-fast-022-001.i | 0.9883 | 0.9992 |
| pu-met-fast-024-001.i | 0.9856 | 0.9784 |
| pu-met-fast-023-001.i | 0.9855 | 0.9777 |
| pu-met-fast-001-001.i | 0.9829 | 0.9574 |
| pu-met-fast-018-001.i | 0.9802 | 0.9367 |
| pu-met-fast-036-001.i | 0.9764 | 0.9069 |
| pu-met-fast-044-001.i | 0.9758 | 0.9028 |
| mix-met-fast-009-001.i | 0.9753 | 0.8989 |
| pu-met-fast-005-001.i | 0.9732 | 0.8827 |
| pu-met-fast-021-002.i | 0.9727 | 0.8789 |
| pu-met-fast-035-001.i | 0.9721 | 0.8743 |
| pu-met-fast-025-001.i | 0.9704 | 0.8612 |
| pu-met-fast-044-005.i | 0.9641 | 0.8122 |
| pu-met-fast-009-001.i | 0.9633 | 0.8057 |
| pu-met-fast-019-001.i | 0.9588 | 0.7714 |
| pu-met-fast-044-002.i | 0.9577 | 0.7632 |
| pu-met-fast-029-001.i | 0.9572 | 0.7588 |
| pu-met-fast-038-001.i | 0.9522 | 0.7207 |
| pu-met-fast-008-001.i | 0.9508 | 0.7098 |
| pu-met-fast-030-001.i | 0.9506 | 0.7081 |
| pu-met-fast-044-004.i | 0.9474 | 0.6829 |
| mix-met-fast-007-022.i | 0.9416 | 0.6383 |
| mix-met-fast-007-014.i | 0.9403 | 0.6287 |
| pu-met-fast-045-005.i | 0.9320 | 0.5647 |
| pu-met-fast-045-006.i | 0.9284 | 0.5368 |
| pu-met-fast-045-004.i | 0.9264 | 0.5212 |
| pu-met-fast-031-001.i | 0.9227 | 0.4929 |
| pu-met-fast-045-003.i | 0.9217 | 0.4851 |
| pu-met-fast-011-001.i | 0.9197 | 0.4697 |
| pu-met-fast-045-007.i | 0.9136 | 0.4221 |
| pu-met-fast-045-001.i | 0.9115 | 0.4058 |

| | | |
|---|---|---|
| mix-met-fast-007-015.i | 0.9077 | 0.3771 |
| pu-met-fast-045-002.i | 0.9078 | 0.3771 |
| mix-met-fast-007-007.i | 0.9038 | 0.3464 |
| mix-met-fast-007-023.i | 0.9010 | 0.3253 |
| pu-met-fast-003-103.i | 0.8960 | 0.2860 |
| mix-met-fast-007-019.i | 0.8848 | 0.1998 |
| pu-met-fast-032-001.i | 0.8762 | 0.1336 |
| pu-met-fast-027-001.i | 0.8727 | 0.1063 |
| mix-met-fast-001-001.i | 0.8697 | 0.0833 |
| pu-met-fast-040-001.i | 0.8648 | 0.0454 |
| pu-met-fast-026-001.i | 0.8596 | 0.0052 |

**Table V. Calculational Margin for Pu-Metal Sphere Reflected by Different Materials of Varied Thickness**

| Reflector Material | 2 cm | 5 cm | 10 cm | 20 cm | 30 cm |
|---|---|---|---|---|---|
| Water (H2O) | 0.01280 | 0.01282 | 0.01277 | 0.01277 | 0.01277 |
| Heavy Water (D2O) | 0.01285 | 0.01291 | 0.01292 | 0.01290 | 0.01287 |
| Polyethylene | 0.01272 | 0.01269 | 0.01267 | 0.01267 | 0.01268 |
| Borated Poly | 0.01272 | 0.01271 | 0.01271 | 0.01271 | 0.01271 |
| Lucite | 0.01276 | 0.01277 | 0.01273 | 0.01271 | 0.01271 |
| PVDF (Kynar) | 0.01277 | 0.01280 | 0.01279 | 0.01278 | 0.01277 |
| Mock HE | 0.01280 | 0.01284 | 0.01285 | 0.01286 | 0.01285 |
| BISCO | 0.01276 | 0.01277 | 0.01277 | 0.01277 | 0.01278 |
| Fire-Rated BISCO | 0.01279 | 0.01281 | 0.01282 | 0.01282 | 0.01282 |
| PVC | 0.01278 | 0.01283 | 0.01284 | 0.01284 | 0.01284 |
| Bromobenzene | 0.01272 | 0.01273 | 0.01274 | 0.01274 | 0.01274 |
| LiH | 0.01272 | 0.01271 | 0.01271 | 0.01270 | 0.01270 |
| Be Metal | 0.01275 | 0.01266 | 0.01258 | 0.01250 | 0.01249 |
| BeO | 0.01292 | 0.01291 | 0.01289 | 0.01286 | 0.01284 |
| B4C | 0.01275 | 0.01277 | 0.01276 | 0.01276 | 0.01276 |
| Graphite | 0.01272 | 0.01273 | 0.01275 | 0.01277 | 0.01276 |
| PF-5050 | 0.01278 | 0.01284 | 0.01288 | 0.01290 | 0.01291 |
| SiO2 | 0.01288 | 0.01295 | 0.01296 | 0.01296 | 0.01297 |
| Borosilicate Glass | 0.01285 | 0.01293 | 0.01295 | 0.01295 | 0.01294 |
| Vermiculite | 0.01287 | 0.01290 | 0.01284 | 0.01282 | 0.01282 |
| VAF | 0.01293 | 0.01296 | 0.01299 | 0.01299 | 0.01299 |
| Foray | 0.01281 | 0.01284 | 0.01280 | 0.01280 | 0.01280 |
| Los Alamos Concrete | 0.01284 | 0.01293 | 0.01295 | 0.01295 | 0.01295 |
| NaCl | 0.01272 | 0.01273 | 0.01276 | 0.01278 | 0.01279 |
| NaHCO3 | 0.01287 | 0.01293 | 0.01292 | 0.01289 | 0.01288 |
| MgO2 | 0.01298 | 0.01310 | 0.01312 | 0.01311 | 0.01310 |
| Al Metal | 0.01273 | 0.01275 | 0.01275 | 0.01275 | 0.01275 |
| Alumina (Al2O3) | 0.01294 | 0.01297 | 0.01298 | 0.01298 | 0.01297 |
| SS-304 | 0.01267 | 0.01266 | 0.01266 | 0.01266 | 0.01266 |
| Carbon Steel | 0.01264 | 0.01262 | 0.01260 | 0.01259 | 0.01259 |
| Inconel | 0.01275 | 0.01277 | 0.01279 | 0.01279 | 0.01279 |
| Pewter | 0.01276 | 0.01286 | 0.01295 | 0.01303 | 0.01307 |
| Copper | 0.01571 | 0.01704 | 0.01721 | 0.01723 | 0.01724 |
| Titanium | 0.01272 | 0.01275 | 0.01277 | 0.01280 | 0.01283 |
| Molybdenum | 0.01269 | 0.01488 | 0.01583 | 0.01606 | 0.01603 |
| Zirconium | 0.01302 | 0.01354 | 0.01605 | 0.01671 | 0.01680 |
| Zirconium Hydride (ZrH) | 0.01301 | 0.01362 | 0.01523 | 0.01524 | 0.01520 |
| Cadmium | 0.01285 | 0.01302 | 0.01312 | 0.01348 | 0.01316 |
| Zinc | 0.01279 | 0.01286 | 0.01292 | 0.01296 | 0.01296 |
| Vanadium | 0.01282 | 0.01292 | 0.01297 | 0.01300 | 0.01300 |
| Tantalum | 0.01614 | 0.02610 | 0.02704 | 0.02621 | 0.02614 |
| Lead | 0.01271 | 0.01271 | 0.01271 | 0.01271 | 0.01271 |
| Bismuth | 0.01272 | 0.01273 | 0.01275 | 0.01276 | 0.01276 |
| Tungsten | 0.01412 | 0.01475 | 0.01484 | 0.01486 | 0.01487 |
| Tungsten Carbide (WC) | 0.01279 | 0.01465 | 0.01485 | 0.01481 | 0.01481 |
| Thorium Metal | 0.01272 | 0.01275 | 0.01272 | 0.01270 | 0.01270 |
| Natural Uranium Metal | 0.01251 | 0.01235 | 0.01235 | 0.01236 | 0.01237 |
| LEU (3%) Metal | 0.01249 | 0.01234 | 0.01232 | 0.01234 | 0.01242 |
| HEU (93.1%) Metal | 0.01232 | 0.01136 | 0.01081 | 0.01181 | 0.01255 |
| U233 Metal | 0.01298 | 0.01598 | 0.02772 | 0.04084 | 0.04425 |

### 5.2. Pu Solutions

For the process model considered, there is a strong trend in the calculational margin with Pu solution (metal-water mix) concentration and corresponding EALF. Figures 4 and 5 give the calculational margin curve as a function of Pu solution concentration (in g/L) and EALF (in MeV), respectively.

Tables VI.1-3 give the benchmarks, $c_k$ values, and weighting factors used for the validation at 15, 40, and 150 g/L; this represents three typical points on the calculational margin curve. In the 40 g/L case, there are numerous benchmarks that are highly similar, with 45 benchmarks having a $c_k$ exceeding 0.97, indicating the coverage for this solution concentration is very good. The benchmarks also tend to calculate high in this regime, so the calculational margin required is lower. No credit is taken for positive bias directly; however, the presence of benchmarks that compute high do not incur a penalty.

For the more dilute 15-g/L case, there is still reasonable coverage, with 52 benchmarks having $c_k$ exceeding 0.978. The bias is higher in this region because a few benchmarks compute a larger bias (in particular, the PST-011 cases drive the calculational margin) and have a greater uncertainty.

For the more concentrated 150 g/L Pu metal-water mix, the coverage is not as good. The maximum $c_k$ is 0.971 and therefore 62 benchmarks are required to meet the criteria with some having as low a $c_k$ as 0.89. This is a consequence of the benchmark data beyond 150 g/L being quite sparse. To meet the required total weight, the validation needed to use some of the mixed solutions and oxides. This tends to drive the calculational margin upward from the 40-g/L case.

Because of the strong trend in Pu solution concentration, this curve is used directly in determining a bounding USL for Pu solutions. Section 7 will give the USL and the rationale for its selection.

**Table VI.1 Benchmarks Used, Correlation Coefficients, and Weighting Factors for Pu-Solution/Metal-Water Mix Validation (15 g/L case)**

| Benchmark | ck | weight |
|---|---|---|
| pu-sol-therm-011-181.i | 0.9970 | 1.0000 |
| pu-sol-therm-011-183.i | 0.9963 | 0.9638 |
| pu-sol-therm-011-182.i | 0.9960 | 0.9452 |
| pu-sol-therm-006-001.i | 0.9954 | 0.9174 |
| pu-sol-therm-011-187.i | 0.9954 | 0.9172 |
| pu-sol-therm-011-184.i | 0.9954 | 0.9166 |
| pu-sol-therm-006-002.i | 0.9947 | 0.8801 |
| pu-sol-therm-011-185.i | 0.9943 | 0.8563 |
| pu-sol-therm-004-001.i | 0.9934 | 0.8094 |
| pu-sol-therm-004-002.i | 0.9933 | 0.8028 |
| pu-sol-therm-006-003.i | 0.9931 | 0.7916 |
| pu-sol-therm-004-005.i | 0.9926 | 0.7650 |
| pu-sol-therm-004-006.i | 0.9922 | 0.7459 |
| pu-sol-therm-004-003.i | 0.9921 | 0.7424 |
| pu-sol-therm-004-013.i | 0.9912 | 0.6927 |
| pu-sol-therm-004-012.i | 0.9911 | 0.6894 |
| pu-sol-therm-004-007.i | 0.9911 | 0.6856 |
| pu-sol-therm-005-001.i | 0.9910 | 0.6853 |
| pu-sol-therm-004-004.i | 0.9909 | 0.6751 |
| pu-sol-therm-011-186.i | 0.9905 | 0.6587 |
| pu-sol-therm-005-002.i | 0.9905 | 0.6571 |
| pu-sol-therm-004-008.i | 0.9904 | 0.6532 |
| pu-sol-therm-005-008.i | 0.9902 | 0.6411 |
| pu-sol-therm-010-014.i | 0.9895 | 0.6060 |
| pu-sol-therm-005-003.i | 0.9889 | 0.5734 |
| pu-sol-therm-005-009.i | 0.9888 | 0.5650 |
| pu-sol-therm-004-009.i | 0.9881 | 0.5313 |

| | | |
|---|---|---|
| mix-sol-therm-003-005.i | 0.9874 | 0.4930 |
| mix-sol-therm-003-009.i | 0.9872 | 0.4844 |
| pu-sol-therm-005-004.i | 0.9861 | 0.4267 |
| pu-sol-therm-003-001.i | 0.9859 | 0.4136 |
| pu-sol-therm-003-007.i | 0.9847 | 0.3486 |
| pu-sol-therm-032-009.i | 0.9844 | 0.3367 |
| pu-sol-therm-003-002.i | 0.9843 | 0.3304 |
| mix-sol-therm-003-010.i | 0.9841 | 0.3179 |
| pu-sol-therm-032-008.i | 0.9839 | 0.3086 |
| pu-sol-therm-003-008.i | 0.9833 | 0.2746 |
| pu-sol-therm-032-007.i | 0.9826 | 0.2422 |
| pu-sol-therm-032-010.i | 0.9826 | 0.2379 |
| pu-sol-therm-005-005.i | 0.9825 | 0.2345 |
| pu-sol-therm-004-010.i | 0.9825 | 0.2327 |
| pu-sol-therm-003-003.i | 0.9817 | 0.1939 |
| pu-sol-therm-032-011.i | 0.9815 | 0.1793 |
| pu-sol-therm-032-006.i | 0.9814 | 0.1751 |
| pu-sol-therm-003-004.i | 0.9806 | 0.1332 |
| pu-sol-therm-010-008.i | 0.9806 | 0.1332 |
| pu-sol-therm-032-012.i | 0.9805 | 0.1279 |
| pu-sol-therm-011-161.i | 0.9805 | 0.1274 |
| pu-sol-therm-032-017.i | 0.9798 | 0.0941 |
| pu-sol-therm-011-162.i | 0.9794 | 0.0728 |
| pu-sol-therm-005-006.i | 0.9788 | 0.0372 |
| pu-sol-therm-032-016.i | 0.9785 | 0.0209 |

**Table VI.2 Benchmarks Used, Correlation Coefficients, and Weighting Factors for Pu-Solution/Metal-Water Mix Validation (40 g/L case)**

| | | |
|---|---|---|
| pu-sol-therm-011-165.i | 0.9949 | 1.0000 |
| pu-sol-therm-011-164.i | 0.9942 | 0.9453 |
| pu-sol-therm-002-001.i | 0.9938 | 0.9190 |
| pu-sol-therm-002-002.i | 0.9938 | 0.9170 |
| pu-sol-therm-011-162.i | 0.9934 | 0.8896 |
| pu-sol-therm-002-003.i | 0.9934 | 0.8862 |
| pu-sol-therm-011-161.i | 0.9930 | 0.8625 |
| pu-sol-therm-010-006.i | 0.9926 | 0.8307 |
| pu-sol-therm-010-010.i | 0.9926 | 0.8285 |
| pu-sol-therm-003-006.i | 0.9925 | 0.8265 |
| pu-sol-therm-010-011.i | 0.9925 | 0.8216 |
| pu-sol-therm-010-003.i | 0.9923 | 0.8130 |
| pu-sol-therm-002-004.i | 0.9917 | 0.7680 |
| pu-sol-therm-010-004.i | 0.9913 | 0.7407 |
| pu-sol-therm-010-012.i | 0.9913 | 0.7365 |
| pu-sol-therm-010-009.i | 0.9913 | 0.7358 |
| pu-sol-therm-010-005.i | 0.9912 | 0.7345 |
| pu-sol-therm-003-008.i | 0.9912 | 0.7338 |
| pu-sol-therm-003-005.i | 0.9910 | 0.7200 |
| pu-sol-therm-010-007.i | 0.9908 | 0.7020 |
| pu-sol-therm-002-005.i | 0.9906 | 0.6862 |
| pu-sol-therm-003-004.i | 0.9904 | 0.6706 |
| pu-sol-therm-004-011.i | 0.9902 | 0.6603 |
| pu-sol-therm-001-001.i | 0.9899 | 0.6356 |
| pu-sol-therm-003-007.i | 0.9899 | 0.6352 |
| pu-sol-therm-003-003.i | 0.9896 | 0.6172 |
| pu-sol-therm-005-007.i | 0.9891 | 0.5789 |
| pu-sol-therm-003-002.i | 0.9887 | 0.5515 |
| pu-sol-therm-005-006.i | 0.9887 | 0.5503 |
| pu-sol-therm-002-006.i | 0.9880 | 0.5024 |
| pu-sol-therm-003-001.i | 0.9878 | 0.4860 |
| pu-sol-therm-010-002.i | 0.9876 | 0.4745 |
| pu-sol-therm-004-010.i | 0.9875 | 0.4677 |
| pu-sol-therm-010-008.i | 0.9868 | 0.4179 |
| pu-sol-therm-005-005.i | 0.9867 | 0.4078 |
| pu-sol-therm-005-004.i | 0.9851 | 0.2909 |
| pu-sol-therm-004-009.i | 0.9842 | 0.2294 |
| pu-sol-therm-005-003.i | 0.9833 | 0.1663 |

| | | |
|---|---|---|
| pu-sol-therm-005-009.i | 0.9829 | 0.1391 |
| pu-sol-therm-004-004.i | 0.9827 | 0.1229 |
| pu-sol-therm-002-007.i | 0.9826 | 0.1120 |
| pu-sol-therm-011-186.i | 0.9823 | 0.0912 |
| pu-sol-therm-004-008.i | 0.9822 | 0.0844 |
| pu-sol-therm-004-012.i | 0.9814 | 0.0292 |
| pu-sol-therm-005-002.i | 0.9813 | 0.0234 |
| pu-sol-therm-005-008.i | 0.9811 | 0.0062 |

**Table VI.3 Benchmarks Used, Correlation Coefficients, and Weighting Factors for Pu-Solution/Metal-Water Mix Validation (150 g/L case)**

| | | |
|---|---|---|
| pu-sol-therm-001-003.i | 0.9711 | 1.0000 |
| pu-sol-therm-001-004.i | 0.9710 | 0.9996 |
| pu-sol-therm-001-005.i | 0.9705 | 0.9935 |
| pu-sol-therm-007-008.i | 0.9692 | 0.9771 |
| pu-sol-therm-007-009.i | 0.9688 | 0.9713 |
| pu-sol-therm-007-007.i | 0.9686 | 0.9694 |
| pu-sol-therm-007-006.i | 0.9683 | 0.9658 |
| pu-sol-therm-007-005.i | 0.9672 | 0.9510 |
| pu-sol-therm-001-002.i | 0.9664 | 0.9413 |
| pu-sol-therm-007-010.i | 0.9657 | 0.9322 |
| pu-sol-therm-002-007.i | 0.9606 | 0.8684 |
| pu-sol-therm-002-006.i | 0.9548 | 0.7956 |
| pu-sol-therm-034-001.i | 0.9524 | 0.7662 |
| pu-sol-therm-001-001.i | 0.9514 | 0.7534 |
| pu-sol-therm-010-002.i | 0.9509 | 0.7465 |
| pu-sol-therm-002-005.i | 0.9467 | 0.6941 |
| pu-sol-therm-007-003.i | 0.9447 | 0.6686 |
| pu-sol-therm-010-009.i | 0.9428 | 0.6449 |
| pu-sol-therm-002-004.i | 0.9425 | 0.6418 |
| mix-sol-therm-001-008.i | 0.9383 | 0.5888 |
| pu-sol-therm-002-003.i | 0.9379 | 0.5833 |
| pu-sol-therm-007-002.i | 0.9353 | 0.5510 |
| pu-sol-therm-010-004.i | 0.9301 | 0.4850 |
| pu-sol-therm-002-002.i | 0.9297 | 0.4803 |
| pu-sol-therm-011-165.i | 0.9293 | 0.4753 |
| pu-sol-therm-010-003.i | 0.9285 | 0.4661 |
| pu-sol-therm-034-002.i | 0.9282 | 0.4614 |
| pu-sol-therm-002-001.i | 0.9261 | 0.4360 |
| mix-sol-therm-001-006.i | 0.9241 | 0.4101 |
| pu-sol-therm-010-010.i | 0.9237 | 0.4049 |
| pu-sol-therm-032-001.i | 0.9215 | 0.3773 |
| pu-sol-therm-010-011.i | 0.9206 | 0.3664 |
| pu-sol-therm-010-006.i | 0.9198 | 0.3565 |
| pu-sol-therm-022-002.i | 0.9194 | 0.3513 |
| pu-sol-therm-010-005.i | 0.9189 | 0.3451 |
| pu-sol-therm-003-006.i | 0.9181 | 0.3352 |
| mix-sol-therm-001-009.i | 0.9163 | 0.3123 |
| pu-sol-therm-011-164.i | 0.9155 | 0.3017 |
| pu-sol-therm-032-002.i | 0.9144 | 0.2890 |
| pu-sol-therm-005-007.i | 0.9108 | 0.2437 |
| pu-sol-therm-010-012.i | 0.9107 | 0.2416 |
| pu-sol-therm-010-007.i | 0.9104 | 0.2383 |
| pu-sol-therm-001-006.i | 0.9096 | 0.2281 |
| pu-sol-therm-004-011.i | 0.9095 | 0.2273 |
| pu-sol-therm-003-005.i | 0.9082 | 0.2109 |
| pu-sol-therm-022-001.i | 0.9079 | 0.2074 |
| pu-sol-therm-011-162.i | 0.9077 | 0.2049 |
| pu-sol-therm-011-161.i | 0.9062 | 0.1860 |
| mix-comp-therm-001-003.i | 0.9052 | 0.1730 |
| pu-sol-therm-005-006.i | 0.9037 | 0.1538 |
| mix-sol-therm-001-002.i | 0.9033 | 0.1493 |
| pu-sol-therm-003-004.i | 0.9023 | 0.1365 |
| mix-sol-therm-001-001.i | 0.9022 | 0.1357 |
| pu-sol-therm-032-003.i | 0.9021 | 0.1335 |
| pu-sol-therm-003-003.i | 0.8994 | 0.0997 |

| | | |
|---|---|---|
| pu-sol-therm-003-008.i | 0.8992 | 0.0977 |
| pu-sol-therm-010-008.i | 0.8982 | 0.0852 |
| pu-sol-therm-004-010.i | 0.8969 | 0.0685 |
| mix-sol-therm-001-010.i | 0.8966 | 0.0654 |
| pu-sol-therm-003-007.i | 0.8960 | 0.0576 |
| pu-sol-therm-005-005.i | 0.8952 | 0.0471 |
| pu-sol-therm-003-002.i | 0.8938 | 0.0298 |

### 5.3. Pu Oxides

The calculational margin of Pu oxides has a strong dependence on the system EALF. Dry powders have a somewhat softer spectrum (with an EALF in the few- to several hundred-keV range) than metals and tend to be spectrally similar to metals with low-Z reflectors (e.g., water, polyethylene, beryllium) having $c_k$ values greater than 0.9. Therefore the Pu oxides have a similar, but slightly larger, calculational margin compared to the Pu metals. Dilute powders are qualitatively like Pu solutions, having the same dominant isotopes of Pu, hydrogen, and oxygen, but in different proportions, and they also have a similar calculational margin. The damp powders are unlike either, and they have a significantly higher calculational margin.

Figure 8 gives the calculational margin curve as a function of EALF. Note that there is a sharp transition between the regimes at EALF of 400 keV from metal to oxide and another at about 0.2 eV from oxide to solution. These transition bounds correspond to water fractions of 0.125 and 0.99 or Pu-239 concentrations of 890.0 and 12.9 g/L.

The benchmarks used for the dry oxide powder case (water faction of 1e–6 with a Pu-239 concentration of 1014.2 g/L and EALF of 606 keV) are given in Table VII.1. The maximum $c_k$ is 0.980 and 47 benchmarks are required. While more are required, the benchmarks used for the dry oxides are neutronically similar to the metals with low-Z reflectors, and therefore the calculational margin, 0.0129, is similar.

Table VII.2 gives a dilute oxide powder case with a water fraction of 0.995, corresponding to a Pu-239 concentration of 6.53 g/L with an EALF of 0.09 eV. The results show that this case is quite similar to the Pu solutions. The maximum $c_k$ is 0.985 and 46 Pu solution benchmarks are used. This implies that the limits for dilute oxides and solutions are very similar. This makes sense as they share common isotopes and spectra.

The intermediate-spectrum case (water fraction of 0.5 corresponding to a Pu-239 concentration of 516.9 g/L with an EALF of 31.5 keV) is given in Table VII.3. The maximum $c_k$ is 0.950 with the PU-COMP-MIXED-002-008 benchmark being most similar. Fifty-five benchmarks are required to perform the validation. The $c_k$ required to reach the required weight is 0.598, indicating poor coverage; the benchmarks used are a combination of mixed oxides and solutions, Pu oxides, metals, and solutions. Because of the scant benchmark coverage in the intermediate regime, a single benchmark, PU-COMP-MIXED-001-005, drives the calculational margin over a very wide range of EALF. For this specific case, the $c_k$ is 0.877. Because of these factors, the calculational margin in this regime is bounded by 0.035, significantly higher than the other cases.

**Table VII.1 Benchmarks Used, Correlation Coefficients, and Weighting Factors for Pu-Oxide/Oxide-Water Mix Validation (dry case)**

| Benchmark | ck | weight |
|---|---|---|
| pu-met-fast-011-001.i | 0.9703 | 1.0000 |
| pu-met-fast-021-002.i | 0.9640 | 0.9708 |
| pu-met-fast-036-001.i | 0.9607 | 0.9555 |
| pu-met-fast-044-005.i | 0.9577 | 0.9415 |
| pu-met-fast-044-001.i | 0.9570 | 0.9380 |
| pu-met-fast-024-001.i | 0.9553 | 0.9304 |
| pu-met-fast-044-004.i | 0.9533 | 0.9208 |
| pu-met-fast-038-001.i | 0.9464 | 0.8888 |
| pu-met-fast-021-001.i | 0.9373 | 0.8461 |

| | | |
|---|---|---|
| pu-met-fast-044-002.i | 0.9371 | 0.8452 |
| pu-met-fast-031-001.i | 0.9328 | 0.8253 |
| pu-met-fast-018-001.i | 0.9294 | 0.8096 |
| mix-met-fast-007-014.i | 0.9226 | 0.7779 |
| pu-met-fast-019-001.i | 0.9179 | 0.7557 |
| pu-met-fast-023-001.i | 0.9174 | 0.7536 |
| pu-met-fast-027-001.i | 0.9134 | 0.7349 |
| pu-met-fast-005-001.i | 0.9072 | 0.7060 |
| pu-met-fast-022-001.i | 0.9070 | 0.7050 |
| pu-met-fast-045-005.i | 0.8970 | 0.6582 |
| pu-met-fast-009-001.i | 0.8957 | 0.6524 |
| pu-met-fast-001-001.i | 0.8955 | 0.6512 |
| pu-met-fast-035-001.i | 0.8950 | 0.6490 |
| mix-met-fast-009-001.i | 0.8921 | 0.6355 |
| mix-met-fast-007-007.i | 0.8921 | 0.6354 |
| pu-met-fast-045-004.i | 0.8915 | 0.6328 |
| pu-met-fast-025-001.i | 0.8911 | 0.6308 |
| pu-met-fast-045-003.i | 0.8859 | 0.6067 |
| pu-met-fast-045-001.i | 0.8848 | 0.6017 |
| pu-met-fast-045-002.i | 0.8774 | 0.5670 |
| pu-met-fast-045-006.i | 0.8764 | 0.5622 |
| mix-met-fast-007-022.i | 0.8754 | 0.5577 |
| mix-met-fast-007-015.i | 0.8741 | 0.5517 |
| pu-met-fast-030-001.i | 0.8727 | 0.5451 |
| pu-met-fast-045-007.i | 0.8679 | 0.5226 |
| pu-met-fast-029-001.i | 0.8664 | 0.5158 |
| pu-met-fast-008-001.i | 0.8647 | 0.5080 |
| mix-met-fast-007-023.i | 0.8300 | 0.3459 |
| mix-met-fast-007-019.i | 0.8225 | 0.3111 |
| mix-met-fast-007-008.i | 0.8149 | 0.2755 |
| pu-met-fast-040-001.i | 0.8044 | 0.2263 |
| pu-met-fast-014-001.i | 0.7923 | 0.1703 |
| pu-met-fast-032-001.i | 0.7922 | 0.1695 |
| mix-met-fast-001-001.i | 0.7891 | 0.1552 |
| pu-met-fast-003-103.i | 0.7890 | 0.1549 |
| pu-met-fast-026-001.i | 0.7852 | 0.1371 |
| mix-met-fast-007-020.i | 0.7686 | 0.0595 |
| mix-met-fast-005-001.i | 0.7629 | 0.0331 |

**Table VII.2 Benchmarks Used, Correlation Coefficients, and Weighting Factors for Pu-Oxide/Oxide-Water Mix Validation (dilute case; 0.5 atom percent $PuO_2$)**

| Benchmark | ck | weight |
|---|---|---|
| pu-sol-therm-001-001.i | 0.9850 | 1.0000 |
| pu-sol-therm-002-006.i | 0.9848 | 0.9920 |
| pu-sol-therm-002-005.i | 0.9837 | 0.9500 |
| pu-sol-therm-002-004.i | 0.9831 | 0.9278 |
| pu-sol-therm-002-003.i | 0.9830 | 0.9243 |
| pu-sol-therm-010-009.i | 0.9830 | 0.9224 |
| pu-sol-therm-010-002.i | 0.9829 | 0.9196 |
| pu-sol-therm-002-007.i | 0.9824 | 0.9020 |
| pu-sol-therm-007-010.i | 0.9819 | 0.8815 |
| pu-sol-therm-011-165.i | 0.9811 | 0.8514 |
| pu-sol-therm-002-002.i | 0.9804 | 0.8247 |
| pu-sol-therm-001-002.i | 0.9799 | 0.8056 |
| pu-sol-therm-002-001.i | 0.9791 | 0.7755 |
| pu-sol-therm-007-007.i | 0.9791 | 0.7752 |
| pu-sol-therm-010-003.i | 0.9787 | 0.7612 |
| pu-sol-therm-010-004.i | 0.9786 | 0.7597 |
| pu-sol-therm-007-006.i | 0.9786 | 0.7563 |
| pu-sol-therm-007-005.i | 0.9783 | 0.7450 |
| pu-sol-therm-007-009.i | 0.9779 | 0.7300 |
| pu-sol-therm-007-008.i | 0.9777 | 0.7245 |
| pu-sol-therm-010-010.i | 0.9772 | 0.7037 |
| pu-sol-therm-010-011.i | 0.9762 | 0.6675 |
| pu-sol-therm-010-006.i | 0.9759 | 0.6558 |
| pu-sol-therm-011-164.i | 0.9754 | 0.6394 |

| | | |
|---|---|---|
| pu-sol-therm-003-006.i | 0.9750 | 0.6215 |
| pu-sol-therm-010-005.i | 0.9747 | 0.6116 |
| pu-sol-therm-011-162.i | 0.9724 | 0.5263 |
| pu-sol-therm-010-012.i | 0.9716 | 0.4954 |
| pu-sol-therm-011-161.i | 0.9715 | 0.4925 |
| pu-sol-therm-010-007.i | 0.9710 | 0.4711 |
| pu-sol-therm-003-005.i | 0.9704 | 0.4498 |
| pu-sol-therm-004-011.i | 0.9700 | 0.4348 |
| pu-sol-therm-005-007.i | 0.9691 | 0.4017 |
| pu-sol-therm-003-004.i | 0.9679 | 0.3562 |
| pu-sol-therm-003-008.i | 0.9678 | 0.3517 |
| pu-sol-therm-001-003.i | 0.9674 | 0.3360 |
| pu-sol-therm-005-006.i | 0.9665 | 0.3043 |
| pu-sol-therm-003-003.i | 0.9662 | 0.2928 |
| pu-sol-therm-003-007.i | 0.9653 | 0.2580 |
| pu-sol-therm-003-002.i | 0.9638 | 0.2025 |
| pu-sol-therm-004-010.i | 0.9633 | 0.1813 |
| pu-sol-therm-010-008.i | 0.9631 | 0.1766 |
| pu-sol-therm-005-005.i | 0.9619 | 0.1310 |
| pu-sol-therm-003-001.i | 0.9619 | 0.1296 |
| pu-sol-therm-032-001.i | 0.9617 | 0.1230 |
| pu-sol-therm-032-002.i | 0.9602 | 0.0671 |

**Table VII.3 Benchmarks Used, Correlation Coefficients, and Weighting Factors for Pu-Oxide/Oxide-Water Mix Validation (50 atom percent $PuO_2$)**

| Benchmark | ck | weight |
|---|---|---|
| pu-comp-mixed-002-008.i | 0.9498 | 1.0000 |
| pu-comp-mixed-002-009.i | 0.9477 | 0.9940 |
| pu-comp-mixed-001-004.i | 0.9289 | 0.9410 |
| pu-comp-mixed-002-022.i | 0.9263 | 0.9337 |
| pu-comp-mixed-002-021.i | 0.9260 | 0.9328 |
| pu-comp-mixed-002-018.i | 0.9259 | 0.9326 |
| pu-comp-mixed-002-019.i | 0.9258 | 0.9322 |
| pu-comp-mixed-002-020.i | 0.9255 | 0.9315 |
| pu-comp-mixed-002-017.i | 0.9224 | 0.9225 |
| pu-comp-inter-001-001.i | 0.8955 | 0.8468 |
| pu-sol-therm-034-013.i | 0.8890 | 0.8283 |
| pu-sol-therm-034-010.i | 0.8887 | 0.8276 |
| pu-sol-therm-034-011.i | 0.8885 | 0.8269 |
| pu-sol-therm-034-012.i | 0.8882 | 0.8262 |
| pu-sol-therm-034-009.i | 0.8875 | 0.8241 |
| pu-sol-therm-034-014.i | 0.8871 | 0.8230 |
| pu-sol-therm-034-015.i | 0.8869 | 0.8225 |
| pu-sol-therm-034-008.i | 0.8859 | 0.8195 |
| pu-sol-therm-034-007.i | 0.8854 | 0.8182 |
| pu-comp-mixed-001-005.i | 0.8760 | 0.7917 |
| pu-comp-mixed-002-029.i | 0.8655 | 0.7621 |
| pu-comp-mixed-002-028.i | 0.8650 | 0.7606 |
| pu-comp-mixed-002-027.i | 0.8639 | 0.7576 |
| mix-comp-therm-001-001.i | 0.8638 | 0.7573 |
| pu-comp-mixed-002-026.i | 0.8632 | 0.7555 |
| pu-comp-mixed-002-024.i | 0.8618 | 0.7516 |
| pu-comp-mixed-002-025.i | 0.8609 | 0.7490 |
| pu-comp-mixed-002-023.i | 0.8596 | 0.7454 |
| mix-comp-inter-005-001.i | 0.8460 | 0.7069 |
| mix-comp-therm-003-001.i | 0.7752 | 0.5071 |
| pu-sol-therm-001-006.i | 0.7662 | 0.4816 |
| mix-sol-therm-001-007.i | 0.7508 | 0.4383 |
| mix-comp-therm-003-003.i | 0.7386 | 0.4039 |
| pu-sol-therm-007-002.i | 0.7262 | 0.3689 |
| mix-comp-therm-003-002.i | 0.7164 | 0.3411 |
| pu-sol-therm-007-003.i | 0.7093 | 0.3212 |
| mix-comp-therm-001-002.i | 0.7088 | 0.3197 |
| pu-sol-therm-034-006.i | 0.6872 | 0.2589 |
| pu-sol-therm-034-005.i | 0.6808 | 0.2407 |
| pu-met-fast-027-001.i | 0.6798 | 0.2379 |

| | | |
|---|---|---|
| pu-met-fast-016-002.i | 0.6759 | 0.2269 |
| pu-met-fast-016-006.i | 0.6667 | 0.2008 |
| pu-met-fast-016-003.i | 0.6646 | 0.1951 |
| pu-met-fast-016-005.i | 0.6632 | 0.1910 |
| pu-sol-therm-034-004.i | 0.6621 | 0.1878 |
| pu-met-fast-016-004.i | 0.6592 | 0.1797 |
| pu-sol-therm-022-001.i | 0.6568 | 0.1729 |
| pu-sol-therm-034-003.i | 0.6427 | 0.1331 |
| mix-sol-therm-001-005.i | 0.6283 | 0.0926 |
| pu-met-fast-011-001.i | 0.6160 | 0.0579 |
| mix-comp-therm-002-002.i | 0.6154 | 0.0560 |
| pu-sol-therm-034-002.i | 0.6124 | 0.0477 |
| mix-sol-therm-001-006.i | 0.6060 | 0.0296 |
| mix-sol-therm-001-001.i | 0.6007 | 0.0145 |
| mix-sol-therm-001-002.i | 0.5982 | 0.0076 |

**6. Margin of Subcriticality**

ANS-8.24 defines the margin of subcriticality as "an allowance beyond the calculational margin to ensure subcriticality." To guide the selection of the margin, ANS-8.24 Sec. 6.4 states, "A margin of subcriticality shall be applied that is sufficiently large to ensure that calculated conditions will actually be subcritical. The selection of a margin of subcriticality should take into account the sensitivity of the system or process to variations in fissile form, geometry, or other physical characteristics. A single margin might not be appropriate over the entire validation applicability."

This document addresses the issues with codes and the nuclear data libraries towards determining this aspect of the margin of subcriticality. The aspect related to the condition being modeled, which requires a determination by the analyst of the necessity and magnitude of any additional margin of subcriticality necessary to ensure subcriticality, is not included.

The calculational margin determines, for the given area of applicability, what value of $k_{eff}$ calculated by a transport code with an associated nuclear data library is to be treated as critical to within some confidence interval (99% in this case). The phrase "ensure subcriticality" in ANS-8.24 implies that the analyst should not have credible doubt that the condition modeled is actually subcritical. This cannot be done with normal statistical techniques and therefore relies on the expert judgment of the analyst to create models that are bounding of the actual conditions being analyzed.

Finally, as stated in Sec. 5, the arguments for establishing a suitable margin of subcriticality assume a 99% confidence interval bounding the worst-case $k_{eff}$ bias, i.e., the methodology used in this validation. Stated another way, there is a 1% chance that the worst-case bias in $k_{eff}$ among the benchmarks is greater than the calculational margin. Because the calculational margin is based upon the worst-case scenario among numerous benchmarks and not some type of average, a 1% chance of this occurring is deemed acceptable based upon expert judgment given that the other four factors to be discussed are applied.

The margin of subcriticality, again, must be large enough to ensure subcriticality, and the choice of having four considerations discussed in the subsequent subsections is predicated upon these assumptions. If, hypothetically speaking, in a different validation the calculational margin were redefined to, for instance, use a 95% confidence interval instead of a 99% confidence interval, it would invalidate the assumptions herein and this entire section would need to be reconsidered. Additional margin is most likely necessary because there would now be higher probability (5% versus 1% in this hypothetical case) of a benchmark having a bias exceeding the redefined calculational margin. Again and in any case, **it is <u>not possible</u> to change the definition of, or reduce the confidence interval for, the calculational margin without reconsidering the entirety of this section.**

### 6.1. Errors in Monte Carlo Transport Codes and Nuclear Data Processing

Production Monte Carlo transport codes are very complicated pieces of software. The same is true of the entire process of developing nuclear data files that are usable by such codes. Inevitably, despite the best efforts of those developing the codes or preparing the nuclear data, there are going to be undetected problems that may influence results in unpredictable ways that may not be covered by the validation basis.

Several errors in MCNP and the associated nuclear data libraries have been uncovered within the last few years, and there is every reason to expect more will continue to surface. As these are uncovered, the developers address them and the codes and data improve over time, but there must be some allowance for errors that remain undetected but impact calculated results.

In trying to quantify a margin for unknowns that remain undetected in a transport code, expert judgment needs to be applied. This margin can be thought of as a "detection limit." Errors with an effect larger than this detection limit are likely to be or have been flagged and fixed, whereas errors smaller can credibly go unnoticed by either the analyst performing the calculation or the code developers.

Critical benchmarks that are used as part of the validation were also used in the development of the codes and data. This creates a dependency between the validation, the benchmarks, the codes, and the data that is difficult to quantify. Problems tend to be spotted if there is a large disagreement between calculations and benchmark results. The realistic lower bound on the 1-σ benchmark uncertainty is about 0.001 in $k_{eff}$. Practically speaking, problems do not get noticed until discrepancies are outside the 2σ or 3σ uncertainty band.

Because of the unpredictable effects of code and data errors and the random nature of the Monte Carlo calculation, they may appear in some benchmark calculations and not others or none at all. Essentially, they may escape detection in the analysis done in computing the calculational margin altogether or may be dismissed as outliers, when in actuality they can have a significant impact in specific and not necessarily obvious situations. For the code and data developers, a credible lower bound on this detection limit for errors is 3σ of the benchmark uncertainty of the highest-quality benchmarks, or 0.003. In practice for a given process, however, this detection limit may be higher. Again, the discrepancy must be large enough to have had a qualified user of the code to notice and report to the code developers.

**Based upon expert judgment of the MCNP code developers, a conservative detection limit for hidden, unpredictable errors in MCNP or other mature, widely-used, production Monte Carlo codes and the associated data libraries that can be used to ensure subcriticality past the calculational margin accounting for no other factors is <u>0.005</u>.**

This margin is predicated upon responsible use of the transport code. For codes such as MCNP that employ the power iteration to solve for $k_{eff}$, users must: heed all warnings and address potential problems or understand why they will not impact the calculation adversely, sample the starting source in all fissionable regions, ensure that the fission source distribution has converged using some diagnostic such as the Shannon entropy, run with a batch size of at least 10,000 neutrons per cycle/iteration to ensure the non-conservative bias in $k_{eff}$ is negligible, and run at least 100 active cycles/iterations after convergence to ensure the code performs sound statistical analysis of the results.

Note that the number 0.005 assumes a code that is decades old, under active development, and with thousands of users. This would not apply to a newer code, one that is no longer developed, or one that is not currently used much. In such cases, an additional margin of 0.01 or 0.02 is appropriate depending on these factors. The same applies for cross-section libraries. Those that are widely accepted by the international community (ENDF, JEFF, JENDL, etc.)

are, generally speaking, of high pedigree. Those datasets that are locally generated do not have the same level of review and testing, and a larger margin would also be required in this case.

### 6.2. Margin from Nuclear Data Library Uncertainty and Variability

LANL uses ENDF for historical and geographical reasons, i.e., the ENDF library is developed in the United States. There are, however, data libraries available developed by others, e.g., JEFF, JENDL, BROND, CENDL, etc. The development of any of these nuclear data libraries relies upon expert judgment of evaluators to decide what they feel are the best experimental data, theoretical models, and the best methods to combine them for ultimately determining the final evaluations that go into the data library. There is no technical justification to favor one set of evaluators over another, so a natural question to ask is what difference it would have made in the $k_{eff}$ results had a different nuclear data library been chosen instead of ENDF.

An approach is to find an estimate of the uncertainty in $k_{eff}$ from the nuclear data. This can be done with the same sensitivity coefficients and covariance data discussed in Sec. 3.1 via application of the "sandwich rule." The nuclear data uncertainties in $k_{eff}$ from this approach tend to be quite large, and empirically it has been observed that the 1σ normal distribution (68%) confidence interval tends to bound most of the computational biases observed in practice.

Everything being equal and assuming that most of the bias is from nuclear data uncertainties, one would expect the observed computational bias to follow standard rules of normal distributions (i.e., 68% within 1σ, 95% within 2σ, etc.). The reason that the benchmarks perform better than the raw covariance data would indicate is because the evaluators consider the integral benchmark experiments as part of producing the nuclear data evaluations. In other words, the expert judgment used to make an evaluation is constrained to be within the nuclear data uncertainties and such that the expert judgment-based adjustments do not too adversely impact critical experiment results. This introduces a dependency between the benchmark experiments and the nuclear data such that the true nuclear data covariances for this application set are smaller than the differential data alone would indicate.

The GLLS nuclear data adjustment method provides a way to find a more representative set of nuclear covariances that considers both the prior covariance data and the benchmark experiments. The details of how the GLLS nuclear data adjustment reduces the nuclear data covariances are given in Ref. 15. This adjusted covariance library can be thought of as producing the practical bounds that an evaluator can use in formulating a nuclear data evaluation using expert judgment.

This adjusted nuclear covariance library can be used with the sensitivity profiles of the processes being analyzed to get an estimate of the variability in $k_{eff}$ from using different nuclear data evaluations. The 99% confidence level is used to set this portion of the margin of subcriticality.

Note that trending the margin of subcriticality is consistent with ANSI/ANS-8.24. Section 6.4 of ANSI/ANS-8.24 states that "A single margin might not be appropriate over the entire validation applicability." This implies that trending on physical parameters is permitted.

As a side study, completely separate from the margin of subcriticality and for reference alone, Appendix B shows how $k_{eff}$ results of the LANL NCS suite discussed in Ref. 8 change when using different ENDF versions over time.

#### 6.2.1. Pu Metals

For the Pu-metal cylinders on a stainless steel floor and with water reflection, the bounding adjusted $k_{eff}$ uncertainty from the nuclear data is very small, ~0.0008, indicating that the adjustment could constrain all the relevant benchmark data in the fast Pu regime, and there is very little uncertainty incurred from using a different nuclear data

evaluation. The bounding margin of subcriticality (using a 99% confidence level or 2.6σ) from nuclear data uncertainty and variability for the Pu metals is 0.0021.

As a check, the validation was performed using the techniques in Ref. 18 where JEFF-3.1 nuclear data libraries [19] were used in place of ENDF/B-VII.1. The change in the calculational margin observed was 0.0016, which is consistent with the 0.0021 number found from the data adjustment.

For the Pu-metal sphere reflected by different materials with various thicknesses, Table VIII gives the $k_{eff}$ uncertainties (1σ) from the nuclear data. The margin of subcriticality for nuclear data uncertainty and variability (at the 99% confidence level) is 2.6 multiplied by the numbers in Table VIII.

**Table VIII. Nuclear Data Uncertainty/Variability (1σ) for Pu-Metal Sphere Reflected by Different Materials of Varied Thickness**

| Reflector Material | 2 cm | 5 cm | 10 cm | 20 cm | 30 cm |
|---|---|---|---|---|---|
| Water (H2O) | 0.00077 | 0.00079 | 0.00073 | 0.00075 | 0.00075 |
| Heavy Water (D2O) | 0.00105 | 0.00144 | 0.00182 | 0.00204 | 0.00216 |
| Polyethylene | 0.00076 | 0.00071 | 0.00070 | 0.00069 | 0.00072 |
| Borated Poly | 0.00072 | 0.00068 | 0.00066 | 0.00067 | 0.00067 |
| Lucite | 0.00068 | 0.00069 | 0.00067 | 0.00066 | 0.00064 |
| PVDF (Kynar) | 0.00165 | 0.00243 | 0.00273 | 0.00277 | 0.00274 |
| Mock HE | 0.00070 | 0.00076 | 0.00079 | 0.00076 | 0.00075 |
| BISCO | 0.00069 | 0.00064 | 0.00064 | 0.00065 | 0.00065 |
| Fire-Rated BISCO | 0.00069 | 0.00066 | 0.00064 | 0.00067 | 0.00065 |
| PVC | 0.00084 | 0.00097 | 0.00104 | 0.00103 | 0.00104 |
| Bromobenzene | 0.00097 | 0.00123 | 0.00145 | 0.00153 | 0.00155 |
| LiH | 0.00072 | 0.00072 | 0.00072 | 0.00072 | 0.00072 |
| Be Metal | 0.00068 | 0.00075 | 0.00086 | 0.00096 | 0.00112 |
| BeO | 0.00086 | 0.00105 | 0.00119 | 0.00124 | 0.00130 |
| B4C | 0.00098 | 0.00120 | 0.00121 | 0.00118 | 0.00121 |
| Graphite | 0.00068 | 0.00078 | 0.00087 | 0.00097 | 0.00099 |
| PF-5050 | 0.00190 | 0.00288 | 0.00346 | 0.00390 | 0.00398 |
| SiO2 | 0.00083 | 0.00096 | 0.00114 | 0.00125 | 0.00129 |
| Borosilicate Glass | 0.00076 | 0.00088 | 0.00099 | 0.00103 | 0.00100 |
| Vermiculite | 0.00084 | 0.00104 | 0.00114 | 0.00111 | 0.00112 |
| VAF | 0.00080 | 0.00102 | 0.00124 | 0.00131 | 0.00133 |
| Foray | 0.00082 | 0.00093 | 0.00093 | 0.00092 | 0.00093 |
| Los Alamos Concrete | 0.00073 | 0.00084 | 0.00091 | 0.00104 | 0.00099 |
| NaCl | 0.00121 | 0.00165 | 0.00209 | 0.00247 | 0.00265 |
| NaHCO3 | 0.00081 | 0.00104 | 0.00120 | 0.00123 | 0.00124 |
| MgO2 | 0.00394 | 0.00576 | 0.00662 | 0.00665 | 0.00660 |
| Al Metal | 0.00077 | 0.00083 | 0.00092 | 0.00095 | 0.00097 |
| Alumina (Al2O3) | 0.00085 | 0.00115 | 0.00132 | 0.00141 | 0.00148 |
| SS-304 | 0.00090 | 0.00111 | 0.00124 | 0.00135 | 0.00132 |
| Carbon Steel | 0.00075 | 0.00081 | 0.00084 | 0.00084 | 0.00084 |
| Inconel | 0.00096 | 0.00124 | 0.00143 | 0.00152 | 0.00150 |
| Pewter | 0.00249 | 0.00422 | 0.00574 | 0.00744 | 0.00832 |
| Copper | 0.00118 | 0.00154 | 0.00168 | 0.00152 | 0.00137 |
| Titanium | 0.00088 | 0.00110 | 0.00134 | 0.00164 | 0.00187 |
| Molybdenum | 0.00099 | 0.00138 | 0.00157 | 0.00176 | 0.00186 |
| Zirconium | 0.00271 | 0.00442 | 0.00575 | 0.00680 | 0.00713 |
| Zirconium Hydride (ZrH) | 0.00256 | 0.00384 | 0.00420 | 0.00411 | 0.00408 |
| Cadmium | 0.00404 | 0.00709 | 0.00959 | 0.01104 | 0.01065 |
| Zinc | 0.00213 | 0.00332 | 0.00420 | 0.00471 | 0.00467 |
| Vanadium | 0.00126 | 0.00172 | 0.00201 | 0.00211 | 0.00210 |
| Tantalum | 0.00967 | 0.01411 | 0.01481 | 0.01380 | 0.01375 |
| Lead | 0.00073 | 0.00074 | 0.00077 | 0.00077 | 0.00079 |
| Bismuth | 0.00089 | 0.00109 | 0.00125 | 0.00137 | 0.00141 |
| Tungsten | 0.00082 | 0.00107 | 0.00127 | 0.00140 | 0.00141 |
| Tungsten Carbide (WC) | 0.00072 | 0.00108 | 0.00139 | 0.00114 | 0.00118 |
| Thorium Metal | 0.00073 | 0.00071 | 0.00070 | 0.00067 | 0.00067 |
| Natural Uranium Metal | 0.00062 | 0.00066 | 0.00073 | 0.00077 | 0.00079 |
| LEU (3%) Metal | 0.00061 | 0.00064 | 0.00072 | 0.00077 | 0.00079 |

| | | | | | |
|---|---|---|---|---|---|
| HEU (93.1%) Metal | 0.00052 | 0.00060 | 0.00137 | 0.00288 | 0.00363 |
| U233 Metal | 0.00113 | 0.00163 | 0.00248 | 0.00374 | 0.00437 |

### 6.2.2. Pu Solutions

Figures 9 and 10 give the margin of subcriticality for the nuclear data variations of the Pu solutions or metal-water mixes as a function of EALF and Pu concentration in g/L.

For the Pu solutions (metal-water mixes), the margin of subcriticality starts higher at the dilute limit (additional margin of subcriticality of 0.006), decreases where there is a large amount of consistent benchmark data near optimal moderation, and steadily increases as the Pu becomes more concentrated. The reason for the dip near optimal moderation is because there are a relatively large number of consistent benchmarks in that physical regime and the nuclear data adjustment is therefore able to reduce the uncertainties more than in others. As the solutions become more concentrated, the data adjustment cannot perform as well because of fewer benchmarks and the presence of the Pu oxide benchmarks, which are generally considered to be not of very high quality.

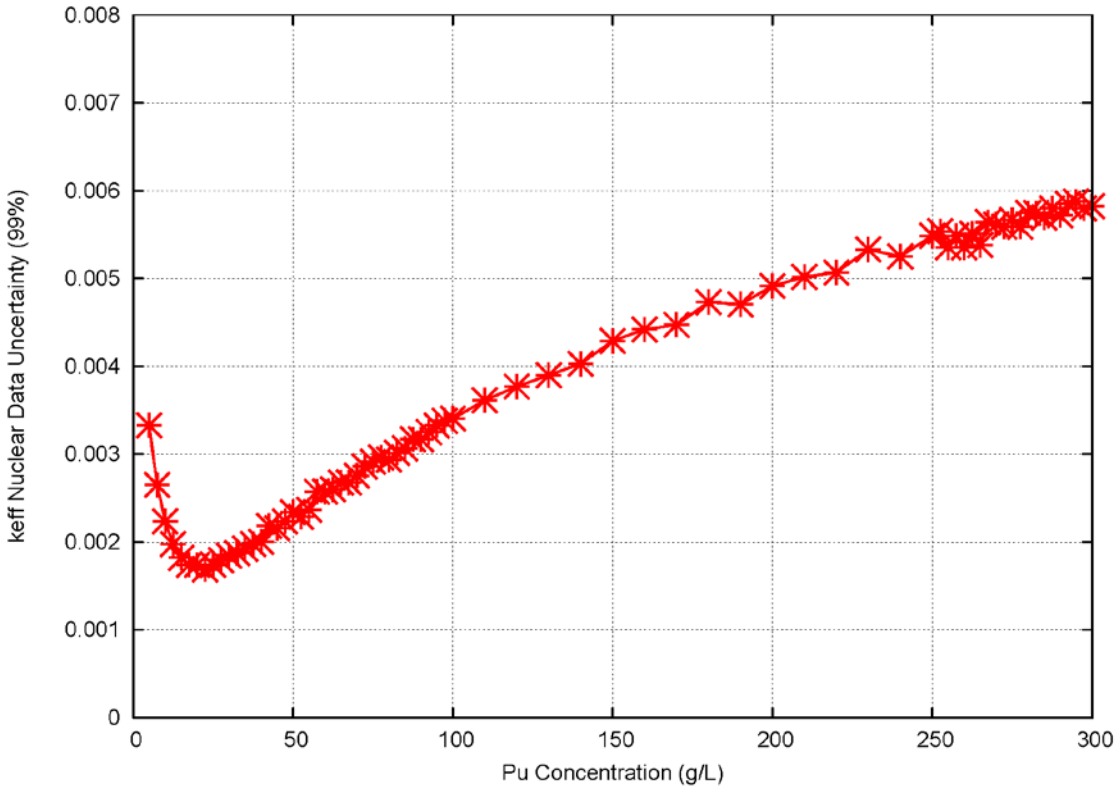


**Fig. 9. Residual uncertainty at the 99% confidence level from nuclear data in $k_{eff}$ after generalized linear least squares nuclear data adjustment for Pu solution/metal-water mix systems as a function of Pu solution concentration in g/L.**

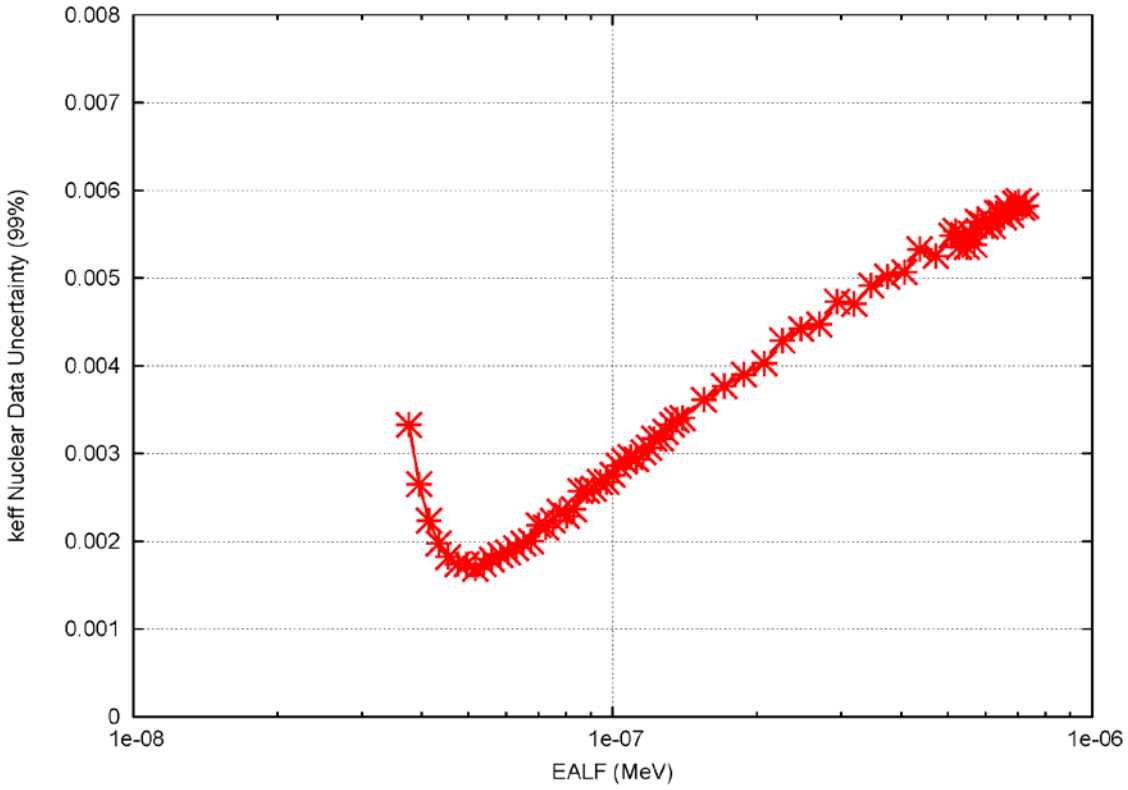


**Fig. 10. Residual uncertainty at the 99% confidence level from nuclear data in $k_{eff}$ after generalized linear least squares nuclear data adjustment for Pu solution/metal-water mix systems as a function of Energy of Average Lethargy causing Fission (EALF).**

### 6.2.3. Pu Oxides

Figure 11 gives the margin of subcriticality for the nuclear data variations of the Pu oxides as a function of EALF.

The Pu oxide margin of subcriticality is lower for the dry limits where the system is fast and, as seen from the metals, can be adjusted to fit the data well. Likewise, similar trends for the thermal spectrum cases are observed for the solutions. The intermediate-spectrum or very dilute oxide cases have a large nuclear data uncertainty (additional margin of subcriticality of 0.006) because of the lack of good quality, consistent Pu intermediate benchmarks.

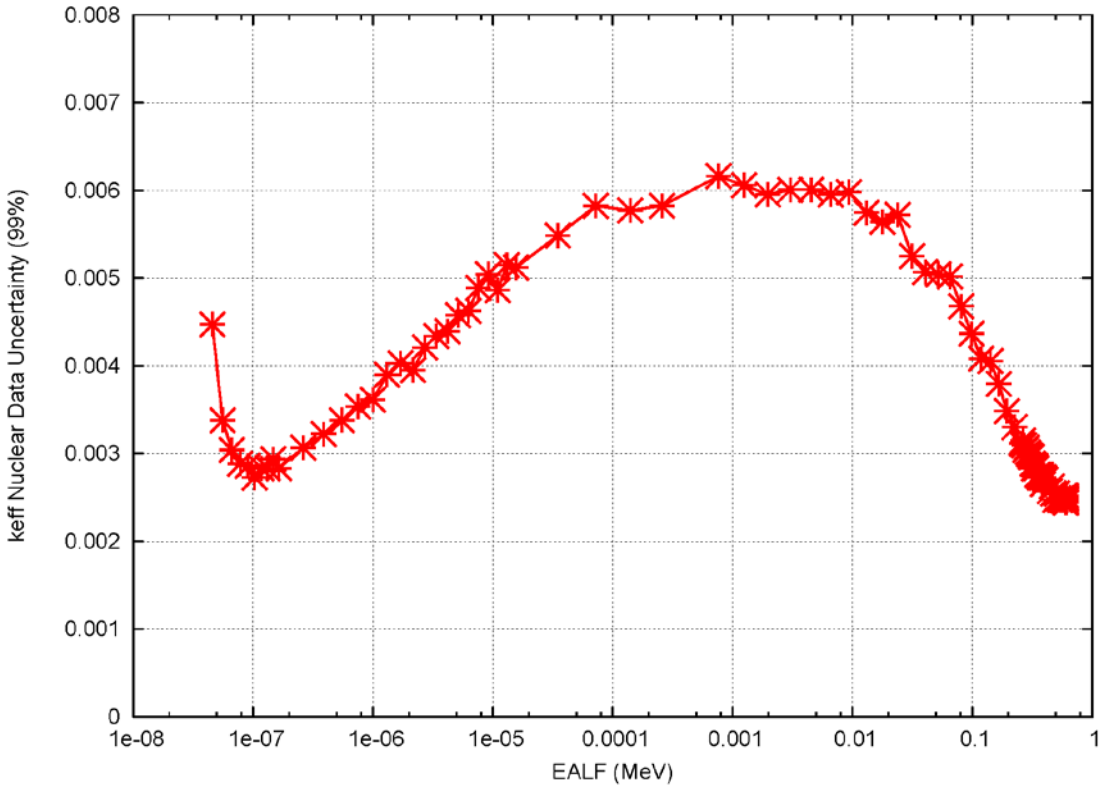


**Fig. 11. Residual uncertainty at the 99% confidence level from nuclear data in $k_{eff}$ after generalized linear least squares nuclear data adjustment for Pu oxide/oxide-water mix systems as a function of Energy of Average Lethargy causing Fission (EALF).**

### 6.3. Sensitivity to Process Conditions and Area of Applicability

In performing the evaluation using transport software, it is important to study the parameter space through numerous computational models (e.g., different mass loadings, solution concentrations, reflection thicknesses, etc.). It is not only important to understand how $k_{eff}$ varies as a function of these conditions, but to understand how the predictive capability of $k_{eff}$ does as well, and consequently, the USL. The behavior of $k_{eff}$ can often be assessed with physical arguments, whereas the behavior of the USL is not always obvious.

In order for the results of a bounding computational model to be considered subcritical, the computed $k_{eff}$ must be less than the USL for the AOA that the computational models lie within. A conservative approach is to adopt the lowest USL for all such computational models, but parameterization of the USL based upon physical properties is permitted if operationally required. The concern is that the analyst be aware of any abrupt changes in the USL as a result of changes in process conditions, such as those observed in the Pu-oxide models (see Sec. 7.3).

This validation report uses certain representative models (described in Sec. 4) for determining the USL values of the different classes of problems that are typical of the models developed for nuclear criticality safety analysis. It is the responsibility of the analyst to ensure that the model being simulated is neutronically similar to those used in the

validation. If the process models differ significantly from those, then the analyst should perform sensitivity studies to ensure that the deviations do not have a significant effect on $k_{eff}$, and if the deviations do, then the analyst should either conservatively substitute materials for those in the validation to make the process model look more like those in this validation or perform a new validation study to determine the USL for those model configurations.

### 6.4. Additional Discussion

To conclude this discussion, recall that **$k_{eff}$ in a transport calculation is purely a non-physical, mathematical quantity** that adjusts the fission multiplication to provide balance between gains and losses. **It does not, by itself, relate to the safety of a process.** Other facilities often prescribe an administrative margin such as 0.02 or greater to be applied as a minimum margin of subcriticality. While this may be appropriate at some facilities considering their processes, the application of such arbitrary margins for the wide variety of processes at LANL may not be in the best interests of criticality safety. **Such ad hoc margins without due consideration for the physics and uncertainties about process conditions are meaningless at best, and, at worst, may even create a false sense of safety.**

When determining what margin of subcriticality is appropriate, it is important to consider the many coupled factors related to the entire operational organization: conduct of operations, material controls and accountability, fidelity of computational resources and data, built-in conservatisms to the model, etc. **The decision for a margin of subcriticality must be made holistically and the analysts should always ask themselves if they would be comfortable being present during those process conditions using their analysis when deciding a margin of subcriticality.**

## 7. Upper Subcritical Limit

The USL is determined by

$$\text{USL} = 1.0 - \text{Calculational Margin} - \text{Margin of Subcriticality}.$$

The USL determines the value of $k_{eff}$ where the analyst can treat the calculated $k_{eff}$ as being subcritical. Each class of problems is discussed separately.

**None of these values consider other process uncertainties and conservatisms, and the value here must be adjusted as appropriate for the system being analyzed to ensure subcriticality.**

### 7.1. Pu Metals

A USL is first given for the case of the three Pu-metal cylinders on a stainless steel floor and with water reflection. Next, a set of values is given for the Pu spheres surrounded by various reflectors of different thicknesses. The former USL represents the upper limit or “best case” that applies to bare Pu metal or models that are similar to the Pu-metal model (three Pu-metal cylinders on a stainless steel floor and with water reflection). When there is significant reflection, the lower USLs in the reflection study should be used.

The bounding calculational margin is 0.0127. The bounding margin of subcriticality from nuclear data variability is 0.0021. The additional margin of subcriticality for transport and data processing software is 0.005.

**The USL for Pu-metal systems is <u>0.980</u>.**

In using this USL, the analyst should check that the EALF is 790 keV or greater. Extrapolation is permitted for systems with an EALF of 400 keV based upon the USLs set for the Pu oxide systems. If the EALF falls below 400 keV, a significantly lower USL may be required based upon the oxide limits that consider intermediate spectra.

Table IX gives the USLs for the Pu-metal sphere reflected by different materials at varied thicknesses. These are always 0.980 or lower (i.e., less than or equal to the USL for the Pu-metal system). Typically, the 2-cm value is appropriate for thin reflectors or where the reflection is partial and not the dominant neutronic property of the model. For thick reflectors, the 30-cm value may be used as it is always bounding.

The reflector study provides a USL that is consistent with the one obtained for the other Pu-metal model considered, the cylinders on a stainless steel floor and with water reflection. Using the 2-cm thickness values for water and SS-304 is appropriate because the reflection by both materials is thin and partial. The USL obtained using either approach is 0.980.

**Table IX. Upper Subcritical Limits for Pu-Metal Sphere Reflected by Different Materials of Varied Thickness**

| Reflector Material | 2 cm | 5 cm | 10 cm | 20 cm | 30 cm |
|---|---|---|---|---|---|
| Water (H2O) | 0.980 | 0.980 | 0.980 | 0.980 | 0.980 |
| Heavy Water (D2O) | 0.979 | 0.978 | 0.977 | 0.976 | 0.976 |
| Polyethylene | 0.980 | 0.980 | 0.980 | 0.980 | 0.980 |
| Borated Polyethylene | 0.980 | 0.980 | 0.980 | 0.980 | 0.980 |
| Lucite | 0.980 | 0.980 | 0.980 | 0.980 | 0.980 |
| PVDF (Kynar) | 0.977 | 0.975 | 0.975 | 0.975 | 0.975 |
| Mock HE | 0.980 | 0.980 | 0.980 | 0.980 | 0.980 |
| BISCO | 0.980 | 0.980 | 0.980 | 0.980 | 0.980 |
| Fire-Rated BISCO | 0.980 | 0.980 | 0.980 | 0.980 | 0.980 |
| PVC | 0.980 | 0.979 | 0.979 | 0.979 | 0.979 |
| Bromobenzene | 0.979 | 0.979 | 0.978 | 0.978 | 0.978 |
| LiH | 0.980 | 0.980 | 0.980 | 0.980 | 0.980 |
| Be Metal | 0.980 | 0.980 | 0.980 | 0.980 | 0.979 |
| BeO | 0.979 | 0.979 | 0.979 | 0.978 | 0.978 |
| B4C | 0.979 | 0.979 | 0.979 | 0.979 | 0.979 |
| Graphite | 0.980 | 0.980 | 0.979 | 0.979 | 0.979 |
| PF-5050 | 0.977 | 0.974 | 0.973 | 0.971 | 0.971 |
| SiO2 | 0.979 | 0.979 | 0.979 | 0.978 | 0.978 |
| Borosilicate Glass | 0.980 | 0.979 | 0.979 | 0.979 | 0.979 |
| Vermiculite | 0.979 | 0.979 | 0.979 | 0.979 | 0.979 |
| VAF | 0.980 | 0.979 | 0.978 | 0.978 | 0.978 |
| Foray | 0.980 | 0.979 | 0.979 | 0.979 | 0.979 |
| Los Alamos Concrete | 0.980 | 0.979 | 0.979 | 0.979 | 0.979 |
| NaCl | 0.979 | 0.977 | 0.976 | 0.975 | 0.975 |
| NaHCO3 | 0.980 | 0.979 | 0.978 | 0.978 | 0.978 |
| MgO2 | 0.971 | 0.966 | 0.964 | 0.964 | 0.964 |
| Al Metal | 0.980 | 0.980 | 0.979 | 0.979 | 0.979 |
| Alumina (Al2O3) | 0.979 | 0.979 | 0.978 | 0.978 | 0.978 |
| SS-304 | 0.980 | 0.979 | 0.979 | 0.978 | 0.978 |
| Carbon Steel | 0.980 | 0.980 | 0.980 | 0.980 | 0.980 |
| Inconel | 0.979 | 0.979 | 0.978 | 0.978 | 0.978 |
| Pewter | 0.975 | 0.971 | 0.967 | 0.962 | 0.960 |
| Copper | 0.976 | 0.973 | 0.973 | 0.973 | 0.973 |
| Titanium | 0.979 | 0.979 | 0.978 | 0.977 | 0.977 |
| Molybdenum | 0.979 | 0.976 | 0.975 | 0.974 | 0.974 |
| Zirconium | 0.974 | 0.969 | 0.964 | 0.960 | 0.959 |
| Zirconium Hydride (ZrH) | 0.975 | 0.971 | 0.968 | 0.968 | 0.968 |
| Cadmium | 0.971 | 0.963 | 0.956 | 0.952 | 0.952 |
| Zinc | 0.976 | 0.973 | 0.971 | 0.969 | 0.969 |
| Vanadium | 0.978 | 0.977 | 0.976 | 0.976 | 0.976 |
| Tantalum | 0.953 | 0.932 | 0.929 | 0.929 | 0.929 |
| Lead | 0.980 | 0.980 | 0.980 | 0.980 | 0.980 |
| Bismuth | 0.979 | 0.979 | 0.979 | 0.978 | 0.978 |
| Tungsten | 0.978 | 0.977 | 0.976 | 0.976 | 0.976 |

| | | | | | |
|---|---|---|---|---|---|
| Tungsten Carbide (WC) | 0.980 | 0.977 | 0.976 | 0.976 | 0.976 |
| Thorium Metal | 0.980 | 0.980 | 0.980 | 0.980 | 0.980 |
| Natural Uranium Metal | 0.980 | 0.980 | 0.980 | 0.980 | 0.980 |
| LEU (3%) Metal | 0.980 | 0.980 | 0.980 | 0.980 | 0.980 |
| HEU (93.1%) Metal | 0.980 | 0.980 | 0.980 | 0.975 | 0.973 |
| U233 Metal | 0.979 | 0.974 | 0.960 | 0.944 | 0.939 |

### 7.2. Pu Solutions

Figures 12 and 13 give curves for the computed USL of Pu metal-water mixes as a function of Pu concentration and EALF. A conservative USL is selected that is bounding over the entire range from 5 to 300 g/L and 0.038 to 0.73 eV. The additional margin of subcriticality for transport and data processing software is 0.0050.

**The USL for Pu-solution systems is <u>0.973</u>.**

Use of this USL assumes the case being analyzed falls within this region in both Pu concentration and EALF. Extrapolation is permitted, but additional margin or supporting analysis is required.

A higher USL is permitted to be used for specific Pu concentrations and EALF within this range as both operationally necessary and supported by the calculated trending curves for EALF and Pu concentration in Figs. 12 and 13, using the most conservative value.

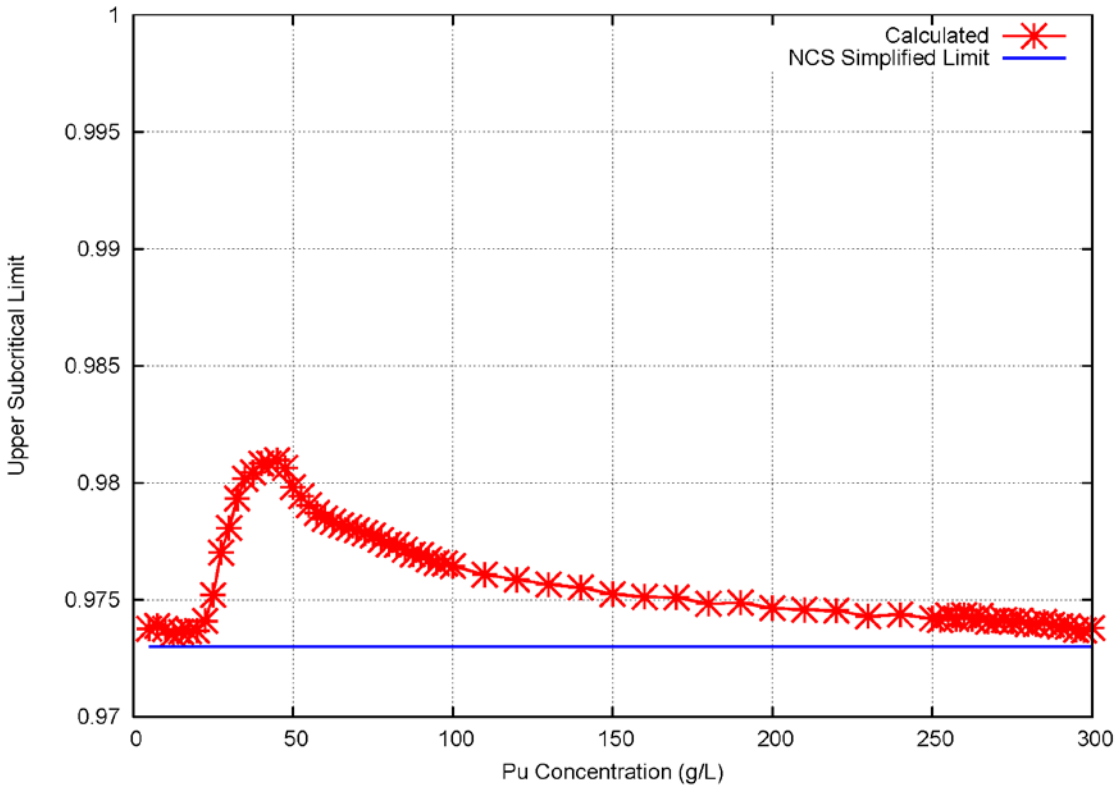


**Fig. 12. Upper subcritical limit (USL) for Pu solution/metal-water mix systems as a function of Pu solution concentration in g/L. The USL in the blue curve represents the simple conservative bounding limit to be normally used by the NCS division. The USL in the red curve is permitted to be used if operationally necessary and it is the most conservative of both the Pu concentration and Energy Average Lethargy causing Fission (EALF).**

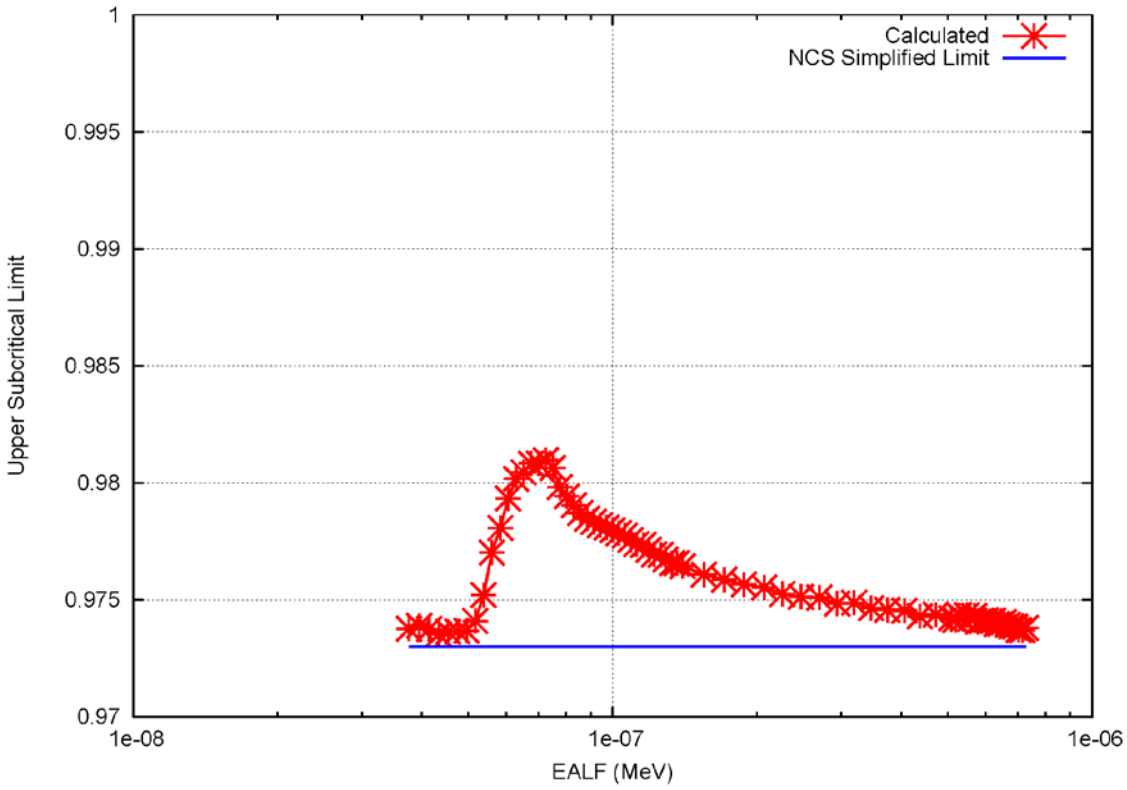


**Fig. 13. Upper subcritical limit (USL) for Pu solution/metal-water mix systems as a function of Energy Average Lethargy causing Fission (EALF). The USL in the blue curve represents the simple conservative bounding limit to be normally used by the NCS division. The USL in the red curve is permitted to be used if operationally necessary and it is the most conservative of both the Pu concentration and Energy Average Lethargy causing Fission (EALF).**

### 7.3. Pu Oxides

The Pu oxides have the most complicated USL behavior, and the USL is broken down by spectrum because of the abrupt changes. Figure 14 gives the curve for the USL (calculated in red, the simplified model to be used by NCS in blue) of the Pu oxide-water mixes as a function of EALF.

USLs are set to be conservatively bounding for each regime. For the fast regime, the USL is lower than for the metals because of a higher uncertainty from nuclear cross sections for the oxides, and an extra margin of 0.002 bounds the deviation of using oxides versus metals. A conservatively bounding additional margin of 0.003 is applied to the thermal oxide-water mixes for the same reason. The additional margin of subcriticality for transport and data processing software is 0.005.

**The USL for Pu-oxide systems with an EALF > 400 keV is 0.978;**
**the USL for Pu-oxide systems with an EALF < 0.3 eV is 0.970;**
**and the USL for Pu-oxide systems with 0.3 eV < EALF < 400 keV is 0.953.**

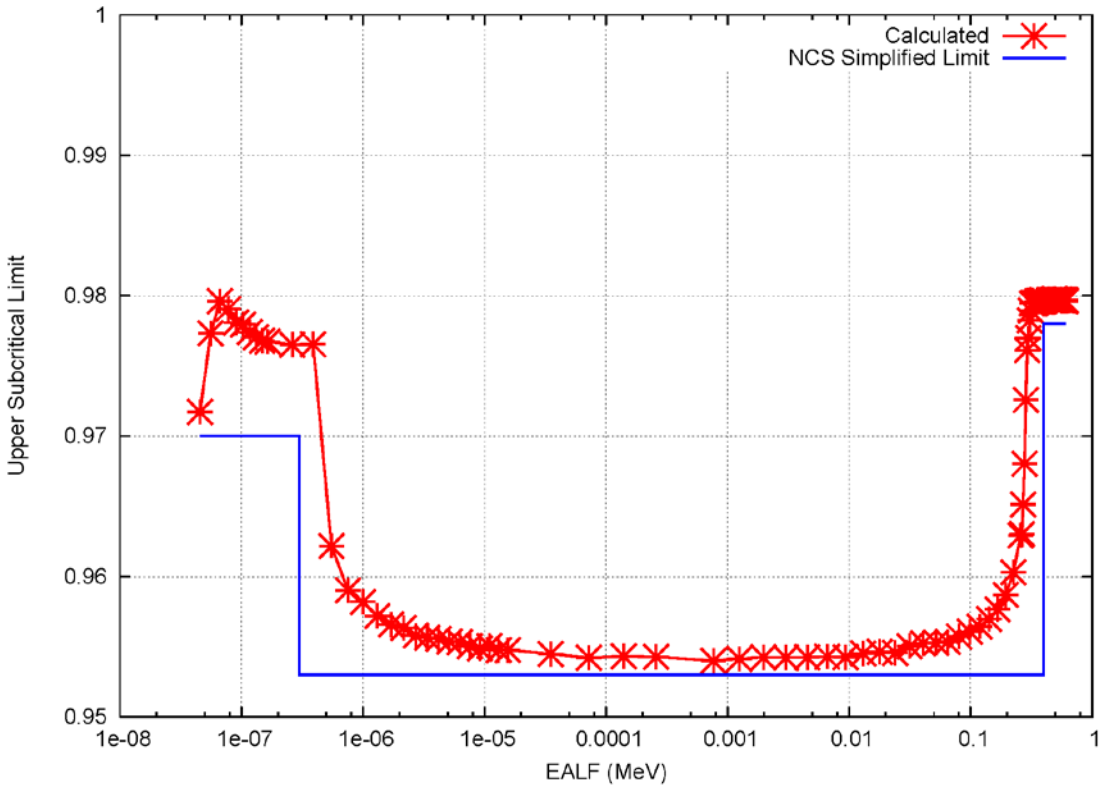


**Fig. 14. Upper subcritical limit (USL) for Pu oxide/oxide-water mix systems as a function of Energy Average Lethargy causing Fission (EALF). The USL in the blue curve represents the simple conservative bounding limit to be normally used by the NCS division. The USL in the red curve is permitted to be used if operationally necessary.**

### 7.4. Combinations of Pu Metals, Oxides, and/or Solutions

Cases where there is more than one class of Pu system (e.g., a system with metal and solution) normally require using the most conservative USL. This bounds the appropriate limit, which is given by the region where most of the fission occurs.

The analyst may use the less conservative USL if it can be shown computationally that one of the classes of problems dominate the $k_{eff}$ calculation (> 90% of the fission in that particular class).

Alternatively, as with any other case, the NCS analyst may use the validation tools used in this validation to set an appropriate limit.

### 7.5. Extensions to Other Systems

The AOA of this validation is defined by the application models discussed in Sec. 4, which are representative of the metals, solutions, and oxides in configurations typically modeled for nuclear criticality safety. Extensions of the

AOA are permitted, but it is the responsibility of the analyst to ensure that the extension to the AOA does not have a significant impact on the predictive capability of the validated code and data (MCNP6.1 with ENDF/B-VII.1).

In any case, the method and computational tools may be used by the NCS analyst to help guide the setting of appropriate USLs. This is the preferred approach for an unknown system, as it should give a not-overly conservative USL.

In the case where all benchmarks in the suite post rejection are considered with unit weight in the EVT analysis, the resulting calculational margin is 0.049. As for the margin of subcriticality, 0.015 is the observed bounding 1σ nuclear data uncertainty after the GLLS adjustment, giving a margin of 0.039 for the effect from nuclear data variability, and 0.005 is still acceptable for the undetected errors in transport codes and data processing. These margins lead to a conservative **USL of 0.907**.

This conservative, bounding USL may be used provided there is an overlap of the neutronically significant properties of the application model and at least one of the benchmark models in the suite. To use this number, the NCS analyst should identify which benchmarks are relevant.

**8. Compliance with ANS-8.24**

Appendix C gives a matrix explaining how this validation meets the applicable requirements outlined in ANS-8.24.

**References**

[1] American National Standard ANSI/ANS-8.24-2007.

[2] J.T. Goorley et al., "Initial MCNP6 Release Overview - MCNP6 version 1.0," LA-UR-13-22934, Los Alamos National Laboratory Report (2013).

[3] F.B. Brown, B.C. Kiedrowski, J.S. Bull, "Verification of MCNP5-1.60 and MCNP6.1 for Criticality Safety Applications," LA-UR-13-22196, Los Alamos National Laboratory Report (2013).

[4] M.B. Chadwick et. al. "ENDF/B-VII.1: Nuclear Data for Science and Technology: Cross Sections, Covariances, Fission Product Yields and Decay Data," *Nucl. Data Sheets*, **112,** 2887 (2011).

[5] J.L. Conlin et al., "Continuous Energy Neutron Cross Section Data Tables Based upon ENDF/B-VII.1," LA-UR-13-20137, Los Alamos National Laboratory Report (2013).

[6] A. Sood, R.A. Forster, D.K. Parsons, "Analytical Benchmark Test Set for Criticality Code Verification," *Prog. Nucl. Enrgy.*, **42**, 55-106 (2003).

[7] NEA Nuclear Science Committee, "International Handbook of Evaluated Criticality Safety Benchmark Experiments," NEA/NSC/DOC(95)03 (2012).

[8] R.J. Kamm, "Validation of MCNP5 on the Ganglion Cyst Computer Cluster with Various Cross Section Libraries," NCS-TECH-007-002, Los Alamos National Laboratory Internal Report (2007).

[9] R.D. Mosteller, "An Expanded Criticality Validation Suite for MCNP," LA-UR-10-06230, Rev3, Los Alamos National Laboratory Report (2010).

[10] A.C. Kahler et. al., "ENDF/B-VII.1 Neutron Cross Section Data Testing with Critical Assembly Benchmark and Reactor Experiments," *Nucl. Data Sheets*, **112**, 2997 (2011).

[11] J.C. Dean, R.W. Tayloe, Jr., "Guide for Validation of Nuclear Criticality Safety Calculational Methodology," NUREG/CR-6698, U.S. Nuclear Regulatory Commission Report (2001).

[12] B.L. Broadhead, et. al., "Sensitivity- and Uncertainty-Based Criticality Safety Validation Techniques," *Nucl. Sci. Eng.*, **146**, 340-366 (2004).

[13] B.C. Kiedrowski, "Methodology for Sensitivity and Uncertainty-Based Criticality Safety Validation," LA-UR-14-23202, Los Alamos National Laboratory Report (2014).

[14] B.C. Kiedrowski, F.B. Brown, "Adjoint-Based k-Eigenvalue Sensitivity Coefficients to Nuclear Data Using Continuous-Energy Monte Carlo," *Nucl. Sci. Eng.*, **174**, 227-244 (2013).

[15] B. L. Broadhead, "SCALE 5.1 Cross-Section Covariance Libraries," (ORNL/TM-2005/39, Version 5.1, Vol. I, Book 3, Sect. M19).

[16] "Database for the International Criticality Safety Benchmark Evaluation Project (DICE)," OECD/NEA, https://www.oecd-nea.org/science/wpncs/icsbep/dice.html (accessed Apr. 18, 2014).

[17] K.D. Kimball, E.F. Trumble, "Statistical Methods for Accurately Determining Criticality Code Bias," *Proc. Topl. Mtg. Criticality Safety Challenges in the Next Decade*, Chelan, Washington, Sep. 7-11 (1997).

[18] B.C. Kiedrowski et. al., "Validation of MCNP6.1 for Criticality Safety of Fast-Spectrum Pu-Metal Systems, Bare and Reflected by Water and/or Steel," XCP-DO:14-008, Los Alamos National Laboratory Internal Report (2014).

[19] OECD/NEA Data Bank, "The JEFF-3.1 Nuclear Data Library," JEFF Report 21, OECD/NEA Data Bank (2006).

**Appendix A: Full List of Benchmarks** (Rejected benchmarks are colored **red**; estimated uncertainties are colored **blue**)

| | Benchmark | | Calculated | | Bias | | EALF |
|---|---|---|---|---|---|---|---|
| Benchmark | keff | Unc. | keff | Unc. | keff | Unc | (MeV) |
| heu-comp-inter-003-006 | 1.00000 | 0.00470 | 0.99558 | 0.00011 | 0.00442 | 0.00470 | 5.43E-03 |
| heu-comp-therm-002-001 | 1.00110 | 0.00690 | 1.01150 | 0.00013 | -0.01040 | 0.00690 | 1.35E-07 |
| heu-comp-therm-002-002 | 1.00110 | 0.00690 | 1.01385 | 0.00013 | -0.01275 | 0.00690 | 9.69E-08 |
| heu-comp-therm-002-003 | 1.00110 | 0.00690 | 1.01666 | 0.00012 | -0.01556 | 0.00690 | 8.00E-08 |
| heu-comp-therm-002-004 | 1.00110 | 0.00690 | 1.01599 | 0.00012 | -0.01489 | 0.00690 | 7.08E-08 |
| heu-comp-therm-002-005 | 1.00110 | 0.00690 | 1.01700 | 0.00013 | -0.01590 | 0.00690 | 6.48E-08 |
| heu-comp-therm-002-006 | 1.00110 | 0.00690 | 1.01718 | 0.00011 | -0.01608 | 0.00690 | 6.07E-08 |
| heu-comp-therm-002-007 | 1.00110 | 0.00690 | 1.01738 | 0.00011 | -0.01628 | 0.00690 | 5.75E-08 |
| heu-comp-therm-002-008 | 1.00110 | 0.00690 | 1.01748 | 0.00011 | -0.01638 | 0.00690 | 5.54E-08 |
| heu-comp-therm-002-009 | 1.00110 | 0.00690 | 1.01882 | 0.00010 | -0.01772 | 0.00690 | 5.35E-08 |
| heu-comp-therm-002-010 | 1.00110 | 0.00690 | 1.01562 | 0.00010 | -0.01452 | 0.00690 | 5.20E-08 |
| heu-comp-therm-002-011 | 1.00110 | 0.00530 | 1.01446 | 0.00013 | -0.01336 | 0.00530 | 1.01E-07 |
| heu-comp-therm-002-012 | 1.00110 | 0.00550 | 1.01370 | 0.00012 | -0.01260 | 0.00550 | 7.01E-08 |
| **heu-comp-therm-002-013** | **1.00110** | **0.00550** | **1.01791** | **0.00012** | **-0.01681** | **0.00550** | **6.43E-08** |
| heu-comp-therm-002-014 | 1.00110 | 0.00550 | 1.01767 | 0.00011 | -0.01657 | 0.00550 | 5.99E-08 |
| **heu-comp-therm-002-015** | **1.00110** | **0.00550** | **1.01916** | **0.00011** | **-0.01806** | **0.00550** | **5.69E-08** |
| **heu-comp-therm-002-016** | **1.00110** | **0.00530** | **1.01879** | **0.00010** | **-0.01769** | **0.00530** | **5.29E-08** |
| **heu-comp-therm-002-017** | **1.00110** | **0.00530** | **1.02344** | **0.00010** | **-0.02234** | **0.00530** | **5.14E-08** |
| **heu-comp-therm-002-018** | **1.00200** | **0.00430** | **1.01569** | **0.00013** | **-0.01369** | **0.00430** | **1.15E-07** |
| heu-comp-therm-002-019 | 1.00200 | 0.00430 | 1.01291 | 0.00012 | -0.01091 | 0.00430 | 7.50E-08 |
| **heu-comp-therm-002-020** | **1.00200** | **0.00430** | **1.01552** | **0.00011** | **-0.01352** | **0.00430** | **6.19E-08** |
| **heu-comp-therm-002-021** | **1.00200** | **0.00430** | **1.01677** | **0.00012** | **-0.01477** | **0.00430** | **5.72E-08** |
| **heu-comp-therm-002-022** | **1.00200** | **0.00430** | **1.01724** | **0.00011** | **-0.01524** | **0.00430** | **5.25E-08** |
| heu-comp-therm-002-023 | 1.00080 | 0.00850 | 1.01438 | 0.00012 | -0.01358 | 0.00850 | 7.89E-08 |
| heu-comp-therm-002-024 | 1.00080 | 0.00850 | 1.01501 | 0.00012 | -0.01421 | 0.00850 | 6.38E-08 |
| heu-comp-therm-002-025 | 1.00080 | 0.00850 | 1.01358 | 0.00012 | -0.01278 | 0.00850 | 5.87E-08 |
| heu-met-fast-001-001 | 1.00000 | 0.00100 | 1.00000 | 0.00008 | 0.00000 | 0.00100 | 8.20E-01 |
| heu-met-fast-002-001 | 1.00000 | 0.00300 | 1.00150 | 0.00009 | -0.00150 | 0.00300 | 7.38E-01 |
| heu-met-fast-002-002 | 1.00000 | 0.00300 | 1.00193 | 0.00009 | -0.00193 | 0.00300 | 7.28E-01 |
| heu-met-fast-002-003 | 1.00000 | 0.00300 | 1.00037 | 0.00009 | -0.00037 | 0.00300 | 7.22E-01 |
| heu-met-fast-002-004 | 1.00000 | 0.00300 | 0.99946 | 0.00009 | 0.00054 | 0.00300 | 7.13E-01 |
| heu-met-fast-002-005 | 1.00000 | 0.00300 | 1.00000 | 0.00009 | 0.00000 | 0.00300 | 7.09E-01 |
| heu-met-fast-002-006 | 1.00000 | 0.00300 | 1.00129 | 0.00009 | -0.00129 | 0.00300 | 7.15E-01 |
| heu-met-fast-003-001 | 1.00000 | 0.00500 | 0.99492 | 0.00009 | 0.00508 | 0.00500 | 7.87E-01 |
| heu-met-fast-003-002 | 1.00000 | 0.00500 | 0.99434 | 0.00009 | 0.00566 | 0.00500 | 7.80E-01 |
| heu-met-fast-003-003 | 1.00000 | 0.00500 | 0.99916 | 0.00009 | 0.00084 | 0.00500 | 7.70E-01 |
| heu-met-fast-003-004 | 1.00000 | 0.00300 | 0.99718 | 0.00009 | 0.00282 | 0.00300 | 7.63E-01 |
| heu-met-fast-003-005 | 1.00000 | 0.00300 | 1.00158 | 0.00009 | -0.00158 | 0.00300 | 7.45E-01 |
| heu-met-fast-003-006 | 1.00000 | 0.00300 | 1.00150 | 0.00009 | -0.00150 | 0.00300 | 7.38E-01 |
| heu-met-fast-003-007 | 1.00000 | 0.00300 | 1.00199 | 0.00009 | -0.00199 | 0.00300 | 7.20E-01 |
| heu-met-fast-003-008 | 1.00000 | 0.00500 | 1.00220 | 0.00009 | -0.00220 | 0.00500 | 6.38E-01 |
| heu-met-fast-003-009 | 1.00000 | 0.00500 | 1.00267 | 0.00009 | -0.00267 | 0.00500 | 5.79E-01 |
| heu-met-fast-003-010 | 1.00000 | 0.00500 | 1.00491 | 0.00009 | -0.00491 | 0.00500 | 5.31E-01 |
| heu-met-fast-003-011 | 1.00000 | 0.00500 | 1.00875 | 0.00009 | -0.00875 | 0.00500 | 5.14E-01 |
| heu-met-fast-003-012 | 1.00000 | 0.00300 | 1.00864 | 0.00009 | -0.00864 | 0.00300 | 6.48E-01 |
| heu-met-fast-004-001 | 0.99850 | **0.00300** | 0.99406 | 0.00011 | 0.00444 | 0.00011 | 2.60E-02 |
| heu-met-fast-005-001 | 1.00000 | 0.00360 | 0.99510 | 0.00009 | 0.00490 | 0.00360 | 5.88E-01 |
| heu-met-fast-005-002 | 1.00070 | 0.00360 | 0.99795 | 0.00010 | 0.00275 | 0.00360 | 3.84E-01 |
| heu-met-fast-005-003 | 0.99960 | 0.00360 | 1.00046 | 0.00010 | -0.00086 | 0.00360 | 2.37E-01 |
| heu-met-fast-005-004 | 0.99890 | 0.00360 | 0.99438 | 0.00011 | 0.00452 | 0.00360 | 1.72E-01 |
| heu-met-fast-005-005 | 0.99800 | 0.00360 | 0.99909 | 0.00010 | -0.00109 | 0.00360 | 2.98E-01 |
| heu-met-fast-005-006 | 0.99870 | 0.00360 | 0.99792 | 0.00009 | 0.00078 | 0.00360 | 4.05E-01 |
| heu-met-fast-007-001 | 0.99500 | 0.00240 | 0.99245 | 0.00009 | 0.00255 | 0.00240 | 8.32E-01 |
| heu-met-fast-007-002 | 0.99640 | 0.00140 | 0.99832 | 0.00009 | -0.00192 | 0.00140 | 4.45E-01 |
| heu-met-fast-007-003 | 0.99900 | 0.00130 | 0.99976 | 0.00010 | -0.00076 | 0.00130 | 3.34E-01 |
| heu-met-fast-007-004 | 0.99480 | 0.00130 | 0.99766 | 0.00010 | -0.00286 | 0.00130 | 2.96E-01 |
| heu-met-fast-007-005 | 0.99780 | 0.00180 | 0.99971 | 0.00010 | -0.00191 | 0.00180 | 2.25E-01 |
| **heu-met-fast-007-006** | **1.00060** | **0.00130** | **1.00560** | **0.00009** | **-0.00500** | **0.00130** | **1.42E-01** |
| heu-met-fast-007-007 | 0.99740 | 0.00140 | 1.00118 | 0.00010 | -0.00378 | 0.00140 | 1.75E-01 |
| heu-met-fast-007-008 | 0.99730 | 0.00130 | 0.99925 | 0.00010 | -0.00195 | 0.00130 | 1.82E-01 |
| heu-met-fast-007-009 | 0.99950 | 0.00560 | 1.00209 | 0.00010 | -0.00259 | 0.00560 | 1.59E-01 |
| heu-met-fast-007-010 | 0.99810 | 0.00120 | 0.99901 | 0.00011 | -0.00091 | 0.00121 | 2.33E-02 |
| heu-met-fast-007-011 | 0.99580 | 0.00130 | 0.99725 | 0.00011 | -0.00145 | 0.00130 | 4.98E-03 |
| heu-met-fast-007-012 | 0.99320 | 0.00120 | 0.99280 | 0.00012 | 0.00040 | 0.00121 | 3.68E-03 |
| heu-met-fast-007-013 | 0.99900 | 0.00120 | 1.00088 | 0.00013 | -0.00188 | 0.00121 | 2.24E-03 |

| | | | | | | | |
|---|---|---|---|---|---|---|---|
| heu-met-fast-007-014 | 0.99640 | 0.00120 | 0.99703 | 0.00012 | -0.00063 | 0.00121 | 3.38E-03 |
| heu-met-fast-007-015 | 0.99590 | 0.00120 | 0.99671 | 0.00012 | -0.00081 | 0.00121 | 2.49E-03 |
| heu-met-fast-007-016 | 0.99690 | 0.00120 | 0.99723 | 0.00012 | -0.00033 | 0.00121 | 2.45E-03 |
| heu-met-fast-007-017 | 0.99530 | 0.00120 | 0.99584 | 0.00013 | -0.00054 | 0.00121 | 3.42E-04 |
| heu-met-fast-007-018 | 0.99720 | 0.00120 | 0.99818 | 0.00013 | -0.00098 | 0.00121 | 3.25E-04 |
| heu-met-fast-007-019 | 0.99560 | 0.00150 | 0.99614 | 0.00009 | -0.00054 | 0.00150 | 8.26E-01 |
| heu-met-fast-007-020 | 0.99500 | 0.00170 | 0.99776 | 0.00010 | -0.00276 | 0.00170 | 1.89E-01 |
| heu-met-fast-007-021 | 0.99560 | 0.00180 | 0.99845 | 0.00010 | -0.00285 | 0.00180 | 1.74E-01 |
| heu-met-fast-007-022 | 0.99630 | 0.00190 | 0.99926 | 0.00011 | -0.00296 | 0.00190 | 1.60E-01 |
| heu-met-fast-007-023 | 0.99620 | 0.00170 | 0.99902 | 0.00010 | -0.00282 | 0.00170 | 5.43E-02 |
| heu-met-fast-007-024 | 0.99700 | 0.00180 | 0.99954 | 0.00011 | -0.00254 | 0.00180 | 5.07E-02 |
| heu-met-fast-007-025 | 0.99590 | 0.00180 | 0.99811 | 0.00011 | -0.00221 | 0.00180 | 2.30E-02 |
| heu-met-fast-007-026 | 0.99660 | 0.00170 | 0.99837 | 0.00012 | -0.00177 | 0.00170 | 2.14E-02 |
| heu-met-fast-007-027 | 0.99480 | 0.00140 | 0.99673 | 0.00010 | -0.00193 | 0.00140 | 4.18E-01 |
| heu-met-fast-007-028 | 0.99700 | 0.00230 | 0.99804 | 0.00010 | -0.00104 | 0.00230 | 2.47E-01 |
| heu-met-fast-007-029 | 0.99610 | 0.00140 | 0.99865 | 0.00011 | -0.00255 | 0.00140 | 1.44E-01 |
| heu-met-fast-007-030 | 0.99640 | 0.00210 | 0.99730 | 0.00011 | -0.00090 | 0.00210 | 1.55E-02 |
| heu-met-fast-007-031 | 0.99960 | 0.00220 | 1.00107 | 0.00012 | -0.00147 | 0.00220 | 1.49E-03 |
| **heu-met-fast-007-032** | **0.99410** | **0.00120** | **1.00450** | **0.00009** | **-0.01040** | **0.00120** | **7.26E-01** |
| **heu-met-fast-007-033** | **0.99770** | **0.00190** | **1.01394** | **0.00009** | **-0.01624** | **0.00190** | **6.66E-01** |
| **heu-met-fast-007-034** | **0.99590** | **0.00170** | **1.01733** | **0.00010** | **-0.02143** | **0.00170** | **6.14E-01** |
| heu-met-fast-007-035 | 1.00030 | 0.00180 | 0.99489 | 0.00011 | 0.00541 | 0.00180 | 6.92E-03 |
| **heu-met-fast-007-036** | **0.99990** | **0.00070** | **1.00354** | **0.00012** | **-0.00364** | **0.00071** | **3.55E-03** |
| **heu-met-fast-007-037** | **0.99880** | **0.00080** | **1.00182** | **0.00012** | **-0.00302** | **0.00081** | **1.79E-03** |
| **heu-met-fast-007-038** | **1.00000** | **0.00080** | **1.00267** | **0.00011** | **-0.00267** | **0.00081** | **1.63E-03** |
| **heu-met-fast-007-039** | **1.00180** | **0.00140** | **1.00636** | **0.00011** | **-0.00456** | **0.00140** | **1.61E-03** |
| **heu-met-fast-007-040** | **1.00130** | **0.00080** | **1.00598** | **0.00011** | **-0.00468** | **0.00081** | **1.63E-03** |
| heu-met-fast-007-041 | 0.99940 | 0.00090 | 1.00093 | 0.00012 | -0.00153 | 0.00091 | 3.04E-04 |
| heu-met-fast-007-042 | 1.00160 | 0.00090 | 1.00292 | 0.00012 | -0.00132 | 0.00091 | 2.88E-04 |
| heu-met-fast-007-043 | 0.99980 | 0.00080 | 1.00040 | 0.00013 | -0.00060 | 0.00081 | 3.42E-05 |
| heu-met-fast-008-001 | 0.99890 | 0.00160 | 0.99583 | 0.00008 | 0.00307 | 0.00160 | 8.06E-01 |
| heu-met-fast-009-001 | 0.99920 | 0.00150 | 0.99763 | 0.00009 | 0.00157 | 0.00150 | 6.74E-01 |
| heu-met-fast-009-002 | 0.99920 | 0.00150 | 0.99649 | 0.00009 | 0.00271 | 0.00150 | 6.94E-01 |
| heu-met-fast-010-001 | 0.99920 | 0.00150 | 0.99829 | 0.00009 | 0.00091 | 0.00150 | 6.54E-01 |
| heu-met-fast-010-002 | 0.99920 | 0.00150 | 0.99789 | 0.00009 | 0.00131 | 0.00150 | 6.65E-01 |
| heu-met-fast-011-001 | 0.99890 | 0.00150 | 0.99887 | 0.00011 | 0.00003 | 0.00150 | 2.41E-02 |
| heu-met-fast-012-001 | 0.99920 | 0.00180 | 0.99823 | 0.00009 | 0.00097 | 0.00180 | 7.84E-01 |
| heu-met-fast-013-001 | 0.99900 | 0.00150 | 0.99752 | 0.00009 | 0.00148 | 0.00150 | 7.66E-01 |
| heu-met-fast-014-001 | 0.99890 | 0.00170 | 0.99777 | 0.00009 | 0.00113 | 0.00170 | 7.67E-01 |
| heu-met-fast-015-001 | 0.99960 | 0.00170 | 0.99470 | 0.00009 | 0.00490 | 0.00170 | 8.31E-01 |
| heu-met-fast-016-001 | 0.99960 | 0.00180 | 1.00163 | 0.00009 | -0.00203 | 0.00180 | 5.09E-01 |
| heu-met-fast-016-002 | 0.99960 | 0.00180 | 1.00263 | 0.00009 | -0.00303 | 0.00180 | 5.67E-01 |
| heu-met-fast-017-001 | 0.99930 | 0.00140 | 1.00058 | 0.00010 | -0.00128 | 0.00140 | 4.79E-01 |
| heu-met-fast-018-002 | 1.00000 | 0.00140 | 0.99971 | 0.00008 | 0.00029 | 0.00140 | 8.05E-01 |
| heu-met-fast-019-001 | 1.00000 | 0.00300 | 1.00708 | 0.00009 | -0.00708 | 0.00300 | 7.39E-01 |
| heu-met-fast-020-002 | 1.00000 | 0.00280 | 1.00063 | 0.00010 | -0.00063 | 0.00280 | 4.26E-01 |
| heu-met-fast-021-002 | 1.00000 | 0.00240 | 0.99760 | 0.00009 | 0.00240 | 0.00240 | 7.38E-01 |
| heu-met-fast-022-002 | 1.00000 | 0.00190 | 0.99763 | 0.00009 | 0.00237 | 0.00190 | 7.69E-01 |
| heu-met-fast-025-001 | 0.99870 | 0.00140 | 0.99907 | 0.00009 | -0.00037 | 0.00140 | 8.14E-01 |
| heu-met-fast-025-002 | 0.99900 | 0.00160 | 1.00124 | 0.00009 | -0.00224 | 0.00160 | 8.02E-01 |
| heu-met-fast-025-003 | 0.99910 | 0.00160 | 1.00369 | 0.00009 | -0.00459 | 0.00160 | 7.85E-01 |
| **heu-met-fast-025-004** | **0.99950** | **0.00160** | **1.00544** | **0.00009** | **-0.00594** | **0.00160** | **7.72E-01** |
| **heu-met-fast-025-005** | **0.99910** | **0.00160** | **1.00557** | **0.00009** | **-0.00647** | **0.00160** | **7.69E-01** |
| heu-met-fast-026-011 | 1.00000 | 0.00380 | 1.00330 | 0.00011 | -0.00330 | 0.00380 | 1.10E-02 |
| heu-met-fast-027-001 | 1.00000 | 0.00250 | 1.00058 | 0.00009 | -0.00058 | 0.00250 | 7.77E-01 |
| heu-met-fast-028-001 | 1.00000 | 0.00300 | 1.00298 | 0.00009 | -0.00298 | 0.00300 | 7.42E-01 |
| heu-met-fast-029-001 | 1.00000 | 0.00200 | 1.00572 | 0.00009 | -0.00572 | 0.00200 | 7.66E-01 |
| heu-met-fast-030-001 | 1.00000 | 0.00090 | 1.00219 | 0.00010 | -0.00219 | 0.00091 | 2.02E-01 |
| heu-met-fast-031-001 | 1.00000 | 0.00590 | 1.00487 | 0.00010 | -0.00487 | 0.00590 | 5.97E-03 |
| heu-met-fast-032-001 | 1.00000 | 0.00160 | 1.00411 | 0.00009 | -0.00411 | 0.00160 | 7.69E-01 |
| heu-met-fast-032-002 | 1.00000 | 0.00270 | 1.00487 | 0.00009 | -0.00487 | 0.00270 | 7.72E-01 |
| heu-met-fast-032-003 | 1.00000 | 0.00170 | 1.00017 | 0.00009 | -0.00017 | 0.00170 | 7.90E-01 |
| heu-met-fast-032-004 | 1.00000 | 0.00170 | 1.00100 | 0.00009 | -0.00100 | 0.00170 | 8.02E-01 |
| heu-met-fast-033-001 | 0.99910 | 0.00140 | 0.99902 | 0.00011 | 0.00008 | 0.00140 | 1.39E-02 |
| heu-met-fast-033-002 | 0.99910 | 0.00140 | 0.99769 | 0.00011 | 0.00141 | 0.00140 | 1.85E-03 |
| heu-met-fast-034-001 | 0.99900 | 0.00120 | 0.99703 | 0.00011 | 0.00197 | 0.00121 | 1.41E-02 |
| heu-met-fast-034-002 | 0.99900 | 0.00120 | 0.99873 | 0.00011 | 0.00027 | 0.00121 | 1.40E-02 |
| heu-met-fast-034-003 | 0.99900 | 0.00120 | 0.99767 | 0.00011 | 0.00133 | 0.00121 | 1.30E-02 |
| heu-met-fast-036-001 | 0.99930 | 0.00150 | 0.99908 | 0.00011 | 0.00022 | 0.00150 | 3.92E-03 |
| heu-met-fast-036-002 | 0.99930 | 0.00130 | 0.99837 | 0.00010 | 0.00093 | 0.00130 | 2.36E-02 |
| heu-met-fast-037-001 | 0.99970 | 0.00110 | 1.00215 | 0.00011 | -0.00245 | 0.00111 | 2.10E-03 |

| | | | | | | | |
|---|---|---|---|---|---|---|---|
| heu-met-fast-037-002 | 0.99970 | 0.00110 | 0.99779 | 0.00011 | 0.00191 | 0.00111 | 1.44E-02 |
| **heu-met-fast-038-001** | **0.99990** | **0.00070** | **1.00303** | **0.00010** | **-0.00313** | **0.00071** | **2.14E-01** |
| heu-met-fast-038-002 | 0.99990 | 0.00090 | 1.00186 | 0.00010 | -0.00196 | 0.00091 | 1.19E-01 |
| **heu-met-fast-040-001** | **0.99910** | **0.00110** | **1.00453** | **0.00009** | **-0.00543** | **0.00110** | **7.28E-01** |
| heu-met-fast-041-001 | 1.00130 | 0.00300 | 1.00687 | 0.00009 | -0.00557 | 0.00300 | 5.14E-01 |
| heu-met-fast-041-002 | 1.00220 | 0.00430 | 1.00517 | 0.00011 | -0.00297 | 0.00430 | 1.30E-01 |
| heu-met-fast-041-003 | 1.00060 | 0.00290 | 1.00240 | 0.00009 | -0.00180 | 0.00290 | 7.19E-01 |
| heu-met-fast-041-004 | 1.00060 | 0.00250 | 1.00725 | 0.00009 | -0.00665 | 0.00250 | 6.10E-01 |
| heu-met-fast-041-005 | 1.00060 | 0.00310 | 1.00287 | 0.00009 | -0.00227 | 0.00310 | 4.87E-01 |
| heu-met-fast-041-006 | 1.00060 | 0.00450 | 1.00434 | 0.00010 | -0.00374 | 0.00450 | 3.73E-01 |
| heu-met-fast-043-001 | 0.99950 | 0.00180 | 0.99900 | 0.00008 | 0.00050 | 0.00180 | 8.21E-01 |
| heu-met-fast-043-002 | 0.99950 | 0.00190 | 0.99821 | 0.00009 | 0.00129 | 0.00190 | 8.13E-01 |
| heu-met-fast-043-003 | 0.99950 | 0.00210 | 0.99880 | 0.00009 | 0.00070 | 0.00210 | 8.05E-01 |
| heu-met-fast-043-004 | 0.99950 | 0.00150 | 0.99725 | 0.00009 | 0.00225 | 0.00150 | 7.93E-01 |
| heu-met-fast-043-005 | 0.99950 | 0.00150 | 0.99826 | 0.00009 | 0.00124 | 0.00150 | 7.91E-01 |
| heu-met-fast-044-001 | 0.99950 | 0.00190 | 1.00000 | 0.00008 | -0.00050 | 0.00190 | 8.20E-01 |
| heu-met-fast-044-002 | 0.99950 | 0.00170 | 0.99962 | 0.00008 | -0.00012 | 0.00170 | 8.14E-01 |
| heu-met-fast-044-003 | 0.99950 | 0.00190 | 0.99993 | 0.00009 | -0.00043 | 0.00190 | 8.05E-01 |
| heu-met-fast-044-004 | 0.99950 | 0.00140 | 0.99931 | 0.00009 | 0.00019 | 0.00140 | 7.98E-01 |
| heu-met-fast-044-005 | 0.99950 | 0.00150 | 0.99989 | 0.00008 | -0.00039 | 0.00150 | 7.97E-01 |
| heu-met-fast-049-001 | 0.99900 | 0.00160 | 0.99808 | 0.00009 | 0.00092 | 0.00160 | 8.03E-01 |
| heu-met-fast-049-002 | 0.99940 | 0.00150 | 0.99963 | 0.00009 | -0.00023 | 0.00150 | 7.65E-01 |
| heu-met-fast-049-003 | 0.99940 | 0.00160 | 0.99886 | 0.00009 | 0.00054 | 0.00160 | 7.27E-01 |
| heu-met-fast-050-001 | 0.99900 | 0.00120 | 0.99803 | 0.00009 | 0.00097 | 0.00120 | 6.47E-01 |
| **heu-met-fast-051-001** | **0.99710** | **0.00050** | **0.99505** | **0.00009** | **0.00205** | **0.00051** | **8.28E-01** |
| heu-met-fast-051-002 | 0.99680 | 0.00050 | 0.99546 | 0.00009 | 0.00134 | 0.00051 | 8.28E-01 |
| **heu-met-fast-051-003** | **0.99740** | **0.00050** | **0.99497** | **0.00009** | **0.00243** | **0.00051** | **8.29E-01** |
| heu-met-fast-051-004 | 0.99690 | 0.00050 | 0.99517 | 0.00009 | 0.00173 | 0.00051 | 8.30E-01 |
| **heu-met-fast-051-009** | **0.99820** | **0.00020** | **0.99489** | **0.00009** | **0.00331** | **0.00022** | **8.31E-01** |
| **heu-met-fast-051-014** | **0.99960** | **0.00020** | **0.99861** | **0.00008** | **0.00099** | **0.00022** | **8.21E-01** |
| **heu-met-fast-051-015** | **0.99980** | **0.00010** | **0.99805** | **0.00008** | **0.00175** | **0.00013** | **8.25E-01** |
| **heu-met-fast-051-016** | **0.99810** | **0.00010** | **0.99636** | **0.00009** | **0.00174** | **0.00013** | **8.29E-01** |
| **heu-met-fast-051-017** | **0.99690** | **0.00010** | **0.99546** | **0.00008** | **0.00144** | **0.00013** | **8.31E-01** |
| **heu-met-fast-051-018** | **0.99840** | **0.00020** | **0.99387** | **0.00009** | **0.00453** | **0.00022** | **8.34E-01** |
| **heu-met-fast-057-001** | **1.00000** | **0.00200** | **0.98964** | **0.00009** | **0.01036** | **0.00200** | **7.48E-01** |
| heu-met-fast-057-002 | 1.00000 | 0.00230 | 0.99824 | 0.00009 | 0.00176 | 0.00230 | 7.67E-01 |
| **heu-met-fast-057-003** | **1.00000** | **0.00320** | **1.01718** | **0.00010** | **-0.01718** | **0.00320** | **7.43E-01** |
| heu-met-fast-057-004 | 1.00000 | 0.00400 | 0.98783 | 0.00009 | 0.01217 | 0.00400 | 7.73E-01 |
| **heu-met-fast-057-005** | **1.00000** | **0.00190** | **1.02180** | **0.00009** | **-0.02180** | **0.00190** | **7.34E-01** |
| heu-met-fast-057-006 | 1.00000 | 0.00290 | 0.99667 | 0.00009 | 0.00333 | 0.00290 | 7.50E-01 |
| heu-met-fast-058-001 | 1.00000 | 0.00260 | 1.00323 | 0.00012 | -0.00323 | 0.00260 | 3.47E-02 |
| heu-met-fast-058-002 | 1.00000 | 0.00350 | 1.00499 | 0.00010 | -0.00499 | 0.00350 | 2.22E-01 |
| heu-met-fast-058-003 | 1.00000 | 0.00270 | 1.00285 | 0.00011 | -0.00285 | 0.00270 | 4.60E-01 |
| heu-met-fast-058-004 | 1.00000 | 0.00210 | 1.00208 | 0.00009 | -0.00208 | 0.00210 | 6.15E-01 |
| heu-met-fast-058-005 | 1.00000 | 0.00330 | 1.00098 | 0.00009 | -0.00098 | 0.00330 | 6.85E-01 |
| heu-met-fast-063-001 | 0.99930 | 0.00490 | 1.00064 | 0.00009 | -0.00134 | 0.00490 | 6.95E-01 |
| heu-met-fast-063-002 | 0.99880 | 0.00470 | 1.00094 | 0.00009 | -0.00214 | 0.00470 | 6.55E-01 |
| **heu-met-fast-064-001** | **0.99960** | **0.00080** | **0.99537** | **0.00009** | **0.00423** | **0.00081** | **7.47E-01** |
| heu-met-fast-064-002 | 0.99960 | 0.00100 | 0.99562 | 0.00009 | 0.00398 | 0.00100 | 6.91E-01 |
| **heu-met-fast-064-003** | **0.99960** | **0.00090** | **0.99360** | **0.00009** | **0.00600** | **0.00090** | **6.90E-01** |
| heu-met-fast-065-002 | 0.99950 | 0.00130 | 0.99812 | 0.00009 | 0.00138 | 0.00130 | 8.31E-01 |
| heu-met-fast-066-001 | 1.00300 | 0.00330 | 1.00374 | 0.00010 | -0.00074 | 0.00330 | 2.04E-01 |
| heu-met-fast-066-002 | 1.00230 | 0.00290 | 1.00192 | 0.00010 | 0.00038 | 0.00290 | 4.15E-01 |
| heu-met-fast-066-003 | 1.00230 | 0.00260 | 1.00466 | 0.00010 | -0.00236 | 0.00260 | 5.18E-01 |
| heu-met-fast-066-004 | 1.00430 | 0.00430 | 1.00496 | 0.00011 | -0.00066 | 0.00430 | 5.49E-02 |
| heu-met-fast-066-005 | 1.00300 | 0.00330 | 1.00431 | 0.00010 | -0.00131 | 0.00330 | 2.13E-01 |
| heu-met-fast-066-006 | 1.00280 | 0.00300 | 1.00343 | 0.00010 | -0.00063 | 0.00300 | 3.46E-01 |
| heu-met-fast-066-007 | 1.00480 | 0.00390 | 1.00578 | 0.00011 | -0.00098 | 0.00390 | 1.97E-01 |
| heu-met-fast-066-008 | 1.00390 | 0.00400 | 1.00458 | 0.00011 | -0.00068 | 0.00400 | 8.81E-02 |
| heu-met-fast-066-009 | 1.00270 | 0.00360 | 1.00289 | 0.00010 | -0.00019 | 0.00360 | 2.18E-01 |
| **heu-met-fast-067-001** | **1.00860** | **0.00040** | **1.00112** | **0.00008** | **0.00748** | **0.00041** | **1.22E-01** |
| heu-met-fast-067-002 | 0.99380 | 0.00240 | 0.99620 | 0.00008 | -0.00240 | 0.00240 | 2.19E-01 |
| heu-met-fast-072-001 | 0.99910 | 0.00240 | 1.00867 | 0.00010 | -0.00957 | 0.00240 | 2.23E-01 |
| heu-met-fast-072-003 | 1.00160 | 0.00690 | 1.01221 | 0.00009 | -0.01061 | 0.00690 | 4.08E-02 |
| heu-met-fast-073-001 | 1.00040 | 0.00160 | 1.00806 | 0.00009 | -0.00766 | 0.00160 | 4.16E-01 |
| heu-met-fast-077-001 | 1.00010 | 0.00310 | 1.00068 | 0.00010 | -0.00058 | 0.00310 | 2.01E-01 |
| heu-met-fast-077-002 | 0.99950 | 0.00270 | 1.00068 | 0.00010 | -0.00118 | 0.00270 | 4.29E-01 |
| heu-met-fast-077-003 | 0.99950 | 0.00400 | 0.99787 | 0.00011 | 0.00163 | 0.00400 | 5.00E-02 |
| heu-met-fast-077-004 | 0.99980 | 0.00320 | 0.99836 | 0.00010 | 0.00144 | 0.00320 | 2.19E-01 |
| heu-met-fast-077-005 | 0.99940 | 0.00270 | 1.00012 | 0.00009 | -0.00072 | 0.00270 | 3.67E-01 |
| heu-met-fast-077-006 | 0.99960 | 0.00330 | 0.99969 | 0.00010 | -0.00009 | 0.00330 | 2.00E-01 |

| | | | | | | | |
|---|---|---|---|---|---|---|---|
| heu-met-fast-077-007 | 0.99940 | 0.00560 | 1.00057 | 0.00010 | -0.00117 | 0.00560 | 4.97E-01 |
| heu-met-fast-077-008 | 0.99940 | 0.00350 | 0.99833 | 0.00010 | 0.00107 | 0.00350 | 2.83E-01 |
| heu-met-fast-078-001 | 0.99950 | 0.00180 | 0.99457 | 0.00011 | 0.00493 | 0.00180 | 8.16E-02 |
| heu-met-fast-078-003 | 0.99940 | 0.00220 | 0.99591 | 0.00010 | 0.00349 | 0.00220 | 3.14E-01 |
| heu-met-fast-078-005 | 0.99910 | 0.00190 | 0.99636 | 0.00010 | 0.00274 | 0.00190 | 1.09E-01 |
| heu-met-fast-078-007 | 1.00000 | 0.00190 | 0.99845 | 0.00011 | 0.00155 | 0.00190 | 1.10E-02 |
| heu-met-fast-078-009 | 0.99970 | 0.00220 | 0.99568 | 0.00010 | 0.00402 | 0.00220 | 7.80E-02 |
| heu-met-fast-078-011 | 0.99950 | 0.00150 | 0.99582 | 0.00010 | 0.00368 | 0.00150 | 7.30E-02 |
| heu-met-fast-078-013 | 1.00000 | 0.00170 | 0.99727 | 0.00010 | 0.00273 | 0.00170 | 7.23E-02 |
| heu-met-fast-078-015 | 0.99910 | 0.00180 | 0.99655 | 0.00010 | 0.00255 | 0.00180 | 7.21E-02 |
| heu-met-fast-078-017 | 0.99950 | 0.00180 | 0.99657 | 0.00010 | 0.00293 | 0.00180 | 7.21E-02 |
| heu-met-fast-078-023 | 0.99920 | 0.00220 | 0.99824 | 0.00009 | 0.00096 | 0.00220 | 7.95E-01 |
| heu-met-fast-078-025 | 0.99920 | 0.00250 | 0.99742 | 0.00010 | 0.00178 | 0.00250 | 7.59E-01 |
| heu-met-fast-078-027 | 0.99920 | 0.00210 | 0.99595 | 0.00009 | 0.00325 | 0.00210 | 6.68E-01 |
| heu-met-fast-078-029 | 1.00000 | 0.00250 | 1.00212 | 0.00010 | -0.00212 | 0.00250 | 4.63E-01 |
| heu-met-fast-078-031 | 0.99940 | 0.00200 | 0.99519 | 0.00010 | 0.00421 | 0.00200 | 6.54E-01 |
| heu-met-fast-078-033 | 0.99960 | 0.00260 | 0.99588 | 0.00009 | 0.00372 | 0.00260 | 4.37E-01 |
| heu-met-fast-078-035 | 0.99910 | 0.00220 | 0.99445 | 0.00010 | 0.00465 | 0.00220 | 6.43E-01 |
| heu-met-fast-078-037 | 0.99860 | 0.00210 | 0.99620 | 0.00009 | 0.00240 | 0.00210 | 6.32E-01 |
| heu-met-fast-078-039 | 0.99890 | 0.00210 | 0.99694 | 0.00010 | 0.00196 | 0.00210 | 6.28E-01 |
| heu-met-fast-078-041 | 0.99920 | 0.00250 | 0.99664 | 0.00009 | 0.00256 | 0.00250 | 8.33E-01 |
| heu-met-fast-078-043 | 1.00000 | 0.00190 | 0.99765 | 0.00009 | 0.00235 | 0.00190 | 4.17E-01 |
| heu-met-fast-079-001 | 0.99960 | 0.00150 | 0.99984 | 0.00008 | -0.00024 | 0.00150 | 8.19E-01 |
| heu-met-fast-079-002 | 0.99960 | 0.00140 | 0.99921 | 0.00009 | 0.00039 | 0.00140 | 8.14E-01 |
| heu-met-fast-079-003 | 0.99960 | 0.00150 | 1.00009 | 0.00009 | -0.00049 | 0.00150 | 8.03E-01 |
| heu-met-fast-079-004 | 0.99960 | 0.00140 | 1.00113 | 0.00009 | -0.00153 | 0.00140 | 7.94E-01 |
| heu-met-fast-079-005 | 0.99960 | 0.00150 | 0.99981 | 0.00009 | -0.00021 | 0.00150 | 7.93E-01 |
| heu-met-fast-084-001 | 0.99940 | 0.00190 | 0.99881 | 0.00009 | 0.00059 | 0.00190 | 7.88E-01 |
| heu-met-fast-084-002 | 0.99940 | 0.00210 | 0.99948 | 0.00009 | -0.00008 | 0.00210 | 7.66E-01 |
| heu-met-fast-084-003 | 0.99930 | 0.00210 | 0.99988 | 0.00009 | -0.00058 | 0.00210 | 6.53E-01 |
| heu-met-fast-084-004 | 0.99940 | 0.00200 | 0.99868 | 0.00009 | 0.00072 | 0.00200 | 7.63E-01 |
| heu-met-fast-084-005 | 0.99930 | 0.00210 | 1.00497 | 0.00009 | -0.00567 | 0.00210 | 7.58E-01 |
| heu-met-fast-084-006 | 0.99940 | 0.00240 | 0.99858 | 0.00008 | 0.00082 | 0.00240 | 7.54E-01 |
| heu-met-fast-084-007 | 0.99950 | 0.00200 | 0.99740 | 0.00009 | 0.00210 | 0.00200 | 7.87E-01 |
| heu-met-fast-084-008 | 0.99940 | 0.00340 | 1.00840 | 0.00009 | -0.00900 | 0.00340 | 7.35E-01 |
| heu-met-fast-084-009 | 0.99930 | 0.00540 | 1.00246 | 0.00009 | -0.00316 | 0.00540 | 7.28E-01 |
| heu-met-fast-084-010 | 0.99930 | 0.00220 | 1.00106 | 0.00009 | -0.00176 | 0.00220 | 7.61E-01 |
| heu-met-fast-084-011 | 0.99950 | 0.00190 | 1.00146 | 0.00010 | -0.00196 | 0.00190 | 1.45E-01 |
| heu-met-fast-084-012 | 0.99940 | 0.00200 | 0.99740 | 0.00009 | 0.00200 | 0.00200 | 7.91E-01 |
| heu-met-fast-084-013 | 0.99940 | 0.00220 | 0.99897 | 0.00009 | 0.00043 | 0.00220 | 7.95E-01 |
| heu-met-fast-084-014 | 0.99940 | 0.00190 | 0.99987 | 0.00009 | -0.00047 | 0.00190 | 7.28E-01 |
| heu-met-fast-084-015 | 0.99950 | 0.00210 | 0.99790 | 0.00009 | 0.00160 | 0.00210 | 7.91E-01 |
| heu-met-fast-084-016 | 0.99940 | 0.00200 | 0.99912 | 0.00009 | 0.00028 | 0.00200 | 7.42E-01 |
| heu-met-fast-084-017 | 0.99950 | 0.00190 | 1.00036 | 0.00009 | -0.00086 | 0.00190 | 7.84E-01 |
| heu-met-fast-084-018 | 0.99950 | 0.00220 | 0.99743 | 0.00008 | 0.00207 | 0.00220 | 7.83E-01 |
| heu-met-fast-084-019 | 0.99960 | 0.00190 | 0.99768 | 0.00009 | 0.00192 | 0.00190 | 8.01E-01 |
| heu-met-fast-084-020 | 0.99950 | 0.00250 | 1.00304 | 0.00009 | -0.00354 | 0.00250 | 7.73E-01 |
| heu-met-fast-084-021 | 0.99950 | 0.00450 | 1.00023 | 0.00009 | -0.00073 | 0.00450 | 7.70E-01 |
| heu-met-fast-084-022 | 0.99940 | 0.00200 | 0.99824 | 0.00009 | 0.00116 | 0.00200 | 7.84E-01 |
| heu-met-fast-084-023 | 0.99930 | 0.00240 | 0.99956 | 0.00010 | -0.00026 | 0.00240 | 4.55E-01 |
| heu-met-fast-084-024 | 0.99960 | 0.00180 | 0.99862 | 0.00009 | 0.00098 | 0.00180 | 8.06E-01 |
| heu-met-fast-084-025 | 0.99950 | 0.00200 | 0.99808 | 0.00008 | 0.00142 | 0.00200 | 7.70E-01 |
| heu-met-fast-084-026 | 0.99930 | 0.00220 | 1.00039 | 0.00009 | -0.00109 | 0.00220 | 7.08E-01 |
| heu-met-fast-084-027 | 0.99940 | 0.00200 | 0.99769 | 0.00009 | 0.00171 | 0.00200 | 6.93E-01 |
| heu-met-fast-087-001 | 0.99870 | 0.00130 | 0.99840 | 0.00009 | 0.00030 | 0.00130 | 7.51E-01 |
| heu-met-fast-088-001 | 0.99930 | 0.00080 | 0.99681 | 0.00010 | 0.00249 | 0.00081 | 1.33E-02 |
| heu-met-fast-088-002 | 0.99930 | 0.00070 | 0.99672 | 0.00011 | 0.00258 | 0.00071 | 2.15E-03 |
| heu-met-fast-089-001 | 0.99910 | 0.00140 | 1.00008 | 0.00009 | -0.00098 | 0.00140 | 7.71E-01 |
| **heu-met-fast-090-001** | **0.99940** | **0.00070** | **1.00567** | **0.00011** | **-0.00627** | **0.00071** | **6.26E-03** |
| **heu-met-fast-090-002** | **0.99930** | **0.00070** | **1.00226** | **0.00011** | **-0.00296** | **0.00071** | **1.09E-03** |
| heu-met-fast-091-001 | 0.99960 | 0.00090 | 0.99957 | 0.00011 | 0.00003 | 0.00091 | 8.48E-03 |
| heu-met-fast-092-001 | 0.99860 | 0.00110 | 1.00105 | 0.00008 | -0.00245 | 0.00110 | 8.05E-01 |
| heu-met-fast-092-002 | 0.99890 | 0.00130 | 1.00279 | 0.00009 | -0.00389 | 0.00130 | 7.72E-01 |
| **heu-met-fast-092-003** | **0.99930** | **0.00120** | **1.00397** | **0.00009** | **-0.00467** | **0.00120** | **7.39E-01** |
| **heu-met-fast-092-004** | **0.99930** | **0.00130** | **1.00361** | **0.00009** | **-0.00431** | **0.00130** | **7.37E-01** |
| **heu-met-fast-093-001** | **0.99780** | **0.00120** | **1.00328** | **0.00008** | **-0.00548** | **0.00120** | **6.55E-01** |
| heu-met-fast-094-001 | 0.99940 | 0.00120 | 1.00347 | 0.00010 | -0.00407 | 0.00120 | 1.76E-01 |
| **heu-met-fast-094-002** | **0.99930** | **0.00100** | **1.00366** | **0.00010** | **-0.00436** | **0.00100** | **1.34E-01** |
| heu-met-fast-100-001 | 1.00310 | 0.00070 | 1.00486 | 0.00008 | -0.00176 | 0.00070 | 8.15E-01 |
| heu-met-fast-100-002 | 0.99660 | 0.00070 | 0.99878 | 0.00008 | -0.00218 | 0.00070 | 8.17E-01 |
| **heu-met-inter-006-001** | **0.99770** | **0.00080** | **0.99293** | **0.00010** | **0.00477** | **0.00081** | **4.93E-03** |

| | | | | | | | |
|---|---|---|---|---|---|---|---|
| heu-met-inter-006-002 | 1.00010 | 0.00080 | 0.99682 | 0.00011 | 0.00328 | 0.00081 | 1.01E-02 |
| heu-met-inter-006-003 | 1.00150 | 0.00090 | 1.00071 | 0.00011 | 0.00079 | 0.00091 | 2.35E-02 |
| **heu-met-inter-006-004** | **1.00160** | **0.00080** | **1.00728** | **0.00011** | **-0.00568** | **0.00081** | **7.98E-02** |
| heu-met-mixed-001-001 | 0.99950 | 0.00130 | 1.00227 | 0.00011 | -0.00277 | 0.00130 | 2.09E-03 |
| heu-met-mixed-002-001 | 1.00000 | 0.00370 | 1.00647 | 0.00012 | -0.00647 | 0.00370 | 1.08E-03 |
| heu-met-mixed-003-001 | 1.00000 | 0.00380 | 1.00760 | 0.00011 | -0.00760 | 0.00380 | 1.07E-03 |
| heu-met-mixed-004-001 | 0.99990 | 0.00090 | 1.00249 | 0.00009 | -0.00259 | 0.00090 | 4.31E-04 |
| heu-met-mixed-015-001 | 0.99960 | 0.00080 | 0.99701 | 0.00012 | 0.00259 | 0.00081 | 9.56E-05 |
| heu-met-mixed-016-001 | 0.99950 | 0.00080 | 1.00156 | 0.00012 | -0.00206 | 0.00081 | 1.06E-04 |
| **heu-met-mixed-016-002** | **0.99950** | **0.00070** | **1.00250** | **0.00011** | **-0.00300** | **0.00071** | **6.38E-05** |
| heu-met-mixed-017-001 | 0.99950 | 0.00080 | 0.99547 | 0.00011 | 0.00403 | 0.00081 | 1.77E-04 |
| heu-met-therm-010-001 | 1.00650 | 0.00720 | 1.00875 | 0.00012 | -0.00225 | 0.00720 | 7.54E-08 |
| **heu-met-therm-012-001** | **0.99710** | **0.00250** | **1.00919** | **0.00012** | **-0.01209** | **0.00250** | **1.32E-07** |
| **heu-met-therm-014-001** | **0.99390** | **0.00150** | **1.00795** | **0.00013** | **-0.01405** | **0.00151** | **1.24E-07** |
| heu-met-therm-031-001 | 1.00370 | 0.00240 | 1.00850 | 0.00011 | -0.00480 | 0.00240 | 6.34E-08 |
| heu-sol-therm-001-001 | 1.00000 | 0.00250 | 0.99828 | 0.00016 | 0.00172 | 0.00251 | 8.05E-08 |
| heu-sol-therm-001-002 | 1.00000 | 0.00250 | 0.99603 | 0.00015 | 0.00397 | 0.00250 | 2.71E-07 |
| heu-sol-therm-001-003 | 1.00000 | 0.00250 | 1.00177 | 0.00016 | -0.00177 | 0.00251 | 7.91E-08 |
| heu-sol-therm-001-004 | 1.00000 | 0.00250 | 0.99852 | 0.00015 | 0.00148 | 0.00250 | 2.89E-07 |
| heu-sol-therm-001-005 | 1.00000 | 0.00250 | 0.99868 | 0.00014 | 0.00132 | 0.00250 | 4.26E-08 |
| heu-sol-therm-001-006 | 1.00000 | 0.00250 | 1.00196 | 0.00013 | -0.00196 | 0.00250 | 4.41E-08 |
| heu-sol-therm-001-007 | 1.00000 | 0.00250 | 0.99779 | 0.00014 | 0.00221 | 0.00250 | 7.64E-08 |
| heu-sol-therm-001-008 | 1.00000 | 0.00250 | 0.99823 | 0.00015 | 0.00177 | 0.00250 | 8.07E-08 |
| **heu-sol-therm-001-009** | **1.00000** | **0.00250** | **0.99435** | **0.00015** | **0.00565** | **0.00250** | **2.90E-07** |
| **heu-sol-therm-001-010** | **1.00000** | **0.00250** | **0.99257** | **0.00013** | **0.00743** | **0.00250** | **4.56E-08** |
| heu-sol-therm-009-001 | 0.99900 | 0.00430 | 1.00215 | 0.00014 | -0.00315 | 0.00430 | 5.12E-07 |
| heu-sol-therm-009-002 | 1.00000 | 0.00390 | 1.00249 | 0.00014 | -0.00249 | 0.00390 | 3.14E-07 |
| heu-sol-therm-009-003 | 1.00000 | 0.00360 | 1.00211 | 0.00013 | -0.00211 | 0.00360 | 1.57E-07 |
| heu-sol-therm-010-001 | 1.00000 | 0.00290 | 1.00115 | 0.00012 | -0.00115 | 0.00290 | 5.20E-08 |
| heu-sol-therm-011-001 | 1.00000 | 0.00230 | 1.00481 | 0.00012 | -0.00481 | 0.00230 | 3.95E-08 |
| heu-sol-therm-011-002 | 1.00000 | 0.00230 | 1.00072 | 0.00011 | -0.00072 | 0.00230 | 3.93E-08 |
| heu-sol-therm-012-001 | 0.99990 | 0.00580 | 1.00088 | 0.00008 | -0.00098 | 0.00580 | 3.23E-08 |
| heu-sol-therm-013-001 | 1.00120 | 0.00260 | 0.99862 | 0.00008 | 0.00258 | 0.00260 | 3.23E-08 |
| heu-sol-therm-013-002 | 1.00070 | 0.00360 | 0.99781 | 0.00008 | 0.00289 | 0.00360 | 3.37E-08 |
| heu-sol-therm-013-003 | 1.00090 | 0.00360 | 0.99415 | 0.00010 | 0.00675 | 0.00360 | 3.51E-08 |
| heu-sol-therm-013-004 | 1.00030 | 0.00360 | 0.99600 | 0.00010 | 0.00430 | 0.00360 | 3.58E-08 |
| heu-sol-therm-019-001 | 0.99910 | 0.00410 | 0.99737 | 0.00014 | 0.00173 | 0.00410 | 3.06E-07 |
| heu-sol-therm-019-002 | 0.99910 | 0.00410 | 0.99895 | 0.00013 | 0.00015 | 0.00410 | 2.87E-07 |
| heu-sol-therm-019-003 | 0.99910 | 0.00670 | 0.99459 | 0.00013 | 0.00451 | 0.00670 | 3.42E-07 |
| heu-sol-therm-025-001 | 1.00020 | 0.00250 | 1.00093 | 0.00012 | -0.00073 | 0.00250 | 4.02E-08 |
| heu-sol-therm-025-002 | 1.00070 | 0.00250 | 1.00048 | 0.00011 | 0.00022 | 0.00250 | 4.02E-08 |
| heu-sol-therm-025-003 | 1.00020 | 0.00640 | 0.99527 | 0.00010 | 0.00493 | 0.00640 | 4.22E-08 |
| heu-sol-therm-025-004 | 1.00030 | 0.00270 | 1.00083 | 0.00012 | -0.00053 | 0.00270 | 4.10E-08 |
| heu-sol-therm-025-005 | 1.00130 | 0.00300 | 1.00309 | 0.00012 | -0.00179 | 0.00300 | 4.82E-08 |
| heu-sol-therm-025-006 | 1.00020 | 0.00670 | 1.00858 | 0.00011 | -0.00838 | 0.00670 | 4.25E-08 |
| heu-sol-therm-025-007 | 1.00090 | 0.00730 | 1.01263 | 0.00010 | -0.01173 | 0.00730 | 4.66E-08 |
| heu-sol-therm-025-008 | 1.00000 | 0.00670 | 1.01005 | 0.00010 | -0.01005 | 0.00670 | 4.81E-08 |
| heu-sol-therm-025-009 | 1.00020 | 0.00650 | 1.00398 | 0.00011 | -0.00378 | 0.00650 | 5.45E-08 |
| heu-sol-therm-025-010 | 1.00030 | 0.00430 | 1.00818 | 0.00011 | -0.00788 | 0.00430 | 6.94E-08 |
| heu-sol-therm-025-011 | 1.00020 | 0.00450 | 1.00745 | 0.00011 | -0.00725 | 0.00450 | 7.02E-08 |
| heu-sol-therm-025-012 | 1.00020 | 0.00450 | 1.00581 | 0.00011 | -0.00561 | 0.00450 | 8.62E-08 |
| heu-sol-therm-025-013 | 1.00090 | 0.00470 | 1.01360 | 0.00010 | -0.01270 | 0.00470 | 8.72E-08 |
| heu-sol-therm-025-014 | 1.00080 | 0.00530 | 1.00491 | 0.00011 | -0.00411 | 0.00530 | 1.15E-07 |
| heu-sol-therm-025-015 | 1.00020 | 0.00580 | 0.99913 | 0.00011 | 0.00107 | 0.00580 | 1.09E-07 |
| heu-sol-therm-025-016 | 1.00020 | 0.00490 | 1.00921 | 0.00011 | -0.00901 | 0.00490 | 1.78E-07 |
| heu-sol-therm-025-017 | 1.00090 | 0.00550 | 1.00108 | 0.00012 | -0.00018 | 0.00550 | 1.65E-07 |
| heu-sol-therm-025-018 | 1.00000 | 0.00610 | 0.99863 | 0.00011 | 0.00137 | 0.00610 | 1.56E-07 |
| heu-sol-therm-032-001 | 1.00150 | 0.00260 | 0.99945 | 0.00005 | 0.00205 | 0.00260 | 3.09E-08 |
| heu-sol-therm-038-001 | 1.00000 | 0.00250 | 0.99497 | 0.00015 | 0.00503 | 0.00250 | 3.76E-07 |
| heu-sol-therm-038-002 | 1.00000 | 0.00250 | 0.99721 | 0.00014 | 0.00279 | 0.00250 | 2.96E-07 |
| heu-sol-therm-038-003 | 1.00000 | 0.00250 | 0.99782 | 0.00014 | 0.00218 | 0.00250 | 3.47E-07 |
| heu-sol-therm-038-004 | 1.00000 | 0.00250 | 0.99514 | 0.00014 | 0.00486 | 0.00250 | 3.75E-07 |
| heu-sol-therm-038-005 | 1.00000 | 0.00250 | 0.99544 | 0.00014 | 0.00456 | 0.00250 | 3.77E-07 |
| heu-sol-therm-038-006 | 1.00000 | 0.00250 | 0.99635 | 0.00013 | 0.00365 | 0.00250 | 3.00E-07 |
| heu-sol-therm-038-007 | 1.00000 | 0.00320 | 0.99803 | 0.00014 | 0.00197 | 0.00320 | 3.45E-07 |
| heu-sol-therm-038-008 | 1.00000 | 0.00260 | 0.99823 | 0.00013 | 0.00177 | 0.00260 | 3.41E-07 |
| heu-sol-therm-038-009 | 1.00000 | 0.00330 | 0.99854 | 0.00015 | 0.00146 | 0.00330 | 3.38E-07 |
| heu-sol-therm-038-010 | 1.00000 | 0.00260 | 0.99742 | 0.00014 | 0.00258 | 0.00260 | 3.55E-07 |
| heu-sol-therm-038-011 | 1.00000 | 0.00250 | 0.99637 | 0.00014 | 0.00363 | 0.00250 | 3.76E-07 |
| heu-sol-therm-038-012 | 1.00000 | 0.00250 | 0.99573 | 0.00014 | 0.00427 | 0.00250 | 3.74E-07 |
| heu-sol-therm-038-013 | 1.00000 | 0.00500 | 1.00081 | 0.00014 | -0.00081 | 0.00500 | 3.89E-07 |

| | | | | | | | |
|---|---|---|---|---|---|---|---|
| heu-sol-therm-038-014 | 1.00000 | 0.00500 | 1.00131 | 0.00014 | -0.00131 | 0.00500 | 3.93E-07 |
| heu-sol-therm-038-015 | 1.00000 | 0.00500 | 1.00082 | 0.00015 | -0.00082 | 0.00500 | 3.94E-07 |
| heu-sol-therm-038-016 | 1.00000 | 0.00500 | 1.00018 | 0.00014 | -0.00018 | 0.00500 | 3.94E-07 |
| heu-sol-therm-038-017 | 1.00000 | 0.00260 | 0.99681 | 0.00014 | 0.00319 | 0.00260 | 3.78E-07 |
| heu-sol-therm-038-018 | 1.00000 | 0.00320 | 0.99541 | 0.00014 | 0.00459 | 0.00320 | 3.72E-07 |
| heu-sol-therm-038-019 | 1.00000 | 0.00320 | 0.99716 | 0.00015 | 0.00284 | 0.00320 | 3.71E-07 |
| heu-sol-therm-038-020 | 1.00000 | 0.00320 | 0.99721 | 0.00014 | 0.00279 | 0.00320 | 3.71E-07 |
| heu-sol-therm-038-021 | 1.00000 | 0.00250 | 0.99693 | 0.00014 | 0.00307 | 0.00250 | 3.24E-07 |
| heu-sol-therm-038-022 | 1.00000 | 0.00270 | 0.99749 | 0.00015 | 0.00251 | 0.00270 | 3.15E-07 |
| heu-sol-therm-038-023 | 1.00000 | 0.00270 | 0.99694 | 0.00014 | 0.00306 | 0.00270 | 3.16E-07 |
| heu-sol-therm-038-024 | 1.00000 | 0.00260 | 0.99711 | 0.00014 | 0.00289 | 0.00260 | 3.93E-07 |
| heu-sol-therm-038-025 | 1.00000 | 0.00320 | 0.99741 | 0.00014 | 0.00259 | 0.00320 | 3.72E-07 |
| heu-sol-therm-038-026 | 1.00000 | 0.00320 | 0.99748 | 0.00014 | 0.00252 | 0.00320 | 3.72E-07 |
| heu-sol-therm-038-027 | 1.00000 | 0.00320 | 0.99718 | 0.00014 | 0.00282 | 0.00320 | 3.82E-07 |
| heu-sol-therm-038-028 | 1.00000 | 0.00250 | 0.99749 | 0.00014 | 0.00251 | 0.00250 | 3.58E-07 |
| heu-sol-therm-042-001 | 0.99570 | 0.00390 | 0.99664 | 0.00007 | -0.00094 | 0.00390 | 3.15E-08 |
| heu-sol-therm-042-002 | 0.99650 | 0.00360 | 0.99660 | 0.00007 | -0.00010 | 0.00360 | 3.14E-08 |
| heu-sol-therm-042-003 | 0.99940 | 0.00280 | 1.00067 | 0.00005 | -0.00127 | 0.00280 | 3.10E-08 |
| heu-sol-therm-042-004 | 1.00000 | 0.00340 | 1.00228 | 0.00004 | -0.00228 | 0.00340 | 3.08E-08 |
| heu-sol-therm-042-005 | 1.00000 | 0.00340 | 0.99992 | 0.00004 | 0.00008 | 0.00340 | 3.06E-08 |
| heu-sol-therm-042-006 | 1.00000 | 0.00370 | 1.00050 | 0.00004 | -0.00050 | 0.00370 | 3.07E-08 |
| heu-sol-therm-042-007 | 1.00000 | 0.00360 | 1.00145 | 0.00004 | -0.00145 | 0.00360 | 3.06E-08 |
| heu-sol-therm-042-008 | 1.00000 | 0.00350 | 1.00204 | 0.00003 | -0.00204 | 0.00350 | 3.05E-08 |
| heu-sol-therm-043-001 | 0.99860 | 0.00310 | 0.99479 | 0.00015 | 0.00381 | 0.00310 | 7.27E-08 |
| heu-sol-therm-043-002 | 0.99950 | 0.00260 | 1.00515 | 0.00009 | -0.00565 | 0.00260 | 3.35E-08 |
| heu-sol-therm-043-003 | 0.99900 | 0.00250 | 1.00100 | 0.00008 | -0.00200 | 0.00250 | 3.22E-08 |
| heu-sol-therm-050-001 | 0.99530 | 0.00860 | 1.00714 | 0.00015 | -0.01184 | 0.00860 | 6.71E-07 |
| heu-sol-therm-050-002 | 0.99870 | 0.00830 | 1.00278 | 0.00015 | -0.00408 | 0.00830 | 6.72E-07 |
| heu-sol-therm-050-003 | 0.99840 | 0.00790 | 1.00473 | 0.00015 | -0.00633 | 0.00790 | 2.25E-06 |
| heu-sol-therm-050-004 | 0.99870 | 0.00840 | 1.00452 | 0.00015 | -0.00582 | 0.00840 | 6.71E-07 |
| heu-sol-therm-050-005 | 0.99850 | 0.00850 | 1.00073 | 0.00015 | -0.00223 | 0.00850 | 2.53E-07 |
| heu-sol-therm-050-006 | 0.99850 | 0.00810 | 1.00902 | 0.00015 | -0.01052 | 0.00810 | 6.71E-07 |
| heu-sol-therm-050-007 | 0.99780 | 0.00780 | 0.99803 | 0.00015 | -0.00023 | 0.00780 | 2.28E-06 |
| heu-sol-therm-050-008 | 0.99750 | 0.00840 | 0.99791 | 0.00015 | -0.00041 | 0.00840 | 6.78E-07 |
| heu-sol-therm-050-009 | 0.99660 | 0.00820 | 0.99724 | 0.00014 | -0.00064 | 0.00820 | 2.30E-06 |
| heu-sol-therm-050-010 | 0.99600 | 0.00900 | 0.97986 | 0.00014 | 0.01614 | 0.00900 | 6.89E-07 |
| heu-sol-therm-050-011 | 0.99640 | 0.00890 | 0.99113 | 0.00015 | 0.00527 | 0.00890 | 2.57E-07 |
| ieu-comp-therm-002-003 | 1.00170 | 0.00440 | 1.00417 | 0.00010 | -0.00247 | 0.00440 | 9.83E-08 |
| ieu-met-fast-001-001 | 0.99880 | **0.00280** | 1.00013 | 0.00009 | -0.00133 | 0.00009 | 6.99E-01 |
| ieu-met-fast-001-002 | 0.99880 | **0.00280** | 1.00022 | 0.00009 | -0.00142 | 0.00009 | 6.98E-01 |
| ieu-met-fast-001-003 | 0.99900 | **0.00280** | 1.00048 | 0.00009 | -0.00148 | 0.00009 | 6.39E-01 |
| ieu-met-fast-001-004 | 0.99900 | **0.00280** | 1.00140 | 0.00008 | -0.00240 | 0.00008 | 6.39E-01 |
| ieu-met-fast-002-001 | 1.00000 | 0.00300 | 0.99891 | 0.00009 | 0.00109 | 0.00300 | 4.83E-01 |
| ieu-met-fast-003-001 | 1.00000 | 0.00170 | 1.00215 | 0.00009 | -0.00215 | 0.00170 | 6.12E-01 |
| ieu-met-fast-004-001 | 1.00000 | 0.00300 | 1.00752 | 0.00009 | -0.00752 | 0.00300 | 5.73E-01 |
| ieu-met-fast-005-001 | 1.00000 | 0.00210 | 1.00184 | 0.00009 | -0.00184 | 0.00210 | 5.76E-01 |
| ieu-met-fast-006-001 | 1.00000 | 0.00230 | 0.99612 | 0.00008 | 0.00388 | 0.00230 | 5.72E-01 |
| ieu-met-fast-007-001 | 1.00450 | 0.00070 | 1.00435 | 0.00007 | 0.00015 | 0.00070 | 4.27E-01 |
| ieu-met-fast-008-001 | 1.00000 | 0.00180 | 1.00539 | 0.00009 | -0.00539 | 0.00180 | 6.05E-01 |
| ieu-met-fast-009-001 | 1.00000 | 0.00530 | 1.01058 | 0.00011 | -0.01058 | 0.00530 | 1.29E-02 |
| leu-comp-therm-001-001 | 0.99980 | 0.00310 | 0.99959 | 0.00009 | 0.00021 | 0.00310 | 9.88E-08 |
| leu-comp-therm-001-002 | 0.99980 | 0.00310 | 0.99878 | 0.00010 | 0.00102 | 0.00310 | 9.80E-08 |
| leu-comp-therm-001-003 | 0.99980 | 0.00300 | 0.99846 | 0.00010 | 0.00134 | 0.00300 | 9.71E-08 |
| leu-comp-therm-001-004 | 0.99980 | 0.00300 | 0.99912 | 0.00009 | 0.00068 | 0.00300 | 9.78E-08 |
| leu-comp-therm-001-005 | 0.99980 | 0.00300 | 0.99691 | 0.00010 | 0.00289 | 0.00300 | 9.64E-08 |
| leu-comp-therm-001-006 | 0.99980 | 0.00300 | 0.99899 | 0.00009 | 0.00081 | 0.00300 | 9.74E-08 |
| leu-comp-therm-001-007 | 0.99980 | 0.00300 | 0.99811 | 0.00009 | 0.00169 | 0.00300 | 9.56E-08 |
| leu-comp-therm-001-008 | 0.99980 | 0.00300 | 0.99718 | 0.00009 | 0.00262 | 0.00300 | 9.68E-08 |
| leu-comp-therm-002-001 | 0.99970 | 0.00200 | 0.99865 | 0.00010 | 0.00105 | 0.00200 | 1.16E-07 |
| leu-comp-therm-002-002 | 0.99970 | 0.00200 | 0.99980 | 0.00010 | -0.00010 | 0.00200 | 1.16E-07 |
| leu-comp-therm-002-003 | 0.99970 | 0.00200 | 0.99923 | 0.00010 | 0.00047 | 0.00200 | 1.15E-07 |
| leu-comp-therm-002-004 | 0.99970 | 0.00200 | 0.99883 | 0.00011 | 0.00087 | 0.00200 | 1.15E-07 |
| leu-comp-therm-002-005 | 0.99970 | 0.00200 | 0.99798 | 0.00011 | 0.00172 | 0.00200 | 1.11E-07 |
| leu-comp-therm-005-001 | 1.00000 | 0.00230 | 1.00275 | 0.00011 | -0.00275 | 0.00230 | 1.53E-07 |
| leu-comp-therm-005-002 | 1.00000 | 0.00210 | 0.99962 | 0.00011 | 0.00038 | 0.00210 | 1.70E-07 |
| leu-comp-therm-005-003 | 1.00000 | 0.00290 | 0.99914 | 0.00010 | 0.00086 | 0.00290 | 2.41E-07 |
| leu-comp-therm-005-004 | 1.00000 | 0.00250 | 0.99778 | 0.00011 | 0.00222 | 0.00250 | 2.49E-07 |
| leu-comp-therm-005-005 | 1.00000 | 0.00470 | 1.00498 | 0.00011 | -0.00498 | 0.00470 | 6.53E-07 |
| leu-comp-therm-005-006 | 1.00000 | 0.00420 | 1.00536 | 0.00011 | -0.00536 | 0.00420 | 8.06E-07 |
| leu-comp-therm-005-007 | 1.00000 | 0.00430 | 1.00137 | 0.00011 | -0.00137 | 0.00430 | 1.04E-06 |
| leu-comp-therm-005-008 | 1.00000 | 0.00210 | 1.00162 | 0.00011 | -0.00162 | 0.00210 | 1.36E-06 |

| | | | | | | | |
|---|---|---|---|---|---|---|---|
| leu-comp-therm-005-009 | 1.00000 | 0.00400 | 1.00216 | 0.00011 | -0.00216 | 0.00400 | 1.55E-06 |
| leu-comp-therm-005-010 | 1.00000 | 0.00280 | 1.00115 | 0.00011 | -0.00115 | 0.00280 | 1.66E-06 |
| leu-comp-therm-005-011 | 1.00000 | 0.00430 | 1.00172 | 0.00011 | -0.00172 | 0.00430 | 1.68E-06 |
| leu-comp-therm-005-012 | 1.00000 | 0.00660 | 1.00657 | 0.00011 | -0.00657 | 0.00660 | 3.23E-06 |
| leu-comp-therm-005-013 | 1.00000 | 0.00640 | 1.01207 | 0.00010 | -0.01207 | 0.00640 | 4.19E-06 |
| leu-comp-therm-006-001 | 1.00000 | 0.00300 | 0.99993 | 0.00010 | 0.00007 | 0.00300 | 2.41E-07 |
| leu-comp-therm-006-002 | 1.00000 | 0.00300 | 1.00050 | 0.00011 | -0.00050 | 0.00300 | 2.48E-07 |
| leu-comp-therm-006-003 | 1.00000 | 0.00300 | 1.00027 | 0.00010 | -0.00027 | 0.00300 | 2.55E-07 |
| leu-comp-therm-006-004 | 1.00000 | 0.00300 | 1.00021 | 0.00010 | -0.00021 | 0.00300 | 1.86E-07 |
| leu-comp-therm-006-005 | 1.00000 | 0.00300 | 0.99971 | 0.00010 | 0.00029 | 0.00300 | 1.92E-07 |
| leu-comp-therm-006-006 | 1.00000 | 0.00300 | 1.00033 | 0.00010 | -0.00033 | 0.00300 | 1.96E-07 |
| leu-comp-therm-006-007 | 1.00000 | 0.00300 | 1.00000 | 0.00011 | 0.00000 | 0.00300 | 2.02E-07 |
| leu-comp-therm-006-008 | 1.00000 | 0.00300 | 1.00014 | 0.00010 | -0.00014 | 0.00300 | 2.07E-07 |
| leu-comp-therm-006-009 | 1.00000 | 0.00300 | 0.99983 | 0.00010 | 0.00017 | 0.00300 | 1.39E-07 |
| leu-comp-therm-006-010 | 1.00000 | 0.00300 | 0.99977 | 0.00010 | 0.00023 | 0.00300 | 1.43E-07 |
| leu-comp-therm-006-011 | 1.00000 | 0.00300 | 0.99990 | 0.00010 | 0.00010 | 0.00300 | 1.46E-07 |
| leu-comp-therm-006-012 | 1.00000 | 0.00300 | 0.99978 | 0.00010 | 0.00022 | 0.00300 | 1.49E-07 |
| leu-comp-therm-006-013 | 1.00000 | 0.00300 | 0.99952 | 0.00009 | 0.00048 | 0.00300 | 1.53E-07 |
| leu-comp-therm-006-014 | 1.00000 | 0.00300 | 0.99977 | 0.00010 | 0.00023 | 0.00300 | 1.18E-07 |
| leu-comp-therm-006-015 | 1.00000 | 0.00300 | 0.99967 | 0.00010 | 0.00033 | 0.00300 | 1.20E-07 |
| leu-comp-therm-006-016 | 1.00000 | 0.00300 | 0.99973 | 0.00010 | 0.00027 | 0.00300 | 1.23E-07 |
| leu-comp-therm-006-017 | 1.00000 | 0.00300 | 0.99939 | 0.00010 | 0.00061 | 0.00300 | 1.26E-07 |
| leu-comp-therm-006-018 | 1.00000 | 0.00300 | 0.99948 | 0.00010 | 0.00052 | 0.00300 | 1.28E-07 |
| leu-comp-therm-007-001 | 1.00000 | 0.00140 | 0.99765 | 0.00012 | 0.00235 | 0.00141 | 2.46E-07 |
| leu-comp-therm-007-002 | 1.00000 | 0.00080 | 0.99889 | 0.00012 | 0.00111 | 0.00081 | 1.11E-07 |
| **leu-comp-therm-007-003** | **1.00000** | **0.00070** | **0.99764** | **0.00010** | **0.00236** | **0.00071** | **7.25E-08** |
| leu-comp-therm-007-004 | 1.00000 | 0.00080 | 0.99806 | 0.00009 | 0.00194 | 0.00081 | 6.19E-08 |
| leu-comp-therm-007-005 | 1.00000 | 0.00140 | 0.99688 | 0.00011 | 0.00312 | 0.00140 | 2.69E-07 |
| leu-comp-therm-007-006 | 1.00000 | 0.00080 | 0.99877 | 0.00011 | 0.00123 | 0.00081 | 1.12E-07 |
| leu-comp-therm-007-007 | 1.00000 | 0.00070 | 0.99848 | 0.00010 | 0.00152 | 0.00071 | 7.23E-08 |
| leu-comp-therm-007-008 | 1.00000 | 0.00140 | 0.99820 | 0.00011 | 0.00180 | 0.00140 | 2.54E-07 |
| leu-comp-therm-007-009 | 1.00000 | 0.00080 | 0.99815 | 0.00011 | 0.00185 | 0.00081 | 1.12E-07 |
| leu-comp-therm-007-010 | 1.00000 | 0.00070 | 0.99858 | 0.00010 | 0.00142 | 0.00071 | 7.27E-08 |
| leu-comp-therm-008-001 | 1.00070 | 0.00120 | 1.00057 | 0.00009 | 0.00013 | 0.00120 | 2.83E-07 |
| leu-comp-therm-008-002 | 1.00070 | 0.00120 | 1.00108 | 0.00009 | -0.00038 | 0.00120 | 2.50E-07 |
| leu-comp-therm-008-005 | 1.00070 | 0.00120 | 1.00034 | 0.00010 | 0.00036 | 0.00120 | 2.50E-07 |
| leu-comp-therm-008-007 | 1.00070 | 0.00120 | 1.00006 | 0.00009 | 0.00064 | 0.00120 | 2.49E-07 |
| leu-comp-therm-008-008 | 1.00070 | 0.00120 | 0.99980 | 0.00010 | 0.00090 | 0.00120 | 2.47E-07 |
| leu-comp-therm-008-011 | 1.00070 | 0.00120 | 1.00136 | 0.00010 | -0.00066 | 0.00120 | 2.57E-07 |
| leu-comp-therm-009-001 | 1.00000 | 0.00210 | 0.99911 | 0.00010 | 0.00089 | 0.00210 | 1.15E-07 |
| leu-comp-therm-009-002 | 1.00000 | 0.00210 | 0.99894 | 0.00010 | 0.00106 | 0.00210 | 1.15E-07 |
| leu-comp-therm-009-003 | 1.00000 | 0.00210 | 0.99828 | 0.00010 | 0.00172 | 0.00210 | 1.15E-07 |
| leu-comp-therm-009-004 | 1.00000 | 0.00210 | 0.99931 | 0.00010 | 0.00069 | 0.00210 | 1.15E-07 |
| leu-comp-therm-009-005 | 1.00000 | 0.00210 | 0.99960 | 0.00011 | 0.00040 | 0.00210 | 1.16E-07 |
| leu-comp-therm-009-006 | 1.00000 | 0.00210 | 0.99910 | 0.00010 | 0.00090 | 0.00210 | 1.15E-07 |
| leu-comp-therm-009-007 | 1.00000 | 0.00210 | 0.99995 | 0.00011 | 0.00005 | 0.00210 | 1.16E-07 |
| leu-comp-therm-009-008 | 1.00000 | 0.00210 | 0.99888 | 0.00011 | 0.00112 | 0.00210 | 1.15E-07 |
| leu-comp-therm-009-010 | 1.00000 | 0.00210 | 0.99884 | 0.00010 | 0.00116 | 0.00210 | 1.16E-07 |
| leu-comp-therm-009-011 | 1.00000 | 0.00210 | 0.99900 | 0.00010 | 0.00100 | 0.00210 | 1.15E-07 |
| leu-comp-therm-009-013 | 1.00000 | 0.00210 | 0.99944 | 0.00011 | 0.00056 | 0.00210 | 1.15E-07 |
| leu-comp-therm-009-015 | 1.00000 | 0.00210 | 0.99966 | 0.00011 | 0.00034 | 0.00210 | 1.15E-07 |
| leu-comp-therm-009-016 | 1.00000 | 0.00210 | 0.99893 | 0.00010 | 0.00107 | 0.00210 | 1.16E-07 |
| leu-comp-therm-009-017 | 1.00000 | 0.00210 | 0.99951 | 0.00010 | 0.00049 | 0.00210 | 1.15E-07 |
| leu-comp-therm-009-018 | 1.00000 | 0.00210 | 0.99864 | 0.00010 | 0.00136 | 0.00210 | 1.16E-07 |
| leu-comp-therm-009-019 | 1.00000 | 0.00210 | 0.99958 | 0.00010 | 0.00042 | 0.00210 | 1.16E-07 |
| leu-comp-therm-009-020 | 1.00000 | 0.00210 | 0.99893 | 0.00011 | 0.00107 | 0.00210 | 1.16E-07 |
| leu-comp-therm-009-021 | 1.00000 | 0.00210 | 0.99960 | 0.00010 | 0.00040 | 0.00210 | 1.16E-07 |
| leu-comp-therm-009-022 | 1.00000 | 0.00210 | 0.99927 | 0.00011 | 0.00073 | 0.00210 | 1.17E-07 |
| leu-comp-therm-009-023 | 1.00000 | 0.00210 | 1.00000 | 0.00011 | 0.00000 | 0.00210 | 1.16E-07 |
| leu-comp-therm-009-024 | 1.00000 | 0.00210 | 0.99889 | 0.00010 | 0.00111 | 0.00210 | 1.15E-07 |
| leu-comp-therm-009-025 | 1.00000 | 0.00210 | 0.99910 | 0.00011 | 0.00090 | 0.00210 | 1.14E-07 |
| leu-comp-therm-009-026 | 1.00000 | 0.00210 | 0.99932 | 0.00010 | 0.00068 | 0.00210 | 1.15E-07 |
| leu-comp-therm-009-027 | 1.00000 | 0.00210 | 0.99934 | 0.00010 | 0.00066 | 0.00210 | 1.15E-07 |
| leu-comp-therm-010-001 | 1.00000 | 0.00210 | 1.00472 | 0.00010 | -0.00472 | 0.00210 | 1.21E-07 |
| leu-comp-therm-010-002 | 1.00000 | 0.00210 | 1.00512 | 0.00010 | -0.00512 | 0.00210 | 1.18E-07 |
| leu-comp-therm-010-003 | 1.00000 | 0.00210 | 1.00428 | 0.00011 | -0.00428 | 0.00210 | 1.16E-07 |
| leu-comp-therm-010-004 | 1.00000 | 0.00210 | 0.99677 | 0.00011 | 0.00323 | 0.00210 | 1.13E-07 |
| leu-comp-therm-010-005 | 1.00000 | 0.00210 | 0.99969 | 0.00010 | 0.00031 | 0.00210 | 3.59E-07 |
| leu-comp-therm-010-006 | 1.00000 | 0.00210 | 1.00036 | 0.00010 | -0.00036 | 0.00210 | 2.65E-07 |
| leu-comp-therm-010-007 | 1.00000 | 0.00210 | 1.00139 | 0.00010 | -0.00139 | 0.00210 | 2.12E-07 |
| leu-comp-therm-010-008 | 1.00000 | 0.00210 | 0.99800 | 0.00010 | 0.00200 | 0.00210 | 1.87E-07 |

| | | | | | | | |
|---|---|---|---|---|---|---|---|
| leu-comp-therm-010-009 | 1.00000 | 0.00210 | 0.99964 | 0.00010 | 0.00036 | 0.00210 | 1.25E-07 |
| leu-comp-therm-010-010 | 1.00000 | 0.00210 | 1.00030 | 0.00011 | -0.00030 | 0.00210 | 1.21E-07 |
| leu-comp-therm-010-011 | 1.00000 | 0.00210 | 1.00049 | 0.00010 | -0.00049 | 0.00210 | 1.18E-07 |
| leu-comp-therm-010-012 | 1.00000 | 0.00210 | 0.99973 | 0.00011 | 0.00027 | 0.00210 | 1.15E-07 |
| leu-comp-therm-010-013 | 1.00000 | 0.00210 | 0.99761 | 0.00010 | 0.00239 | 0.00210 | 1.13E-07 |
| leu-comp-therm-011-002 | 1.00090 | 0.00320 | 0.99804 | 0.00009 | 0.00286 | 0.00320 | 2.51E-07 |
| leu-comp-therm-011-003 | 1.00090 | 0.00320 | 0.99799 | 0.00010 | 0.00291 | 0.00320 | 1.97E-07 |
| leu-comp-therm-011-007 | 1.00090 | 0.00320 | 0.99841 | 0.00010 | 0.00249 | 0.00320 | 2.01E-07 |
| leu-comp-therm-011-009 | 1.00090 | 0.00320 | 0.99817 | 0.00010 | 0.00273 | 0.00320 | 2.03E-07 |
| leu-comp-therm-011-015 | 1.00100 | 0.00180 | 0.99619 | 0.00009 | 0.00481 | 0.00180 | 1.42E-07 |
| leu-comp-therm-017-001 | 1.00000 | 0.00310 | 1.00136 | 0.00009 | -0.00136 | 0.00310 | 1.00E-07 |
| leu-comp-therm-017-002 | 1.00000 | 0.00310 | 1.00127 | 0.00009 | -0.00127 | 0.00310 | 9.88E-08 |
| leu-comp-therm-017-003 | 1.00000 | 0.00310 | 0.99967 | 0.00009 | 0.00033 | 0.00310 | 9.69E-08 |
| leu-comp-therm-017-004 | 1.00000 | 0.00310 | 0.99820 | 0.00009 | 0.00180 | 0.00310 | 2.05E-07 |
| leu-comp-therm-017-005 | 1.00000 | 0.00310 | 0.99967 | 0.00009 | 0.00033 | 0.00310 | 1.81E-07 |
| leu-comp-therm-017-006 | 1.00000 | 0.00310 | 0.99998 | 0.00009 | 0.00002 | 0.00310 | 1.71E-07 |
| leu-comp-therm-017-007 | 1.00000 | 0.00310 | 0.99976 | 0.00009 | 0.00024 | 0.00310 | 1.62E-07 |
| leu-comp-therm-017-008 | 1.00000 | 0.00310 | 0.99807 | 0.00009 | 0.00193 | 0.00310 | 1.36E-07 |
| leu-comp-therm-017-009 | 1.00000 | 0.00310 | 0.99767 | 0.00009 | 0.00233 | 0.00310 | 1.11E-07 |
| leu-comp-therm-017-010 | 1.00000 | 0.00310 | 0.99824 | 0.00009 | 0.00176 | 0.00310 | 1.02E-07 |
| leu-comp-therm-017-011 | 1.00000 | 0.00310 | 0.99855 | 0.00009 | 0.00145 | 0.00310 | 1.00E-07 |
| leu-comp-therm-017-012 | 1.00000 | 0.00310 | 0.99860 | 0.00009 | 0.00140 | 0.00310 | 9.90E-08 |
| leu-comp-therm-017-013 | 1.00000 | 0.00310 | 0.99895 | 0.00009 | 0.00105 | 0.00310 | 9.76E-08 |
| leu-comp-therm-017-014 | 1.00000 | 0.00310 | 0.99935 | 0.00009 | 0.00065 | 0.00310 | 9.69E-08 |
| leu-comp-therm-022-001 | 1.00000 | 0.00460 | 1.00304 | 0.00012 | -0.00304 | 0.00460 | 6.78E-07 |
| leu-comp-therm-022-002 | 1.00000 | 0.00460 | 1.00694 | 0.00011 | -0.00694 | 0.00460 | 2.87E-07 |
| leu-comp-therm-022-003 | 1.00000 | 0.00360 | 1.00775 | 0.00011 | -0.00775 | 0.00360 | 1.26E-07 |
| leu-comp-therm-022-004 | 1.00000 | 0.00370 | 1.00799 | 0.00011 | -0.00799 | 0.00370 | 8.35E-08 |
| leu-comp-therm-022-005 | 1.00000 | 0.00380 | 1.00334 | 0.00011 | -0.00334 | 0.00380 | 6.94E-08 |
| leu-comp-therm-022-006 | 1.00000 | 0.00460 | 1.00143 | 0.00009 | -0.00143 | 0.00460 | 5.51E-08 |
| leu-comp-therm-022-007 | 1.00000 | 0.00460 | 1.00394 | 0.00009 | -0.00394 | 0.00460 | 5.46E-08 |
| leu-comp-therm-024-001 | 1.00000 | 0.00540 | 1.00125 | 0.00012 | -0.00125 | 0.00540 | 1.01E-06 |
| leu-comp-therm-024-002 | 1.00000 | 0.00540 | 1.00842 | 0.00011 | -0.00842 | 0.00540 | 1.43E-07 |
| leu-comp-therm-025-001 | 1.00000 | 0.00410 | 0.98838 | 0.00011 | 0.01162 | 0.00410 | 4.31E-07 |
| leu-comp-therm-025-002 | 1.00000 | 0.00440 | 0.99581 | 0.00011 | 0.00419 | 0.00440 | 2.01E-07 |
| leu-comp-therm-025-003 | 1.00000 | 0.00470 | 1.00055 | 0.00011 | -0.00055 | 0.00470 | 9.89E-08 |
| leu-comp-therm-025-004 | 1.00000 | 0.00520 | 1.00258 | 0.00010 | -0.00258 | 0.00520 | 6.98E-08 |
| leu-comp-therm-027-001 | 1.00000 | 0.00110 | 1.00425 | 0.00010 | -0.00425 | 0.00110 | 1.29E-07 |
| **leu-comp-therm-027-002** | **1.00000** | **0.00110** | **1.00664** | **0.00011** | **-0.00664** | **0.00111** | **1.23E-07** |
| **leu-comp-therm-027-003** | **1.00000** | **0.00110** | **1.00699** | **0.00011** | **-0.00699** | **0.00111** | **1.17E-07** |
| **leu-comp-therm-027-004** | **1.00000** | **0.00110** | **1.00921** | **0.00011** | **-0.00921** | **0.00111** | **1.12E-07** |
| leu-comp-therm-028-001 | 0.99980 | 0.00470 | 0.99816 | 0.00011 | 0.00164 | 0.00470 | 2.11E-07 |
| leu-comp-therm-028-002 | 1.00010 | 0.00540 | 0.99927 | 0.00011 | 0.00083 | 0.00540 | 2.35E-07 |
| leu-comp-therm-028-003 | 0.99990 | 0.00510 | 0.99872 | 0.00011 | 0.00118 | 0.00510 | 2.54E-07 |
| leu-comp-therm-028-004 | 1.00000 | 0.00430 | 1.00117 | 0.00011 | -0.00117 | 0.00430 | 2.67E-07 |
| leu-comp-therm-028-005 | 1.00020 | 0.00480 | 1.00000 | 0.00010 | 0.00020 | 0.00480 | 2.31E-07 |
| leu-comp-therm-028-006 | 1.00010 | 0.00450 | 1.00114 | 0.00010 | -0.00104 | 0.00450 | 2.57E-07 |
| leu-comp-therm-028-007 | 0.99980 | 0.00470 | 0.99618 | 0.00011 | 0.00362 | 0.00470 | 2.35E-07 |
| leu-comp-therm-028-008 | 0.99980 | 0.00520 | 0.99401 | 0.00010 | 0.00579 | 0.00520 | 2.55E-07 |
| leu-comp-therm-028-009 | 0.99980 | 0.00470 | 0.99263 | 0.00011 | 0.00717 | 0.00470 | 2.73E-07 |
| leu-comp-therm-028-010 | 1.00040 | 0.00450 | 0.99754 | 0.00010 | 0.00286 | 0.00450 | 1.23E-07 |
| leu-comp-therm-028-011 | 1.00020 | 0.00450 | 0.99794 | 0.00010 | 0.00226 | 0.00450 | 1.31E-07 |
| leu-comp-therm-028-012 | 1.00000 | 0.00490 | 0.99616 | 0.00010 | 0.00384 | 0.00490 | 1.42E-07 |
| leu-comp-therm-028-013 | 0.99980 | 0.00500 | 0.99506 | 0.00010 | 0.00474 | 0.00500 | 1.33E-07 |
| leu-comp-therm-028-014 | 1.00010 | 0.00470 | 0.99292 | 0.00010 | 0.00718 | 0.00470 | 1.43E-07 |
| leu-comp-therm-028-015 | 0.99970 | 0.00440 | 0.99781 | 0.00009 | 0.00189 | 0.00440 | 9.51E-08 |
| leu-comp-therm-028-016 | 1.00000 | 0.00490 | 0.99836 | 0.00008 | 0.00164 | 0.00490 | 9.75E-08 |
| leu-comp-therm-028-017 | 1.00000 | 0.00470 | 0.99832 | 0.00010 | 0.00168 | 0.00470 | 1.03E-07 |
| leu-comp-therm-028-018 | 0.99990 | 0.00470 | 0.99868 | 0.00010 | 0.00122 | 0.00470 | 1.01E-07 |
| leu-comp-therm-028-019 | 1.00020 | 0.00460 | 0.99800 | 0.00009 | 0.00220 | 0.00460 | 9.86E-08 |
| leu-comp-therm-028-020 | 1.00010 | 0.00460 | 0.99575 | 0.00009 | 0.00435 | 0.00460 | 1.01E-07 |
| leu-comp-therm-035-001 | 1.00000 | 0.00180 | 0.99993 | 0.00010 | 0.00007 | 0.00180 | 2.11E-07 |
| leu-comp-therm-035-002 | 1.00000 | 0.00190 | 0.99918 | 0.00011 | 0.00082 | 0.00190 | 2.14E-07 |
| leu-comp-therm-035-003 | 1.00000 | 0.00220 | 0.99533 | 0.00010 | 0.00467 | 0.00220 | 2.12E-07 |
| leu-comp-therm-039-001 | 1.00000 | 0.00140 | 0.99737 | 0.00011 | 0.00263 | 0.00140 | 2.26E-07 |
| leu-comp-therm-039-002 | 1.00000 | 0.00140 | 0.99793 | 0.00011 | 0.00207 | 0.00140 | 2.16E-07 |
| leu-comp-therm-039-003 | 1.00000 | 0.00140 | 0.99739 | 0.00012 | 0.00261 | 0.00141 | 1.96E-07 |
| leu-comp-therm-039-004 | 1.00000 | 0.00140 | 0.99642 | 0.00012 | 0.00358 | 0.00141 | 1.88E-07 |
| leu-comp-therm-039-005 | 1.00000 | 0.00090 | 0.99752 | 0.00011 | 0.00248 | 0.00091 | 1.43E-07 |
| leu-comp-therm-039-006 | 1.00000 | 0.00090 | 0.99725 | 0.00011 | 0.00275 | 0.00091 | 1.49E-07 |
| leu-comp-therm-039-007 | 1.00000 | 0.00120 | 0.99675 | 0.00012 | 0.00325 | 0.00121 | 2.17E-07 |

| | | | | | | | |
|---|---|---|---|---|---|---|---|
| leu-comp-therm-039-008 | 1.00000 | 0.00120 | 0.99722 | 0.00011 | 0.00278 | 0.00121 | 2.07E-07 |
| leu-comp-therm-039-009 | 1.00000 | 0.00120 | 0.99681 | 0.00012 | 0.00319 | 0.00121 | 2.02E-07 |
| leu-comp-therm-039-010 | 1.00000 | 0.00120 | 0.99762 | 0.00011 | 0.00238 | 0.00121 | 1.77E-07 |
| leu-comp-therm-060-001 | 0.99900 | 0.00260 | 0.99866 | 0.00013 | 0.00034 | 0.00260 | 9.51E-08 |
| leu-comp-therm-060-002 | 0.99770 | 0.00260 | 0.99731 | 0.00014 | 0.00039 | 0.00260 | 1.53E-07 |
| leu-comp-therm-060-003 | 1.00010 | 0.00260 | 0.99984 | 0.00014 | 0.00026 | 0.00260 | 1.03E-07 |
| leu-comp-therm-060-004 | 1.00170 | 0.00260 | 0.99947 | 0.00016 | 0.00223 | 0.00260 | 1.66E-07 |
| leu-comp-therm-060-005 | 1.00090 | 0.00260 | 1.00148 | 0.00015 | -0.00058 | 0.00260 | 1.10E-07 |
| leu-comp-therm-060-006 | 0.98940 | 0.00270 | 0.98869 | 0.00018 | 0.00071 | 0.00271 | 1.82E-07 |
| leu-comp-therm-079-001 | 0.99990 | 0.00160 | 0.99818 | 0.00011 | 0.00172 | 0.00160 | 3.01E-07 |
| leu-comp-therm-079-002 | 1.00020 | 0.00160 | 0.99851 | 0.00011 | 0.00169 | 0.00160 | 3.01E-07 |
| leu-comp-therm-079-003 | 1.00050 | 0.00160 | 0.99900 | 0.00011 | 0.00150 | 0.00160 | 3.05E-07 |
| leu-comp-therm-079-004 | 1.00040 | 0.00160 | 0.99950 | 0.00011 | 0.00090 | 0.00160 | 3.08E-07 |
| leu-comp-therm-079-005 | 1.00040 | 0.00160 | 0.99962 | 0.00012 | 0.00078 | 0.00160 | 3.14E-07 |
| leu-comp-therm-079-006 | 0.99940 | 0.00080 | 0.99837 | 0.00011 | 0.00103 | 0.00081 | 1.10E-07 |
| leu-comp-therm-079-007 | 1.00030 | 0.00080 | 0.99778 | 0.00011 | 0.00252 | 0.00081 | 1.10E-07 |
| leu-comp-therm-079-008 | 1.00080 | 0.00080 | 0.99904 | 0.00011 | 0.00176 | 0.00081 | 1.11E-07 |
| leu-comp-therm-079-009 | 1.00030 | 0.00080 | 0.99858 | 0.00011 | 0.00172 | 0.00081 | 1.12E-07 |
| leu-comp-therm-079-010 | 1.00090 | 0.00080 | 0.99951 | 0.00011 | 0.00139 | 0.00081 | 1.13E-07 |
| leu-sol-therm-002-001 | 1.00380 | 0.00400 | 0.99994 | 0.00008 | 0.00386 | 0.00400 | 3.81E-08 |
| leu-sol-therm-002-002 | 1.00240 | 0.00370 | 0.99586 | 0.00009 | 0.00654 | 0.00370 | 4.00E-08 |
| leu-sol-therm-004-001 | 0.99940 | 0.00080 | 1.00042 | 0.00010 | -0.00102 | 0.00081 | 4.15E-08 |
| leu-sol-therm-004-002 | 0.99990 | 0.00090 | 1.00178 | 0.00009 | -0.00188 | 0.00090 | 4.04E-08 |
| leu-sol-therm-004-003 | 0.99990 | 0.00090 | 0.99968 | 0.00009 | 0.00022 | 0.00090 | 3.93E-08 |
| leu-sol-therm-004-004 | 0.99990 | 0.00100 | 1.00194 | 0.00008 | -0.00204 | 0.00100 | 3.85E-08 |
| leu-sol-therm-004-005 | 0.99990 | 0.00100 | 1.00190 | 0.00009 | -0.00200 | 0.00100 | 3.79E-08 |
| leu-sol-therm-004-006 | 0.99940 | 0.00110 | 1.00107 | 0.00008 | -0.00167 | 0.00110 | 3.74E-08 |
| leu-sol-therm-004-007 | 0.99960 | 0.00110 | 1.00118 | 0.00008 | -0.00158 | 0.00110 | 3.71E-08 |
| **leu-sol-therm-007-001** | **0.99940** | **0.00080** | **0.99539** | **0.00010** | **0.00401** | **0.00081** | **4.22E-08** |
| leu-sol-therm-007-002 | 0.99940 | 0.00080 | 0.99742 | 0.00010 | 0.00198 | 0.00081 | 4.09E-08 |
| **leu-sol-therm-007-003** | **0.99940** | **0.00080** | **0.99617** | **0.00009** | **0.00323** | **0.00081** | **3.96E-08** |
| leu-sol-therm-007-004 | 0.99940 | 0.00080 | 0.99866 | 0.00009 | 0.00074 | 0.00081 | 3.88E-08 |
| leu-sol-therm-007-005 | 0.99940 | 0.00080 | 0.99742 | 0.00009 | 0.00198 | 0.00081 | 3.82E-08 |
| leu-sol-therm-007-014 | 0.99610 | 0.00090 | 0.99479 | 0.00010 | 0.00131 | 0.00091 | 4.22E-08 |
| leu-sol-therm-007-030 | 0.99730 | 0.00090 | 0.99741 | 0.00009 | -0.00011 | 0.00090 | 4.09E-08 |
| leu-sol-therm-007-032 | 0.99850 | 0.00100 | 0.99626 | 0.00009 | 0.00224 | 0.00100 | 3.96E-08 |
| leu-sol-therm-007-036 | 0.99880 | 0.00110 | 0.99902 | 0.00009 | -0.00022 | 0.00110 | 3.88E-08 |
| leu-sol-therm-007-049 | 0.99830 | 0.00110 | 0.99753 | 0.00008 | 0.00077 | 0.00110 | 3.82E-08 |
| leu-sol-therm-020-001 | 0.99950 | 0.00100 | 1.00007 | 0.00009 | -0.00057 | 0.00100 | 3.75E-08 |
| leu-sol-therm-020-002 | 0.99960 | 0.00100 | 0.99959 | 0.00008 | 0.00001 | 0.00100 | 3.66E-08 |
| leu-sol-therm-020-003 | 0.99970 | 0.00120 | 0.99898 | 0.00007 | 0.00072 | 0.00120 | 3.57E-08 |
| leu-sol-therm-020-004 | 0.99980 | 0.00120 | 1.00005 | 0.00007 | -0.00025 | 0.00120 | 3.52E-08 |
| leu-sol-therm-021-001 | 0.99830 | 0.00090 | 0.99775 | 0.00009 | 0.00055 | 0.00090 | 3.77E-08 |
| leu-sol-therm-021-002 | 0.99850 | 0.00100 | 0.99821 | 0.00008 | 0.00029 | 0.00100 | 3.68E-08 |
| leu-sol-therm-021-003 | 0.99890 | 0.00110 | 0.99732 | 0.00008 | 0.00158 | 0.00110 | 3.58E-08 |
| leu-sol-therm-021-004 | 0.99930 | 0.00120 | 0.99947 | 0.00007 | -0.00017 | 0.00120 | 3.53E-08 |
| mix-comp-fast-001-001 | 0.98660 | 0.00230 | 0.98716 | 0.00007 | -0.00056 | 0.00230 | 1.15E-01 |
| mix-comp-fast-002-001 | 0.98740 | 0.00220 | 0.98544 | 0.00007 | 0.00196 | 0.00220 | 1.19E-01 |
| mix-comp-inter-005-001 | 1.16020 | 0.00550 | 1.16715 | 0.00009 | -0.00695 | 0.00550 | 1.59E-04 |
| mix-comp-therm-001-001 | 1.00000 | 0.00250 | 1.00086 | 0.00012 | -0.00086 | 0.00250 | 9.59E-07 |
| mix-comp-therm-001-002 | 1.00000 | 0.00260 | 0.99988 | 0.00011 | 0.00012 | 0.00260 | 2.74E-07 |
| mix-comp-therm-001-003 | 1.00000 | 0.00320 | 0.99968 | 0.00012 | 0.00032 | 0.00320 | 1.64E-07 |
| mix-comp-therm-001-004 | 1.00000 | 0.00390 | 1.00138 | 0.00011 | -0.00138 | 0.00390 | 1.15E-07 |
| mix-comp-therm-002-001 | 1.00100 | 0.00590 | 1.00099 | 0.00011 | 0.00001 | 0.00590 | 5.53E-07 |
| mix-comp-therm-002-002 | 1.00090 | 0.00450 | 1.00155 | 0.00011 | -0.00065 | 0.00450 | 7.35E-07 |
| mix-comp-therm-002-003 | 1.00240 | 0.00290 | 1.00242 | 0.00011 | -0.00002 | 0.00290 | 1.90E-07 |
| mix-comp-therm-002-004 | 1.00240 | 0.00210 | 1.00594 | 0.00011 | -0.00354 | 0.00210 | 2.78E-07 |
| mix-comp-therm-002-005 | 1.00380 | 0.00220 | 1.00348 | 0.00010 | 0.00032 | 0.00220 | 1.37E-07 |
| mix-comp-therm-003-001 | 1.00000 | 0.00710 | 1.00010 | 0.00011 | -0.00010 | 0.00710 | 8.61E-07 |
| mix-comp-therm-003-002 | 1.00000 | 0.00570 | 1.00067 | 0.00012 | -0.00067 | 0.00570 | 5.27E-07 |
| mix-comp-therm-003-003 | 1.00000 | 0.00520 | 1.00346 | 0.00013 | -0.00346 | 0.00520 | 6.17E-07 |
| mix-comp-therm-003-004 | 1.00000 | 0.00240 | 1.00003 | 0.00012 | -0.00003 | 0.00240 | 1.84E-07 |
| mix-comp-therm-003-005 | 1.00000 | 0.00280 | 1.00030 | 0.00011 | -0.00030 | 0.00280 | 1.54E-07 |
| mix-comp-therm-003-006 | 1.00000 | 0.00200 | 1.00096 | 0.00011 | -0.00096 | 0.00200 | 1.01E-07 |
| mix-met-fast-001-001 | 1.00000 | 0.00160 | 0.99951 | 0.00008 | 0.00049 | 0.00160 | 1.11E+00 |
| mix-met-fast-002-001 | 1.00000 | 0.00420 | 1.00529 | 0.00010 | -0.00529 | 0.00420 | 8.46E-01 |
| mix-met-fast-002-002 | 1.00000 | 0.00440 | 1.00520 | 0.00010 | -0.00520 | 0.00440 | 8.42E-01 |
| mix-met-fast-002-003 | 1.00000 | 0.00480 | 1.00549 | 0.00010 | -0.00549 | 0.00480 | 8.29E-01 |
| mix-met-fast-003-001 | 0.99930 | 0.00170 | 1.00080 | 0.00009 | -0.00150 | 0.00170 | 1.08E+00 |
| mix-met-fast-004-001 | 0.99930 | 0.00130 | 1.00050 | 0.00009 | -0.00120 | 0.00130 | 8.07E-01 |
| mix-met-fast-004-002 | 0.99930 | 0.00130 | 0.99939 | 0.00009 | -0.00009 | 0.00130 | 8.12E-01 |

| | | | | | | | |
|---|---|---|---|---|---|---|---|
| mix-met-fast-005-001 | 0.99900 | 0.00170 | 1.00393 | 0.00009 | -0.00493 | 0.00170 | 1.05E+00 |
| mix-met-fast-007-001 | 1.00000 | 0.00450 | 1.00313 | 0.00011 | -0.00313 | 0.00450 | 6.24E-02 |
| **mix-met-fast-007-002** | **1.00000** | **0.00230** | **1.00794** | **0.00011** | **-0.00794** | **0.00230** | **9.32E-02** |
| mix-met-fast-007-003 | 1.00000 | 0.00280 | 1.00645 | 0.00010 | -0.00645 | 0.00280 | 3.39E-01 |
| mix-met-fast-007-004 | 1.00000 | 0.00280 | 1.00536 | 0.00010 | -0.00536 | 0.00280 | 5.62E-01 |
| mix-met-fast-007-005 | 1.00000 | 0.00320 | 1.00246 | 0.00009 | -0.00246 | 0.00320 | 7.68E-01 |
| mix-met-fast-007-006 | 1.00000 | 0.00350 | 1.00101 | 0.00009 | -0.00101 | 0.00350 | 8.51E-01 |
| mix-met-fast-007-007 | 1.00000 | 0.00320 | 1.00611 | 0.00011 | -0.00611 | 0.00320 | 1.00E-01 |
| mix-met-fast-007-008 | 1.00000 | 0.00300 | 1.00507 | 0.00011 | -0.00507 | 0.00300 | 1.73E-01 |
| mix-met-fast-007-009 | 1.00000 | 0.00280 | 1.00510 | 0.00010 | -0.00510 | 0.00280 | 2.61E-01 |
| mix-met-fast-007-010 | 1.00000 | 0.00270 | 1.00506 | 0.00010 | -0.00506 | 0.00270 | 5.73E-01 |
| mix-met-fast-007-011 | 1.00000 | 0.00260 | 1.00373 | 0.00010 | -0.00373 | 0.00260 | 7.41E-01 |
| mix-met-fast-007-012 | 1.00000 | 0.00300 | 1.00261 | 0.00009 | -0.00261 | 0.00300 | 8.74E-01 |
| mix-met-fast-007-013 | 1.00000 | 0.00330 | 1.00073 | 0.00009 | -0.00073 | 0.00330 | 9.32E-01 |
| mix-met-fast-007-014 | 1.00000 | 0.00320 | 1.00804 | 0.00010 | -0.00804 | 0.00320 | 3.30E-01 |
| mix-met-fast-007-015 | 1.00000 | 0.00320 | 1.00757 | 0.00010 | -0.00757 | 0.00320 | 4.46E-01 |
| mix-met-fast-007-016 | 1.00000 | 0.00280 | 1.00588 | 0.00009 | -0.00588 | 0.00280 | 7.36E-01 |
| mix-met-fast-007-017 | 1.00000 | 0.00280 | 1.00594 | 0.00009 | -0.00594 | 0.00280 | 8.53E-01 |
| mix-met-fast-007-018 | 1.00000 | 0.00300 | 1.00798 | 0.00009 | -0.00798 | 0.00300 | 9.42E-01 |
| mix-met-fast-007-019 | 1.00000 | 0.00340 | 1.00696 | 0.00009 | -0.00696 | 0.00340 | 8.58E-01 |
| mix-met-fast-007-020 | 1.00000 | 0.00300 | 1.00473 | 0.00009 | -0.00473 | 0.00300 | 9.47E-01 |
| mix-met-fast-007-021 | 1.00000 | 0.00310 | 1.00504 | 0.00009 | -0.00504 | 0.00310 | 1.01E+00 |
| mix-met-fast-007-022 | 1.00000 | 0.00300 | 1.00403 | 0.00009 | -0.00403 | 0.00300 | 9.61E-01 |
| mix-met-fast-007-023 | 1.00000 | 0.00280 | 1.00336 | 0.00009 | -0.00336 | 0.00280 | 1.02E+00 |
| mix-met-fast-009-001 | 1.00000 | 0.00100 | 1.00006 | 0.00008 | -0.00006 | 0.00100 | 1.18E+00 |
| mix-met-fast-010-001 | 1.00000 | 0.00090 | 0.99980 | 0.00009 | 0.00020 | 0.00090 | 1.00E+00 |
| mix-met-mixed-001-001 | 0.99910 | 0.00130 | 0.99973 | 0.00012 | -0.00063 | 0.00131 | 3.20E-03 |
| mix-sol-therm-001-001 | 1.00000 | 0.00160 | 0.99514 | 0.00013 | 0.00486 | 0.00161 | 1.58E-07 |
| mix-sol-therm-001-002 | 1.00000 | 0.00160 | 0.99507 | 0.00012 | 0.00493 | 0.00160 | 1.59E-07 |
| **mix-sol-therm-001-003** | **1.00000** | **0.00160** | **0.98879** | **0.00013** | **0.01121** | **0.00161** | **1.55E-07** |
| **mix-sol-therm-001-004** | **1.00000** | **0.00160** | **0.99435** | **0.00012** | **0.00565** | **0.00160** | **1.68E-07** |
| mix-sol-therm-001-005 | 1.00000 | 0.00160 | 0.99793 | 0.00012 | 0.00207 | 0.00160 | 1.72E-07 |
| mix-sol-therm-001-006 | 1.00000 | 0.00160 | 0.99557 | 0.00012 | 0.00443 | 0.00160 | 1.67E-07 |
| mix-sol-therm-001-007 | 1.00000 | 0.00160 | 1.00026 | 0.00013 | -0.00026 | 0.00161 | 2.78E-07 |
| mix-sol-therm-001-008 | 1.00000 | 0.00160 | 0.99963 | 0.00013 | 0.00037 | 0.00161 | 1.46E-07 |
| mix-sol-therm-001-009 | 1.00000 | 0.00160 | 0.99913 | 0.00012 | 0.00087 | 0.00160 | 9.08E-08 |
| mix-sol-therm-001-010 | 1.00000 | 0.00160 | 0.99971 | 0.00012 | 0.00029 | 0.00160 | 1.14E-07 |
| **mix-sol-therm-001-011** | **1.00000** | **0.00520** | **1.03581** | **0.00012** | **-0.03581** | **0.00520** | **1.08E-07** |
| **mix-sol-therm-003-001** | **0.99850** | **0.00200** | **1.01250** | **0.00013** | **-0.01400** | **0.00013** | **1.36E-07** |
| **mix-sol-therm-003-002** | **0.99600** | **0.00200** | **1.01012** | **0.00013** | **-0.01412** | **0.00013** | **1.40E-07** |
| **mix-sol-therm-003-003** | **0.99350** | **0.00200** | **1.00927** | **0.00013** | **-0.01577** | **0.00013** | **1.41E-07** |
| **mix-sol-therm-003-004** | **0.99090** | **0.00200** | **1.00201** | **0.00013** | **-0.01111** | **0.00013** | **1.41E-07** |
| mix-sol-therm-003-005 | 0.99810 | 0.00220 | 1.00386 | 0.00011 | -0.00576 | 0.00011 | 5.88E-08 |
| **mix-sol-therm-003-006** | **0.99590** | **0.00220** | **1.00708** | **0.00012** | **-0.01118** | **0.00012** | **5.91E-08** |
| **mix-sol-therm-003-007** | **0.99350** | **0.00200** | **1.00231** | **0.00012** | **-0.00881** | **0.00012** | **5.93E-08** |
| **mix-sol-therm-003-008** | **0.99880** | **0.00250** | **1.00655** | **0.00009** | **-0.00775** | **0.00009** | **4.79E-08** |
| mix-sol-therm-003-009 | 0.99580 | 0.00250 | 1.00328 | 0.00010 | -0.00748 | 0.00010 | 4.81E-08 |
| mix-sol-therm-003-010 | 0.99640 | 0.00250 | 1.00337 | 0.00009 | -0.00697 | 0.00009 | 4.72E-08 |
| pu-comp-fast-004-001 | 1.00040 | 0.00440 | 0.99324 | 0.00009 | 0.00716 | 0.00440 | 6.38E-01 |
| pu-comp-inter-001-001 | 1.00000 | 0.01100 | 1.01174 | 0.00007 | -0.01174 | 0.01100 | 2.97E-04 |
| **pu-comp-mixed-001-001** | **0.99860** | **0.00410** | **1.02477** | **0.00009** | **-0.02617** | **0.00410** | **9.69E-01** |
| **pu-comp-mixed-001-002** | **1.00000** | **0.00680** | **1.02778** | **0.00013** | **-0.02778** | **0.00680** | **1.68E-03** |
| **pu-comp-mixed-001-003** | **0.99900** | **0.00670** | **1.02390** | **0.00013** | **-0.02490** | **0.00670** | **3.16E-05** |
| pu-comp-mixed-001-004 | 1.00000 | 0.00660 | 0.99344 | 0.00013 | 0.00656 | 0.00660 | 3.86E-05 |
| pu-comp-mixed-001-005 | 0.99890 | 0.00720 | 0.98030 | 0.00014 | 0.01860 | 0.00720 | 1.75E-06 |
| **pu-comp-mixed-002-001** | **0.99900** | **0.00460** | **1.03110** | **0.00012** | **-0.03210** | **0.00460** | **5.02E-03** |
| **pu-comp-mixed-002-002** | **0.99900** | **0.00460** | **1.02940** | **0.00012** | **-0.03040** | **0.00460** | **4.33E-03** |
| **pu-comp-mixed-002-003** | **0.99900** | **0.00460** | **1.02466** | **0.00011** | **-0.02566** | **0.00460** | **3.58E-03** |
| **pu-comp-mixed-002-004** | **0.99900** | **0.00460** | **1.01474** | **0.00012** | **-0.01574** | **0.00460** | **2.88E-03** |
| **pu-comp-mixed-002-005** | **0.99900** | **0.00460** | **1.01479** | **0.00012** | **-0.01579** | **0.00460** | **1.94E-03** |
| **pu-comp-mixed-002-006** | **1.00000** | **0.00750** | **1.02531** | **0.00012** | **-0.02531** | **0.00750** | **9.51E-05** |
| **pu-comp-mixed-002-007** | **1.00000** | **0.00750** | **1.02368** | **0.00012** | **-0.02368** | **0.00750** | **8.70E-05** |
| pu-comp-mixed-002-008 | 1.00000 | 0.00750 | 1.02227 | 0.00013 | -0.02227 | 0.00750 | 7.02E-05 |
| pu-comp-mixed-002-009 | 1.00000 | 0.00750 | 1.02258 | 0.00013 | -0.02258 | 0.00750 | 5.89E-05 |
| **pu-comp-mixed-002-010** | **1.00000** | **0.00730** | **1.03211** | **0.00013** | **-0.03211** | **0.00730** | **4.26E-06** |
| **pu-comp-mixed-002-011** | **1.00000** | **0.00730** | **1.02949** | **0.00013** | **-0.02949** | **0.00730** | **4.67E-06** |
| **pu-comp-mixed-002-012** | **1.00000** | **0.00730** | **1.02973** | **0.00012** | **-0.02973** | **0.00730** | **5.26E-06** |
| **pu-comp-mixed-002-013** | **1.00000** | **0.00730** | **1.02782** | **0.00014** | **-0.02782** | **0.00730** | **5.56E-06** |
| **pu-comp-mixed-002-014** | **1.00000** | **0.00730** | **1.03191** | **0.00013** | **-0.03191** | **0.00730** | **5.71E-06** |
| **pu-comp-mixed-002-015** | **1.00000** | **0.00730** | **1.02977** | **0.00013** | **-0.02977** | **0.00730** | **5.69E-06** |
| **pu-comp-mixed-002-016** | **1.00000** | **0.00730** | **1.02553** | **0.00013** | **-0.02553** | **0.00730** | **5.28E-06** |

| | | | | | | | |
|---|---|---|---|---|---|---|---|
| pu-comp-mixed-002-017 | 0.99880 | 0.00550 | 1.00738 | 0.00013 | -0.00858 | 0.00550 | 5.07E-06 |
| pu-comp-mixed-002-018 | 0.99880 | 0.00550 | 1.01126 | 0.00012 | -0.01246 | 0.00550 | 6.35E-06 |
| pu-comp-mixed-002-019 | 0.99880 | 0.00550 | 1.01046 | 0.00013 | -0.01166 | 0.00550 | 6.64E-06 |
| pu-comp-mixed-002-020 | 0.99880 | 0.00550 | 1.01050 | 0.00013 | -0.01170 | 0.00550 | 6.81E-06 |
| pu-comp-mixed-002-021 | 0.99880 | 0.00550 | 1.01119 | 0.00012 | -0.01239 | 0.00550 | 6.82E-06 |
| pu-comp-mixed-002-022 | 0.99880 | 0.00550 | 1.01511 | 0.00013 | -0.01631 | 0.00550 | 6.60E-06 |
| pu-comp-mixed-002-023 | 1.00000 | 0.00680 | 1.00690 | 0.00012 | -0.00690 | 0.00680 | 7.08E-07 |
| pu-comp-mixed-002-024 | 1.00000 | 0.00680 | 1.00761 | 0.00013 | -0.00761 | 0.00680 | 7.21E-07 |
| pu-comp-mixed-002-025 | 1.00000 | 0.00680 | 1.00764 | 0.00014 | -0.00764 | 0.00680 | 7.29E-07 |
| pu-comp-mixed-002-026 | 1.00000 | 0.00680 | 1.00871 | 0.00014 | -0.00871 | 0.00680 | 7.36E-07 |
| pu-comp-mixed-002-027 | 1.00000 | 0.00680 | 1.00917 | 0.00013 | -0.00917 | 0.00680 | 7.47E-07 |
| pu-comp-mixed-002-028 | 1.00000 | 0.00680 | 1.00916 | 0.00013 | -0.00916 | 0.00680 | 7.52E-07 |
| pu-comp-mixed-002-029 | 1.00000 | 0.00680 | 1.01014 | 0.00013 | -0.01014 | 0.00680 | 7.60E-07 |
| pu-met-fast-001-001 | 1.00000 | 0.00200 | 1.00001 | 0.00008 | -0.00001 | 0.00200 | 1.25E+00 |
| pu-met-fast-002-001 | 1.00000 | 0.00200 | 1.00000 | 0.00008 | 0.00000 | 0.00200 | 1.27E+00 |
| pu-met-fast-003-103 | 1.00000 | 0.00300 | 0.99873 | 0.00009 | 0.00127 | 0.00300 | 1.24E+00 |
| pu-met-fast-005-001 | 1.00000 | 0.00130 | 1.00125 | 0.00009 | -0.00125 | 0.00130 | 1.01E+00 |
| pu-met-fast-006-001 | 1.00000 | 0.00300 | 1.00107 | 0.00010 | -0.00107 | 0.00300 | 1.06E+00 |
| pu-met-fast-008-001 | 1.00000 | 0.00060 | 0.99814 | 0.00008 | 0.00186 | 0.00061 | 1.07E+00 |
| pu-met-fast-009-001 | 1.00000 | 0.00270 | 1.00573 | 0.00009 | -0.00573 | 0.00270 | 1.14E+00 |
| pu-met-fast-010-001 | 1.00000 | 0.00180 | 0.99968 | 0.00009 | 0.00032 | 0.00180 | 1.17E+00 |
| pu-met-fast-011-001 | 1.00000 | 0.00100 | 1.00014 | 0.00011 | -0.00014 | 0.00101 | 8.24E-02 |
| pu-met-fast-012-001 | 1.00090 | 0.00210 | 1.00300 | 0.00010 | -0.00210 | 0.00210 | 9.50E-01 |
| pu-met-fast-013-001 | 1.00340 | 0.00230 | 1.00820 | 0.00009 | -0.00480 | 0.00230 | 7.83E-01 |
| pu-met-fast-014-001 | 1.00370 | 0.00310 | 1.00646 | 0.00010 | -0.00276 | 0.00310 | 7.91E-01 |
| pu-met-fast-015-001 | 1.00410 | 0.00260 | 0.99995 | 0.00009 | 0.00415 | 0.00260 | 9.62E-01 |
| **pu-met-fast-016-001** | **0.99760** | **0.00420** | **1.01764** | **0.00012** | **-0.02004** | **0.00420** | **1.12E-02** |
| pu-met-fast-016-002 | 1.00000 | 0.00380 | 1.00711 | 0.00011 | -0.00711 | 0.00380 | 8.02E-03 |
| pu-met-fast-016-003 | 1.00000 | 0.00330 | 1.00513 | 0.00011 | -0.00513 | 0.00330 | 7.71E-03 |
| pu-met-fast-016-004 | 1.00000 | 0.00300 | 1.00478 | 0.00011 | -0.00478 | 0.00300 | 7.47E-03 |
| pu-met-fast-016-005 | 1.00000 | 0.00340 | 1.00455 | 0.00011 | -0.00455 | 0.00340 | 7.35E-03 |
| pu-met-fast-016-006 | 1.00000 | 0.00320 | 1.00681 | 0.00010 | -0.00681 | 0.00320 | 7.33E-03 |
| pu-met-fast-018-001 | 1.00000 | 0.00300 | 0.99938 | 0.00009 | 0.00062 | 0.00300 | 9.09E-01 |
| pu-met-fast-019-001 | 0.99920 | 0.00150 | 1.00098 | 0.00010 | -0.00178 | 0.00150 | 7.71E-01 |
| pu-met-fast-020-001 | 0.99930 | 0.00170 | 0.99789 | 0.00009 | 0.00141 | 0.00170 | 1.13E+00 |
| pu-met-fast-021-001 | 1.00000 | 0.00260 | 1.00458 | 0.00009 | -0.00458 | 0.00260 | 7.81E-01 |
| pu-met-fast-021-002 | 1.00000 | 0.00260 | 0.99341 | 0.00010 | 0.00659 | 0.00260 | 8.66E-01 |
| pu-met-fast-022-001 | 1.00000 | 0.00210 | 0.99830 | 0.00008 | 0.00170 | 0.00210 | 1.24E+00 |
| pu-met-fast-023-001 | 1.00000 | 0.00220 | 0.99998 | 0.00009 | 0.00002 | 0.00220 | 1.14E+00 |
| pu-met-fast-024-001 | 1.00000 | 0.00220 | 1.00176 | 0.00009 | -0.00176 | 0.00220 | 6.37E-01 |
| pu-met-fast-025-001 | 1.00000 | 0.00220 | 0.99886 | 0.00009 | 0.00114 | 0.00220 | 1.19E+00 |
| pu-met-fast-026-001 | 1.00000 | 0.00220 | 0.99867 | 0.00009 | 0.00133 | 0.00220 | 1.09E+00 |
| pu-met-fast-027-001 | 1.00000 | 0.00240 | 1.00321 | 0.00010 | -0.00321 | 0.00240 | 7.16E-02 |
| pu-met-fast-028-001 | 1.00000 | 0.00240 | 0.99911 | 0.00009 | 0.00089 | 0.00240 | 1.07E+00 |
| pu-met-fast-029-001 | 1.00000 | 0.00240 | 0.99580 | 0.00008 | 0.00420 | 0.00240 | 1.25E+00 |
| pu-met-fast-030-001 | 1.00000 | 0.00230 | 1.00325 | 0.00009 | -0.00325 | 0.00230 | 1.14E+00 |
| pu-met-fast-031-001 | 1.00000 | 0.00230 | 1.00441 | 0.00010 | -0.00441 | 0.00230 | 1.85E-01 |
| pu-met-fast-032-001 | 1.00000 | 0.00220 | 0.99855 | 0.00009 | 0.00145 | 0.00220 | 1.17E+00 |
| pu-met-fast-035-001 | 1.00000 | 0.00160 | 0.99770 | 0.00008 | 0.00230 | 0.00160 | 1.18E+00 |
| pu-met-fast-036-001 | 1.00000 | 0.00310 | 1.00639 | 0.00009 | -0.00639 | 0.00310 | 6.22E-01 |
| pu-met-fast-038-001 | 1.00070 | 0.00190 | 1.00253 | 0.00010 | -0.00183 | 0.00190 | 5.02E-01 |
| **pu-met-fast-039-001** | **1.00000** | **0.00220** | **0.99220** | **0.00009** | **0.00780** | **0.00220** | **1.16E+00** |
| pu-met-fast-040-001 | 1.00000 | 0.00380 | 0.99667 | 0.00009 | 0.00333 | 0.00380 | 1.15E+00 |
| **pu-met-fast-041-001** | **1.00000** | **0.00160** | **1.00584** | **0.00010** | **-0.00584** | **0.00160** | **1.10E+00** |
| pu-met-fast-044-001 | 0.99770 | 0.00210 | 1.00054 | 0.00009 | -0.00284 | 0.00210 | 4.00E-01 |
| pu-met-fast-044-002 | 0.99800 | 0.00220 | 0.99997 | 0.00010 | -0.00197 | 0.00220 | 3.15E-01 |
| **pu-met-fast-044-003** | **0.99270** | **0.00210** | **0.99938** | **0.00010** | **-0.00668** | **0.00210** | **4.52E-01** |
| pu-met-fast-044-004 | 0.99780 | 0.00260 | 1.00002 | 0.00010 | -0.00222 | 0.00260 | 1.89E-01 |
| pu-met-fast-044-005 | 0.99770 | 0.00240 | 0.99927 | 0.00011 | -0.00157 | 0.00240 | 2.84E-01 |
| pu-met-fast-045-001 | 1.00000 | 0.00470 | 1.00164 | 0.00009 | -0.00164 | 0.00470 | 8.55E-01 |
| pu-met-fast-045-002 | 1.00000 | 0.00460 | 1.00785 | 0.00010 | -0.00785 | 0.00460 | 8.89E-01 |
| pu-met-fast-045-003 | 1.00000 | 0.00440 | 1.00536 | 0.00009 | -0.00536 | 0.00440 | 9.21E-01 |
| pu-met-fast-045-004 | 1.00000 | 0.00460 | 1.00462 | 0.00009 | -0.00462 | 0.00460 | 8.93E-01 |
| pu-met-fast-045-005 | 1.00000 | 0.00450 | 1.00858 | 0.00009 | -0.00858 | 0.00450 | 9.32E-01 |
| pu-met-fast-045-006 | 1.00000 | 0.00490 | 1.00483 | 0.00009 | -0.00483 | 0.00490 | 8.08E-01 |
| pu-met-fast-045-007 | 1.00000 | 0.00500 | 1.00541 | 0.00009 | -0.00541 | 0.00500 | 7.44E-01 |
| pu-sol-therm-001-001 | 1.00000 | 0.00500 | 1.00578 | 0.00013 | -0.00578 | 0.00500 | 8.65E-08 |
| pu-sol-therm-001-002 | 1.00000 | 0.00500 | 1.00730 | 0.00012 | -0.00730 | 0.00500 | 1.09E-07 |
| pu-sol-therm-001-003 | 1.00000 | 0.00500 | 1.01135 | 0.00013 | -0.01135 | 0.00500 | 1.32E-07 |
| pu-sol-therm-001-004 | 1.00000 | 0.00500 | 1.00441 | 0.00013 | -0.00441 | 0.00500 | 1.48E-07 |
| pu-sol-therm-001-005 | 1.00000 | 0.00500 | 1.00870 | 0.00013 | -0.00870 | 0.00500 | 1.56E-07 |

| | | | | | | | |
|---|---|---|---|---|---|---|---|
| pu-sol-therm-001-006 | 1.00000 | 0.00500 | 1.00955 | 0.00014 | -0.00955 | 0.00500 | 3.41E-07 |
| pu-sol-therm-002-001 | 1.00000 | 0.00470 | 1.00384 | 0.00012 | -0.00384 | 0.00470 | 6.99E-08 |
| pu-sol-therm-002-002 | 1.00000 | 0.00470 | 1.00475 | 0.00013 | -0.00475 | 0.00470 | 7.15E-08 |
| pu-sol-therm-002-003 | 1.00000 | 0.00470 | 1.00385 | 0.00013 | -0.00385 | 0.00470 | 7.63E-08 |
| pu-sol-therm-002-004 | 1.00000 | 0.00470 | 1.00667 | 0.00012 | -0.00667 | 0.00470 | 7.98E-08 |
| pu-sol-therm-002-005 | 1.00000 | 0.00470 | 1.00941 | 0.00012 | -0.00941 | 0.00470 | 8.34E-08 |
| pu-sol-therm-002-006 | 1.00000 | 0.00470 | 1.00518 | 0.00012 | -0.00518 | 0.00470 | 9.10E-08 |
| pu-sol-therm-002-007 | 1.00000 | 0.00470 | 1.00772 | 0.00012 | -0.00772 | 0.00470 | 9.84E-08 |
| pu-sol-therm-003-001 | 1.00000 | 0.00470 | 1.00268 | 0.00012 | -0.00268 | 0.00470 | 5.73E-08 |
| pu-sol-therm-003-002 | 1.00000 | 0.00470 | 1.00238 | 0.00012 | -0.00238 | 0.00470 | 5.85E-08 |
| pu-sol-therm-003-003 | 1.00000 | 0.00470 | 1.00513 | 0.00012 | -0.00513 | 0.00470 | 6.08E-08 |
| pu-sol-therm-003-004 | 1.00000 | 0.00470 | 1.00433 | 0.00012 | -0.00433 | 0.00470 | 6.16E-08 |
| pu-sol-therm-003-005 | 1.00000 | 0.00470 | 1.00568 | 0.00012 | -0.00568 | 0.00470 | 6.43E-08 |
| pu-sol-therm-003-006 | 1.00000 | 0.00470 | 1.00605 | 0.00012 | -0.00605 | 0.00470 | 6.81E-08 |
| pu-sol-therm-003-007 | 1.00000 | 0.00470 | 1.00668 | 0.00012 | -0.00668 | 0.00470 | 5.81E-08 |
| pu-sol-therm-003-008 | 1.00000 | 0.00470 | 1.00536 | 0.00011 | -0.00536 | 0.00470 | 5.91E-08 |
| pu-sol-therm-004-001 | 1.00000 | 0.00470 | 1.00399 | 0.00011 | -0.00399 | 0.00470 | 5.24E-08 |
| pu-sol-therm-004-002 | 1.00000 | 0.00470 | 0.99870 | 0.00011 | 0.00130 | 0.00470 | 5.27E-08 |
| pu-sol-therm-004-003 | 1.00000 | 0.00470 | 1.00090 | 0.00011 | -0.00090 | 0.00470 | 5.37E-08 |
| pu-sol-therm-004-004 | 1.00000 | 0.00470 | 0.99898 | 0.00011 | 0.00102 | 0.00470 | 5.50E-08 |
| pu-sol-therm-004-005 | 1.00000 | 0.00470 | 0.99983 | 0.00011 | 0.00017 | 0.00470 | 5.36E-08 |
| pu-sol-therm-004-006 | 1.00000 | 0.00470 | 1.00186 | 0.00011 | -0.00186 | 0.00470 | 5.40E-08 |
| pu-sol-therm-004-007 | 1.00000 | 0.00470 | 1.00564 | 0.00011 | -0.00564 | 0.00470 | 5.49E-08 |
| pu-sol-therm-004-008 | 1.00000 | 0.00470 | 1.00117 | 0.00010 | -0.00117 | 0.00470 | 5.56E-08 |
| pu-sol-therm-004-009 | 1.00000 | 0.00470 | 1.00069 | 0.00011 | -0.00069 | 0.00470 | 5.76E-08 |
| pu-sol-therm-004-010 | 1.00000 | 0.00470 | 1.00234 | 0.00011 | -0.00234 | 0.00470 | 6.20E-08 |
| pu-sol-therm-004-011 | 1.00000 | 0.00470 | 1.00086 | 0.00012 | -0.00086 | 0.00470 | 6.72E-08 |
| pu-sol-therm-004-012 | 1.00000 | 0.00470 | 1.00309 | 0.00012 | -0.00309 | 0.00470 | 5.49E-08 |
| pu-sol-therm-004-013 | 1.00000 | 0.00470 | 1.00035 | 0.00011 | -0.00035 | 0.00470 | 5.46E-08 |
| pu-sol-therm-005-001 | 1.00000 | 0.00470 | 1.00233 | 0.00012 | -0.00233 | 0.00470 | 5.46E-08 |
| pu-sol-therm-005-002 | 1.00000 | 0.00470 | 1.00299 | 0.00012 | -0.00299 | 0.00470 | 5.56E-08 |
| pu-sol-therm-005-003 | 1.00000 | 0.00470 | 1.00354 | 0.00011 | -0.00354 | 0.00470 | 5.66E-08 |
| pu-sol-therm-005-004 | 1.00000 | 0.00470 | 1.00504 | 0.00011 | -0.00504 | 0.00470 | 5.90E-08 |
| pu-sol-therm-005-005 | 1.00000 | 0.00470 | 1.00615 | 0.00011 | -0.00615 | 0.00470 | 6.19E-08 |
| pu-sol-therm-005-006 | 1.00000 | 0.00470 | 1.00584 | 0.00012 | -0.00584 | 0.00470 | 6.49E-08 |
| pu-sol-therm-005-007 | 1.00000 | 0.00470 | 1.00420 | 0.00012 | -0.00420 | 0.00470 | 6.79E-08 |
| pu-sol-therm-005-008 | 1.00000 | 0.00470 | 0.99941 | 0.00011 | 0.00059 | 0.00470 | 5.56E-08 |
| pu-sol-therm-005-009 | 1.00000 | 0.00470 | 1.00215 | 0.00011 | -0.00215 | 0.00470 | 5.70E-08 |
| pu-sol-therm-006-001 | 1.00000 | 0.00350 | 1.00073 | 0.00011 | -0.00073 | 0.00350 | 5.15E-08 |
| pu-sol-therm-006-002 | 1.00000 | 0.00350 | 1.00202 | 0.00011 | -0.00202 | 0.00350 | 5.25E-08 |
| pu-sol-therm-006-003 | 1.00000 | 0.00350 | 1.00158 | 0.00011 | -0.00158 | 0.00350 | 5.43E-08 |
| pu-sol-therm-007-002 | 1.00000 | 0.00470 | 1.00956 | 0.00012 | -0.00956 | 0.00470 | 2.70E-07 |
| pu-sol-therm-007-003 | 1.00000 | 0.00470 | 1.00361 | 0.00013 | -0.00361 | 0.00470 | 2.56E-07 |
| pu-sol-therm-007-005 | 1.00000 | 0.00470 | 1.00928 | 0.00013 | -0.00928 | 0.00470 | 1.10E-07 |
| pu-sol-therm-007-006 | 1.00000 | 0.00470 | 1.00313 | 0.00013 | -0.00313 | 0.00470 | 1.12E-07 |
| pu-sol-therm-007-007 | 1.00000 | 0.00470 | 1.00524 | 0.00013 | -0.00524 | 0.00470 | 1.11E-07 |
| pu-sol-therm-007-008 | 1.00000 | 0.00470 | 0.99868 | 0.00013 | 0.00132 | 0.00470 | 1.13E-07 |
| pu-sol-therm-007-009 | 1.00000 | 0.00470 | 0.99730 | 0.00013 | 0.00270 | 0.00470 | 1.13E-07 |
| pu-sol-therm-007-010 | 1.00000 | 0.00470 | 1.00092 | 0.00012 | -0.00092 | 0.00470 | 1.05E-07 |
| **pu-sol-therm-009-003** | **1.00000** | **0.00330** | **1.01926** | **0.00006** | **-0.01926** | **0.00330** | **4.05E-08** |
| **pu-sol-therm-010-001** | **1.00000** | **0.00480** | **1.01812** | **0.00013** | **-0.01812** | **0.00480** | **1.08E-07** |
| pu-sol-therm-010-002 | 1.00000 | 0.00480 | 1.01428 | 0.00013 | -0.01428 | 0.00480 | 8.77E-08 |
| pu-sol-therm-010-003 | 1.00000 | 0.00480 | 1.00818 | 0.00013 | -0.00818 | 0.00480 | 7.28E-08 |
| pu-sol-therm-010-004 | 1.00000 | 0.00480 | 1.01261 | 0.00013 | -0.01261 | 0.00480 | 7.41E-08 |
| pu-sol-therm-010-005 | 1.00000 | 0.00480 | 1.01057 | 0.00012 | -0.01057 | 0.00480 | 6.87E-08 |
| pu-sol-therm-010-006 | 1.00000 | 0.00480 | 1.00954 | 0.00012 | -0.00954 | 0.00480 | 6.76E-08 |
| pu-sol-therm-010-007 | 1.00000 | 0.00480 | 1.00241 | 0.00012 | -0.00241 | 0.00480 | 6.54E-08 |
| pu-sol-therm-010-008 | 1.00000 | 0.00480 | 1.00377 | 0.00011 | -0.00377 | 0.00480 | 6.30E-08 |
| pu-sol-therm-010-009 | 1.00000 | 0.00480 | 1.01445 | 0.00012 | -0.01445 | 0.00480 | 7.99E-08 |
| pu-sol-therm-010-010 | 1.00000 | 0.00480 | 1.00259 | 0.00012 | -0.00259 | 0.00480 | 6.92E-08 |
| pu-sol-therm-010-011 | 1.00000 | 0.00480 | 1.00985 | 0.00012 | -0.00985 | 0.00480 | 6.85E-08 |
| pu-sol-therm-010-012 | 1.00000 | 0.00480 | 1.00953 | 0.00012 | -0.00953 | 0.00480 | 6.43E-08 |
| **pu-sol-therm-010-013** | **1.00000** | **0.00480** | **1.01576** | **0.00011** | **-0.01576** | **0.00480** | **5.96E-08** |
| pu-sol-therm-010-014 | 1.00000 | 0.00480 | 1.00967 | 0.00011 | -0.00967 | 0.00480 | 5.60E-08 |
| pu-sol-therm-011-161 | 1.00000 | 0.00520 | 1.00962 | 0.00012 | -0.00962 | 0.00520 | 6.23E-08 |
| pu-sol-therm-011-162 | 1.00000 | 0.00520 | 1.01483 | 0.00013 | -0.01483 | 0.00520 | 6.35E-08 |
| **pu-sol-therm-011-163** | **1.00000** | **0.00520** | **1.01657** | **0.00013** | **-0.01657** | **0.00520** | **6.59E-08** |
| pu-sol-therm-011-164 | 1.00000 | 0.00520 | 1.00927 | 0.00012 | -0.00927 | 0.00520 | 6.65E-08 |
| pu-sol-therm-011-165 | 1.00000 | 0.00520 | 1.00642 | 0.00013 | -0.00642 | 0.00520 | 7.39E-08 |
| pu-sol-therm-011-181 | 1.00000 | 0.00520 | 0.99435 | 0.00012 | 0.00565 | 0.00520 | 5.11E-08 |
| pu-sol-therm-011-182 | 1.00000 | 0.00520 | 1.00045 | 0.00012 | -0.00045 | 0.00520 | 5.21E-08 |

| | | | | | | | |
|---|---|---|---|---|---|---|---|
| pu-sol-therm-011-183 | 1.00000 | 0.00520 | 0.99679 | 0.00011 | 0.00321 | 0.00520 | 5.20E-08 |
| pu-sol-therm-011-184 | 1.00000 | 0.00520 | 0.99366 | 0.00011 | 0.00634 | 0.00520 | 5.33E-08 |
| pu-sol-therm-011-185 | 1.00000 | 0.00520 | 1.00372 | 0.00012 | -0.00372 | 0.00520 | 5.47E-08 |
| pu-sol-therm-011-186 | 1.00000 | 0.00520 | 1.00025 | 0.00012 | -0.00025 | 0.00520 | 5.83E-08 |
| pu-sol-therm-011-187 | 1.00000 | 0.00520 | 0.99970 | 0.00011 | 0.00030 | 0.00520 | 5.31E-08 |
| pu-sol-therm-012-001 | 1.00000 | 0.00430 | 1.00536 | 0.00009 | -0.00536 | 0.00430 | 4.74E-08 |
| pu-sol-therm-012-002 | 1.00000 | 0.00430 | 1.00615 | 0.00008 | -0.00615 | 0.00430 | 4.59E-08 |
| pu-sol-therm-012-003 | 1.00000 | 0.00580 | 1.00736 | 0.00008 | -0.00736 | 0.00580 | 4.51E-08 |
| pu-sol-therm-012-004 | 1.00000 | 0.00580 | 1.00746 | 0.00007 | -0.00746 | 0.00580 | 4.36E-08 |
| pu-sol-therm-012-005 | 1.00000 | 0.00580 | 1.00981 | 0.00006 | -0.00981 | 0.00580 | 4.25E-08 |
| **pu-sol-therm-012-006** | **1.00000** | **0.00070** | **1.00659** | **0.00013** | **-0.00659** | **0.00071** | **1.30E-07** |
| **pu-sol-therm-012-007** | **1.00000** | **0.00130** | **1.00537** | **0.00013** | **-0.00537** | **0.00131** | **1.05E-07** |
| **pu-sol-therm-012-008** | **1.00000** | **0.00130** | **1.00417** | **0.00012** | **-0.00417** | **0.00131** | **7.45E-08** |
| pu-sol-therm-012-009 | 1.00000 | 0.00430 | 1.00966 | 0.00011 | -0.00966 | 0.00430 | 5.69E-08 |
| pu-sol-therm-012-010 | 1.00000 | 0.00430 | 1.00409 | 0.00010 | -0.00409 | 0.00430 | 5.30E-08 |
| pu-sol-therm-012-011 | 1.00000 | 0.00430 | 1.00670 | 0.00010 | -0.00670 | 0.00430 | 4.88E-08 |
| pu-sol-therm-012-012 | 1.00000 | 0.00430 | 1.00721 | 0.00009 | -0.00721 | 0.00430 | 4.74E-08 |
| pu-sol-therm-012-013 | 1.00000 | 0.00580 | 1.00964 | 0.00007 | -0.00964 | 0.00580 | 4.25E-08 |
| pu-sol-therm-018-001 | 1.00000 | 0.00340 | 1.00849 | 0.00013 | -0.00849 | 0.00340 | 1.65E-07 |
| **pu-sol-therm-018-002** | **1.00000** | **0.00340** | **1.01189** | **0.00012** | **-0.01189** | **0.00340** | **1.29E-07** |
| pu-sol-therm-018-003 | 1.00000 | 0.00320 | 1.00938 | 0.00012 | -0.00938 | 0.00320 | 1.08E-07 |
| pu-sol-therm-018-004 | 1.00000 | 0.00300 | 1.00765 | 0.00012 | -0.00765 | 0.00300 | 9.36E-08 |
| pu-sol-therm-018-005 | 1.00000 | 0.00300 | 1.00654 | 0.00011 | -0.00654 | 0.00300 | 8.39E-08 |
| pu-sol-therm-018-006 | 1.00000 | 0.00310 | 1.00462 | 0.00012 | -0.00462 | 0.00310 | 7.47E-08 |
| pu-sol-therm-018-007 | 1.00000 | 0.00320 | 1.00399 | 0.00010 | -0.00399 | 0.00320 | 6.75E-08 |
| pu-sol-therm-018-008 | 1.00000 | 0.00330 | 1.00356 | 0.00011 | -0.00356 | 0.00330 | 6.04E-08 |
| pu-sol-therm-018-009 | 1.00000 | 0.00340 | 1.00176 | 0.00010 | -0.00176 | 0.00340 | 5.60E-08 |
| pu-sol-therm-022-001 | 1.00000 | 0.00200 | 0.99953 | 0.00013 | 0.00047 | 0.00200 | 2.06E-07 |
| pu-sol-therm-022-002 | 1.00000 | 0.00160 | 1.00205 | 0.00013 | -0.00205 | 0.00161 | 1.29E-07 |
| pu-sol-therm-022-003 | 1.00000 | 0.00150 | 1.00071 | 0.00012 | -0.00071 | 0.00150 | 8.23E-08 |
| pu-sol-therm-022-004 | 1.00000 | 0.00170 | 1.00135 | 0.00012 | -0.00135 | 0.00170 | 7.23E-08 |
| pu-sol-therm-022-005 | 1.00000 | 0.00190 | 1.00225 | 0.00011 | -0.00225 | 0.00190 | 6.38E-08 |
| pu-sol-therm-022-006 | 1.00000 | 0.00210 | 1.00269 | 0.00011 | -0.00269 | 0.00210 | 5.99E-08 |
| pu-sol-therm-022-007 | 1.00000 | 0.00210 | 1.00423 | 0.00011 | -0.00423 | 0.00210 | 5.76E-08 |
| pu-sol-therm-022-008 | 1.00000 | 0.00230 | 1.00505 | 0.00010 | -0.00505 | 0.00230 | 5.57E-08 |
| pu-sol-therm-022-009 | 1.00000 | 0.00240 | 1.00368 | 0.00010 | -0.00368 | 0.00240 | 5.42E-08 |
| **pu-sol-therm-028-001** | **1.00000** | **0.00120** | **1.00788** | **0.00012** | **-0.00788** | **0.00121** | **1.04E-07** |
| **pu-sol-therm-028-002** | **1.00000** | **0.00120** | **1.00708** | **0.00012** | **-0.00708** | **0.00121** | **9.34E-08** |
| **pu-sol-therm-028-003** | **1.00000** | **0.00120** | **1.00890** | **0.00012** | **-0.00890** | **0.00121** | **8.41E-08** |
| **pu-sol-therm-028-004** | **1.00000** | **0.00120** | **1.00871** | **0.00012** | **-0.00871** | **0.00121** | **7.50E-08** |
| **pu-sol-therm-028-005** | **1.00000** | **0.00120** | **1.00991** | **0.00012** | **-0.00991** | **0.00121** | **7.07E-08** |
| **pu-sol-therm-028-006** | **1.00000** | **0.00120** | **1.01070** | **0.00011** | **-0.01070** | **0.00121** | **6.18E-08** |
| **pu-sol-therm-028-007** | **1.00000** | **0.00120** | **1.00815** | **0.00012** | **-0.00815** | **0.00121** | **9.56E-08** |
| **pu-sol-therm-028-008** | **1.00000** | **0.00120** | **1.00826** | **0.00012** | **-0.00826** | **0.00121** | **8.67E-08** |
| **pu-sol-therm-028-009** | **1.00000** | **0.00120** | **1.00989** | **0.00012** | **-0.00989** | **0.00121** | **7.86E-08** |
| pu-sol-therm-032-001 | 1.00000 | 0.00190 | 0.99617 | 0.00013 | 0.00383 | 0.00190 | 8.56E-08 |
| pu-sol-therm-032-002 | 1.00000 | 0.00190 | 1.00142 | 0.00012 | -0.00142 | 0.00190 | 8.09E-08 |
| pu-sol-therm-032-003 | 1.00000 | 0.00190 | 1.00264 | 0.00012 | -0.00264 | 0.00190 | 7.47E-08 |
| pu-sol-therm-032-004 | 1.00000 | 0.00190 | 1.00255 | 0.00012 | -0.00255 | 0.00190 | 6.98E-08 |
| pu-sol-therm-032-005 | 1.00000 | 0.00190 | 1.00439 | 0.00012 | -0.00439 | 0.00190 | 6.55E-08 |
| pu-sol-therm-032-006 | 1.00000 | 0.00190 | 1.00477 | 0.00011 | -0.00477 | 0.00190 | 6.13E-08 |
| pu-sol-therm-032-007 | 1.00000 | 0.00190 | 1.00496 | 0.00011 | -0.00496 | 0.00190 | 5.96E-08 |
| pu-sol-therm-032-008 | 1.00000 | 0.00190 | 1.00440 | 0.00011 | -0.00440 | 0.00190 | 5.67E-08 |
| pu-sol-therm-032-009 | 1.00000 | 0.00190 | 1.00326 | 0.00011 | -0.00326 | 0.00190 | 5.51E-08 |
| pu-sol-therm-032-010 | 1.00000 | 0.00190 | 1.00514 | 0.00011 | -0.00514 | 0.00190 | 5.36E-08 |
| pu-sol-therm-032-011 | 1.00000 | 0.00190 | 1.00448 | 0.00010 | -0.00448 | 0.00190 | 5.28E-08 |
| pu-sol-therm-032-012 | 1.00000 | 0.00190 | 1.00347 | 0.00010 | -0.00347 | 0.00190 | 5.20E-08 |
| pu-sol-therm-032-013 | 1.00000 | 0.00190 | 1.00230 | 0.00012 | -0.00230 | 0.00190 | 7.23E-08 |
| pu-sol-therm-032-014 | 1.00000 | 0.00190 | 1.00212 | 0.00012 | -0.00212 | 0.00190 | 6.78E-08 |
| pu-sol-therm-032-015 | 1.00000 | 0.00190 | 1.00402 | 0.00011 | -0.00402 | 0.00190 | 6.36E-08 |
| pu-sol-therm-032-016 | 1.00000 | 0.00190 | 1.00382 | 0.00011 | -0.00382 | 0.00190 | 5.97E-08 |
| pu-sol-therm-032-017 | 1.00000 | 0.00190 | 1.00389 | 0.00011 | -0.00389 | 0.00190 | 5.80E-08 |
| pu-sol-therm-034-001 | 1.00000 | 0.00620 | 0.99995 | 0.00013 | 0.00005 | 0.00620 | 1.43E-07 |
| pu-sol-therm-034-002 | 1.00000 | 0.00440 | 1.00148 | 0.00012 | -0.00148 | 0.00440 | 1.71E-07 |
| pu-sol-therm-034-003 | 1.00000 | 0.00400 | 0.99950 | 0.00012 | 0.00050 | 0.00400 | 1.99E-07 |
| pu-sol-therm-034-004 | 1.00000 | 0.00390 | 1.00248 | 0.00012 | -0.00248 | 0.00390 | 2.24E-07 |
| pu-sol-therm-034-005 | 1.00000 | 0.00400 | 0.99991 | 0.00010 | 0.00009 | 0.00400 | 2.50E-07 |
| pu-sol-therm-034-006 | 1.00000 | 0.00420 | 1.00114 | 0.00010 | -0.00114 | 0.00420 | 2.73E-07 |
| pu-sol-therm-034-007 | 1.00000 | 0.00570 | 0.99870 | 0.00012 | 0.00130 | 0.00570 | 1.44E-06 |
| pu-sol-therm-034-008 | 1.00000 | 0.00550 | 0.99889 | 0.00012 | 0.00111 | 0.00550 | 1.53E-06 |
| pu-sol-therm-034-009 | 1.00000 | 0.00520 | 0.99776 | 0.00011 | 0.00224 | 0.00520 | 1.62E-06 |

| | | | | | | | |
|---|---|---|---|---|---|---|---|
| pu-sol-therm-034-010 | 1.00000 | 0.00520 | 0.99732 | 0.00012 | 0.00268 | 0.00520 | 1.78E-06 |
| pu-sol-therm-034-011 | 1.00000 | 0.00480 | 0.99902 | 0.00011 | 0.00098 | 0.00480 | 1.91E-06 |
| pu-sol-therm-034-012 | 1.00000 | 0.00420 | 0.99847 | 0.00011 | 0.00153 | 0.00420 | 2.09E-06 |
| pu-sol-therm-034-013 | 1.00000 | 0.00430 | 0.99696 | 0.00010 | 0.00304 | 0.00430 | 2.26E-06 |
| pu-sol-therm-034-014 | 1.00000 | 0.00440 | 0.99681 | 0.00011 | 0.00319 | 0.00440 | 2.40E-06 |
| pu-sol-therm-034-015 | 1.00000 | 0.00420 | 0.99717 | 0.00011 | 0.00283 | 0.00420 | 2.49E-06 |
| pu-sol-therm-038-001 | 1.00050 | 0.00150 | 1.00318 | 0.00009 | -0.00268 | 0.00150 | 4.65E-08 |
| pu-sol-therm-038-002 | 1.00050 | 0.00150 | 1.00365 | 0.00009 | -0.00315 | 0.00150 | 4.68E-08 |
| pu-sol-therm-038-003 | 1.00050 | 0.00180 | 1.00359 | 0.00007 | -0.00309 | 0.00180 | 4.32E-08 |
| pu-sol-therm-038-004 | 1.00050 | 0.00130 | 1.00173 | 0.00007 | -0.00123 | 0.00130 | 4.27E-08 |
| pu-sol-therm-038-005 | 1.00050 | 0.00130 | 1.00192 | 0.00007 | -0.00142 | 0.00130 | 4.27E-08 |
| u233-comp-therm-001-001 | 1.00060 | 0.00270 | 0.99947 | 0.00013 | 0.00113 | 0.00270 | 5.60E-07 |
| u233-comp-therm-001-002 | 1.00150 | 0.00250 | 1.00208 | 0.00014 | -0.00058 | 0.00250 | 1.55E-06 |
| u233-comp-therm-001-003 | 1.00000 | 0.00240 | 1.00220 | 0.00015 | -0.00220 | 0.00240 | 7.84E-07 |
| u233-comp-therm-001-004 | 1.00070 | 0.00250 | 1.00063 | 0.00012 | 0.00007 | 0.00250 | 4.64E-07 |
| u233-comp-therm-001-005 | 1.00150 | 0.00260 | 1.00018 | 0.00012 | 0.00132 | 0.00260 | 3.08E-07 |
| u233-comp-therm-001-006 | 1.00150 | 0.00280 | 0.99874 | 0.00013 | 0.00276 | 0.00280 | 1.60E-07 |
| u233-comp-therm-001-007 | 0.99950 | 0.00270 | 1.00172 | 0.00014 | -0.00222 | 0.00270 | 3.61E-07 |
| u233-comp-therm-001-008 | 1.00040 | 0.00280 | 0.99948 | 0.00013 | 0.00092 | 0.00280 | 6.01E-07 |
| u233-comp-therm-004-001 | 1.00170 | 0.00180 | 0.99795 | 0.00009 | 0.00375 | 0.00180 | 3.14E-07 |
| u233-met-fast-001-001 | 1.00000 | 0.00100 | 0.99986 | 0.00008 | 0.00014 | 0.00100 | 1.12E+00 |
| u233-met-fast-002-001 | 1.00000 | 0.00100 | 0.99874 | 0.00008 | 0.00126 | 0.00100 | 1.07E+00 |
| u233-met-fast-002-002 | 1.00000 | 0.00110 | 1.00022 | 0.00009 | -0.00022 | 0.00110 | 1.02E+00 |
| u233-met-fast-003-001 | 1.00000 | 0.00100 | 0.99923 | 0.00008 | 0.00077 | 0.00100 | 1.06E+00 |
| u233-met-fast-003-002 | 1.00000 | 0.00100 | 0.99961 | 0.00009 | 0.00039 | 0.00100 | 1.03E+00 |
| u233-met-fast-004-001 | 1.00000 | 0.00070 | 0.99847 | 0.00009 | 0.00153 | 0.00071 | 9.85E-01 |
| **u233-met-fast-004-002** | **1.00000** | **0.00080** | **0.99571** | **0.00010** | **0.00429** | **0.00081** | **8.92E-01** |
| **u233-met-fast-005-001** | **1.00000** | **0.00100** | **0.99608** | **0.00009** | **0.00392** | **0.00100** | **9.53E-01** |
| u233-met-fast-005-002 | 1.00000 | 0.00300 | 0.99510 | 0.00010 | 0.00490 | 0.00300 | 7.78E-01 |
| u233-met-fast-006-001 | 1.00000 | 0.00140 | 0.99902 | 0.00010 | 0.00098 | 0.00140 | 9.56E-01 |
| u233-sol-inter-001-001 | 1.00000 | 0.00830 | 0.98507 | 0.00016 | 0.01493 | 0.00830 | 6.90E-06 |
| u233-sol-inter-001-002 | 1.00000 | 0.00850 | 0.98099 | 0.00015 | 0.01901 | 0.00850 | 8.06E-06 |
| u233-sol-inter-001-003 | 1.00000 | 0.00660 | 0.98188 | 0.00016 | 0.01812 | 0.00660 | 8.66E-06 |
| u233-sol-inter-001-004 | 1.00000 | 0.00610 | 0.99343 | 0.00015 | 0.00657 | 0.00610 | 3.72E-06 |
| u233-sol-inter-001-005 | 1.00000 | 0.00820 | 0.98486 | 0.00015 | 0.01514 | 0.00820 | 9.26E-06 |
| u233-sol-inter-001-006 | 1.00000 | 0.00610 | 0.98657 | 0.00015 | 0.01343 | 0.00610 | 4.28E-06 |
| u233-sol-inter-001-007 | 1.00000 | 0.00590 | 0.98249 | 0.00016 | 0.01751 | 0.00590 | 9.69E-06 |
| **u233-sol-inter-001-008** | **1.00000** | **0.00560** | **0.98182** | **0.00016** | **0.01818** | **0.00560** | **4.54E-06** |
| u233-sol-inter-001-009 | 1.00000 | 0.00680 | 0.97966 | 0.00016 | 0.02034 | 0.00680 | 7.41E-06 |
| **u233-sol-inter-001-010** | **1.00000** | **0.00530** | **0.97897** | **0.00017** | **0.02103** | **0.00530** | **1.02E-05** |
| **u233-sol-inter-001-011** | **1.00000** | **0.00570** | **0.98069** | **0.00017** | **0.01931** | **0.00570** | **7.83E-06** |
| u233-sol-inter-001-012 | 1.00000 | 0.00910 | 0.98156 | 0.00015 | 0.01844 | 0.00910 | 4.49E-06 |
| u233-sol-inter-001-013 | 1.00000 | 0.00710 | 0.98258 | 0.00016 | 0.01742 | 0.00710 | 5.12E-06 |
| u233-sol-inter-001-014 | 1.00000 | 0.00520 | 0.99135 | 0.00015 | 0.00865 | 0.00520 | 2.30E-06 |
| u233-sol-inter-001-015 | 1.00000 | 0.00750 | 0.98048 | 0.00015 | 0.01952 | 0.00750 | 5.50E-06 |
| **u233-sol-inter-001-016** | **1.00000** | **0.00280** | **0.98186** | **0.00015** | **0.01814** | **0.00280** | **1.75E-06** |
| u233-sol-inter-001-017 | 1.00000 | 0.00550 | 0.98956 | 0.00015 | 0.01044 | 0.00550 | 2.55E-06 |
| **u233-sol-inter-001-018** | **1.00000** | **0.00570** | **0.97879** | **0.00015** | **0.02121** | **0.00570** | **5.89E-06** |
| u233-sol-inter-001-019 | 1.00000 | 0.00830 | 0.97595 | 0.00016 | 0.02405 | 0.00830 | 6.13E-06 |
| **u233-sol-inter-001-020** | **1.00000** | **0.00560** | **0.98080** | **0.00016** | **0.01920** | **0.00560** | **3.01E-06** |
| **u233-sol-inter-001-021** | **1.00000** | **0.00500** | **0.97333** | **0.00016** | **0.02667** | **0.00500** | **6.39E-06** |
| **u233-sol-inter-001-022** | **1.00000** | **0.00490** | **0.97873** | **0.00016** | **0.02127** | **0.00490** | **6.54E-06** |
| u233-sol-inter-001-023 | 1.00000 | 0.00470 | 0.99031 | 0.00016 | 0.00969 | 0.00470 | 4.75E-06 |
| u233-sol-inter-001-024 | 1.00000 | 0.00810 | 0.99265 | 0.00015 | 0.00735 | 0.00810 | 2.00E-06 |
| u233-sol-inter-001-025 | 1.00000 | 0.00810 | 0.98564 | 0.00015 | 0.01436 | 0.00810 | 2.29E-06 |
| u233-sol-inter-001-026 | 1.00000 | 0.00650 | 0.98949 | 0.00015 | 0.01051 | 0.00650 | 2.41E-06 |
| u233-sol-inter-001-027 | 1.00000 | 0.00510 | 0.99137 | 0.00016 | 0.00863 | 0.00510 | 1.25E-06 |
| u233-sol-inter-001-028 | 1.00000 | 0.00610 | 0.98406 | 0.00016 | 0.01594 | 0.00610 | 2.57E-06 |
| u233-sol-inter-001-029 | 1.00000 | 0.00980 | 0.97766 | 0.00015 | 0.02234 | 0.00980 | 2.67E-06 |
| **u233-sol-inter-001-030** | **1.00000** | **0.00530** | **0.97875** | **0.00016** | **0.02125** | **0.00530** | **1.46E-06** |
| u233-sol-inter-001-031 | 1.00000 | 0.00710 | 0.99140 | 0.00017 | 0.00860 | 0.00710 | 2.71E-06 |
| **u233-sol-inter-001-032** | **1.00000** | **0.00530** | **0.97609** | **0.00016** | **0.02391** | **0.00530** | **2.82E-06** |
| u233-sol-inter-001-033 | 1.00000 | 0.00460 | 0.99414 | 0.00016 | 0.00586 | 0.00460 | 2.09E-06 |
| u233-sol-therm-001-001 | 1.00000 | 0.00310 | 1.00126 | 0.00008 | -0.00126 | 0.00310 | 3.92E-08 |
| u233-sol-therm-001-002 | 1.00050 | 0.00330 | 1.00140 | 0.00008 | -0.00090 | 0.00330 | 3.98E-08 |
| u233-sol-therm-001-003 | 1.00060 | 0.00330 | 1.00082 | 0.00008 | -0.00022 | 0.00330 | 4.04E-08 |
| u233-sol-therm-001-004 | 0.99980 | 0.00330 | 1.00089 | 0.00009 | -0.00109 | 0.00330 | 4.11E-08 |
| u233-sol-therm-001-005 | 0.99990 | 0.00330 | 0.99994 | 0.00008 | -0.00004 | 0.00330 | 4.17E-08 |
| u233-sol-therm-005-001 | 1.00000 | 0.00400 | 1.00181 | 0.00013 | -0.00181 | 0.00400 | 6.17E-08 |
| u233-sol-therm-005-002 | 1.00000 | 0.00490 | 1.00474 | 0.00012 | -0.00474 | 0.00490 | 5.43E-08 |
| u233-sol-therm-008-001 | 1.00060 | 0.00290 | 1.00136 | 0.00006 | -0.00076 | 0.00290 | 3.70E-08 |

| | | | | | | | |
|---|---|---|---|---|---|---|---|
| u233-sol-therm-009-001 | 0.99660 | 0.00440 | 0.99612 | 0.00006 | 0.00048 | 0.00440 | 3.76E-08 |
| u233-sol-therm-009-002 | 0.99810 | 0.00400 | 0.99929 | 0.00006 | -0.00119 | 0.00400 | 3.73E-08 |
| u233-sol-therm-009-003 | 0.99890 | 0.00380 | 1.00041 | 0.00005 | -0.00151 | 0.00380 | 3.69E-08 |
| u233-sol-therm-009-004 | 0.99980 | 0.00380 | 0.99935 | 0.00005 | 0.00045 | 0.00380 | 3.65E-08 |
| u233-sol-therm-012-001 | 1.00000 | 0.00280 | 1.00080 | 0.00015 | -0.00080 | 0.00280 | 1.72E-07 |
| u233-sol-therm-012-002 | 1.00000 | 0.00250 | 1.00010 | 0.00014 | -0.00010 | 0.00250 | 1.64E-07 |
| **u233-sol-therm-012-003** | **1.00000** | **0.00230** | **1.00947** | **0.00015** | **-0.00947** | **0.00230** | **1.46E-07** |
| u233-sol-therm-012-004 | 1.00000 | 0.00150 | 1.00254 | 0.00014 | -0.00254 | 0.00151 | 1.07E-07 |
| u233-sol-therm-012-005 | 1.00000 | 0.00710 | 1.00515 | 0.00014 | -0.00515 | 0.00710 | 9.11E-08 |
| **u233-sol-therm-012-006** | **1.00000** | **0.00100** | **1.00579** | **0.00014** | **-0.00579** | **0.00101** | **8.01E-08** |
| u233-sol-therm-012-007 | 1.00000 | 0.00380 | 1.00173 | 0.00012 | -0.00173 | 0.00380 | 5.33E-08 |
| u233-sol-therm-012-008 | 1.00000 | 0.00480 | 0.99916 | 0.00012 | 0.00084 | 0.00480 | 5.32E-08 |
| u233-sol-therm-013-001 | 0.99920 | 0.00730 | 1.00528 | 0.00016 | -0.00608 | 0.00730 | 1.57E-07 |
| u233-sol-therm-013-002 | 0.99920 | 0.00700 | 1.00604 | 0.00016 | -0.00684 | 0.00700 | 1.57E-07 |
| u233-sol-therm-013-003 | 0.99920 | 0.00690 | 1.00588 | 0.00016 | -0.00668 | 0.00690 | 1.57E-07 |
| u233-sol-therm-013-004 | 0.99920 | 0.00730 | 1.00657 | 0.00017 | -0.00737 | 0.00730 | 1.57E-07 |
| u233-sol-therm-013-005 | 0.99920 | 0.00670 | 1.00724 | 0.00015 | -0.00804 | 0.00670 | 1.57E-07 |
| u233-sol-therm-013-006 | 0.99920 | 0.00500 | 1.00622 | 0.00016 | -0.00702 | 0.00500 | 1.50E-07 |
| u233-sol-therm-013-007 | 0.99920 | 0.00540 | 1.00610 | 0.00015 | -0.00690 | 0.00540 | 1.50E-07 |
| u233-sol-therm-013-008 | 0.99920 | 0.00500 | 1.00730 | 0.00016 | -0.00810 | 0.00500 | 1.50E-07 |
| u233-sol-therm-013-009 | 0.99920 | 0.00450 | 1.00740 | 0.00016 | -0.00820 | 0.00450 | 1.50E-07 |
| u233-sol-therm-013-010 | 0.99920 | 0.00460 | 1.00825 | 0.00017 | -0.00905 | 0.00460 | 1.50E-07 |
| u233-sol-therm-013-011 | 0.99920 | 0.00540 | 1.00510 | 0.00017 | -0.00590 | 0.00540 | 1.51E-07 |
| u233-sol-therm-013-012 | 0.99920 | 0.00500 | 1.00588 | 0.00016 | -0.00668 | 0.00500 | 1.50E-07 |
| u233-sol-therm-013-013 | 0.99920 | 0.00620 | 1.00354 | 0.00016 | -0.00434 | 0.00620 | 1.51E-07 |
| u233-sol-therm-013-014 | 0.99920 | 0.00510 | 1.00666 | 0.00015 | -0.00746 | 0.00510 | 1.50E-07 |
| u233-sol-therm-013-015 | 0.99960 | 0.00770 | 1.02128 | 0.00016 | -0.02168 | 0.00770 | 1.05E-07 |
| u233-sol-therm-013-016 | 0.99960 | 0.00690 | 0.99376 | 0.00015 | 0.00584 | 0.00690 | 8.87E-08 |
| u233-sol-therm-013-017 | 0.99960 | 0.00520 | 0.99644 | 0.00015 | 0.00316 | 0.00520 | 8.52E-08 |
| u233-sol-therm-013-018 | 0.99960 | 0.00200 | 1.00029 | 0.00016 | -0.00069 | 0.00201 | 8.03E-08 |
| u233-sol-therm-013-019 | 0.99960 | 0.00890 | 0.99625 | 0.00016 | 0.00335 | 0.00890 | 8.05E-08 |
| u233-sol-therm-013-020 | 0.99960 | 0.00560 | 0.99973 | 0.00014 | -0.00013 | 0.00560 | 6.15E-08 |
| u233-sol-therm-013-021 | 0.99960 | 0.00340 | 1.00279 | 0.00013 | -0.00319 | 0.00340 | 5.65E-08 |
| u233-sol-therm-015-001 | 1.00000 | 0.00750 | 0.99033 | 0.00015 | 0.00967 | 0.00750 | 1.11E-06 |
| u233-sol-therm-015-002 | 1.00000 | 0.00700 | 0.98597 | 0.00015 | 0.01403 | 0.00700 | 1.24E-06 |
| u233-sol-therm-015-003 | 1.00000 | 0.00680 | 0.98710 | 0.00015 | 0.01290 | 0.00680 | 1.31E-06 |
| u233-sol-therm-015-004 | 1.00000 | 0.00410 | 0.99033 | 0.00015 | 0.00967 | 0.00410 | 7.20E-07 |
| u233-sol-therm-015-005 | 1.00000 | 0.00550 | 0.98667 | 0.00016 | 0.01333 | 0.00550 | 1.38E-06 |
| u233-sol-therm-015-006 | 1.00000 | 0.00990 | 0.97710 | 0.00016 | 0.02290 | 0.00990 | 1.43E-06 |
| u233-sol-therm-015-007 | 1.00000 | 0.00700 | 0.98796 | 0.00015 | 0.01204 | 0.00700 | 7.94E-07 |
| **u233-sol-therm-015-008** | **1.00000** | **0.00670** | **0.97363** | **0.00015** | **0.02637** | **0.00670** | **1.47E-06** |
| **u233-sol-therm-015-009** | **1.00000** | **0.00500** | **0.96945** | **0.00017** | **0.03055** | **0.00500** | **1.50E-06** |
| u233-sol-therm-015-010 | 1.00000 | 0.00510 | 0.98977 | 0.00016 | 0.01023 | 0.00510 | 1.14E-06 |
| u233-sol-therm-015-011 | 1.00000 | 0.00750 | 0.99361 | 0.00016 | 0.00639 | 0.00750 | 6.97E-07 |
| u233-sol-therm-015-012 | 1.00000 | 0.00690 | 0.99409 | 0.00016 | 0.00591 | 0.00690 | 7.70E-07 |
| u233-sol-therm-015-013 | 1.00000 | 0.00690 | 0.99214 | 0.00017 | 0.00786 | 0.00690 | 8.10E-07 |
| u233-sol-therm-015-014 | 1.00000 | 0.00360 | 0.99852 | 0.00015 | 0.00148 | 0.00360 | 4.64E-07 |
| u233-sol-therm-015-015 | 1.00000 | 0.00600 | 0.98968 | 0.00016 | 0.01032 | 0.00600 | 8.50E-07 |
| u233-sol-therm-015-016 | 1.00000 | 0.00430 | 0.98879 | 0.00016 | 0.01121 | 0.00430 | 8.71E-07 |
| u233-sol-therm-015-017 | 1.00000 | 0.00290 | 0.99807 | 0.00016 | 0.00193 | 0.00290 | 5.04E-07 |
| **u233-sol-therm-015-018** | **1.00000** | **0.00560** | **0.97480** | **0.00016** | **0.02520** | **0.00560** | **9.00E-07** |
| **u233-sol-therm-015-019** | **1.00000** | **0.00520** | **0.97504** | **0.00017** | **0.02496** | **0.00520** | **9.15E-07** |
| u233-sol-therm-015-020 | 1.00000 | 0.00790 | 0.99528 | 0.00015 | 0.00472 | 0.00790 | 2.90E-07 |
| u233-sol-therm-015-021 | 1.00000 | 0.00700 | 0.99805 | 0.00015 | 0.00195 | 0.00700 | 3.16E-07 |
| u233-sol-therm-015-022 | 1.00000 | 0.00620 | 0.99645 | 0.00016 | 0.00355 | 0.00620 | 3.31E-07 |
| u233-sol-therm-015-023 | 1.00000 | 0.00550 | 0.99478 | 0.00015 | 0.00522 | 0.00550 | 3.44E-07 |
| u233-sol-therm-015-024 | 1.00000 | 0.00510 | 0.99088 | 0.00016 | 0.00912 | 0.00510 | 3.52E-07 |
| u233-sol-therm-015-025 | 1.00000 | 0.00230 | 0.99854 | 0.00015 | 0.00146 | 0.00230 | 2.23E-07 |
| u233-sol-therm-015-026 | 1.00000 | 0.00660 | 0.99418 | 0.00015 | 0.00582 | 0.00660 | 1.26E-07 |
| u233-sol-therm-015-027 | 1.00000 | 0.00630 | 0.99908 | 0.00015 | 0.00092 | 0.00630 | 1.31E-07 |
| u233-sol-therm-015-028 | 1.00000 | 0.00580 | 0.99716 | 0.00014 | 0.00284 | 0.00580 | 1.33E-07 |
| u233-sol-therm-015-029 | 1.00000 | 0.00510 | 0.99553 | 0.00015 | 0.00447 | 0.00510 | 1.35E-07 |
| u233-sol-therm-015-030 | 1.00000 | 0.00480 | 0.99477 | 0.00015 | 0.00523 | 0.00480 | 1.36E-07 |
| u233-sol-therm-015-031 | 1.00000 | 0.00550 | 0.99419 | 0.00015 | 0.00581 | 0.00550 | 1.38E-07 |
| u233-sol-therm-016-001 | 0.99870 | 0.00370 | 1.00416 | 0.00016 | -0.00546 | 0.00370 | 2.90E-07 |
| u233-sol-therm-016-002 | 0.99830 | 0.00440 | 1.00487 | 0.00016 | -0.00657 | 0.00440 | 2.90E-07 |
| u233-sol-therm-016-003 | 0.99920 | 0.00360 | 1.00443 | 0.00016 | -0.00523 | 0.00360 | 2.91E-07 |
| u233-sol-therm-016-006 | 0.99930 | 0.00340 | 0.99640 | 0.00017 | 0.00290 | 0.00340 | 2.90E-07 |
| u233-sol-therm-016-007 | 1.00080 | 0.00340 | 0.99710 | 0.00017 | 0.00370 | 0.00340 | 2.90E-07 |
| u233-sol-therm-016-008 | 1.00110 | 0.00280 | 0.99684 | 0.00016 | 0.00426 | 0.00280 | 2.90E-07 |
| u233-sol-therm-016-010 | 1.00000 | 0.00300 | 1.00490 | 0.00017 | -0.00490 | 0.00300 | 2.87E-07 |

| | | | | | | | |
|---|---|---|---|---|---|---|---|
| u233-sol-therm-016-011 | 0.99920 | 0.00410 | 1.00488 | 0.00017 | -0.00568 | 0.00410 | 2.87E-07 |
| u233-sol-therm-016-012 | 0.99920 | 0.00470 | 1.00475 | 0.00018 | -0.00555 | 0.00470 | 2.87E-07 |
| u233-sol-therm-016-013 | 0.99930 | 0.00360 | 1.00505 | 0.00016 | -0.00575 | 0.00360 | 1.44E-07 |
| u233-sol-therm-016-014 | 1.00000 | 0.00260 | 1.00578 | 0.00016 | -0.00578 | 0.00260 | 1.44E-07 |
| u233-sol-therm-016-015 | 1.00000 | 0.00270 | 1.00622 | 0.00016 | -0.00622 | 0.00270 | 1.44E-07 |
| **u233-sol-therm-016-016** | **0.99940** | **0.00310** | **1.00978** | **0.00016** | **-0.01038** | **0.00310** | **1.45E-07** |
| u233-sol-therm-016-017 | 1.00000 | 0.00280 | 0.99551 | 0.00015 | 0.00449 | 0.00280 | 1.45E-07 |
| u233-sol-therm-016-018 | 0.99880 | 0.00360 | 0.99566 | 0.00016 | 0.00314 | 0.00360 | 1.45E-07 |
| **u233-sol-therm-016-021** | **1.00000** | **0.00280** | **1.00969** | **0.00016** | **-0.00969** | **0.00280** | **1.43E-07** |
| u233-sol-therm-016-022 | 1.00000 | 0.00340 | 1.00945 | 0.00016 | -0.00945 | 0.00340 | 1.43E-07 |
| **u233-sol-therm-016-023** | **1.00000** | **0.00310** | **1.01001** | **0.00017** | **-0.01001** | **0.00310** | **1.43E-07** |
| u233-sol-therm-016-025 | 0.99810 | 0.00400 | 1.00042 | 0.00014 | -0.00232 | 0.00400 | 8.07E-08 |
| u233-sol-therm-016-026 | 0.99800 | 0.00340 | 1.00535 | 0.00015 | -0.00735 | 0.00340 | 8.07E-08 |
| u233-sol-therm-016-027 | 0.99880 | 0.00370 | 1.00372 | 0.00015 | -0.00492 | 0.00370 | 8.06E-08 |
| u233-sol-therm-016-028 | 0.99860 | 0.00370 | 0.99915 | 0.00014 | -0.00055 | 0.00370 | 8.04E-08 |
| u233-sol-therm-016-029 | 0.99850 | 0.00310 | 0.99979 | 0.00015 | -0.00129 | 0.00310 | 8.04E-08 |
| u233-sol-therm-016-030 | 0.99930 | 0.00320 | 0.99955 | 0.00016 | -0.00025 | 0.00320 | 8.05E-08 |
| **u233-sol-therm-016-031** | **0.99900** | **0.00340** | **1.01041** | **0.00014** | **-0.01141** | **0.00340** | **5.66E-08** |
| **u233-sol-therm-016-032** | **0.99850** | **0.00320** | **1.01255** | **0.00013** | **-0.01405** | **0.00320** | **5.66E-08** |
| **u233-sol-therm-016-033** | **0.99860** | **0.00390** | **1.01253** | **0.00013** | **-0.01393** | **0.00390** | **5.65E-08** |
| u233-sol-therm-017-001 | 0.99970 | 0.00320 | 1.00427 | 0.00015 | -0.00457 | 0.00320 | 1.15E-07 |
| u233-sol-therm-017-002 | 1.00000 | 0.00250 | 1.00007 | 0.00014 | -0.00007 | 0.00250 | 1.11E-07 |
| u233-sol-therm-017-003 | 1.00010 | 0.00350 | 1.00552 | 0.00015 | -0.00542 | 0.00350 | 1.08E-07 |
| u233-sol-therm-017-004 | 0.99940 | 0.00400 | 1.00549 | 0.00014 | -0.00609 | 0.00400 | 8.24E-08 |
| u233-sol-therm-017-005 | 1.00000 | 0.00290 | 1.00165 | 0.00015 | -0.00165 | 0.00290 | 8.07E-08 |
| u233-sol-therm-017-006 | 1.00000 | 0.00290 | 1.00055 | 0.00013 | -0.00055 | 0.00290 | 5.36E-08 |
| u233-sol-therm-017-007 | 1.00000 | 0.00370 | 1.00063 | 0.00012 | -0.00063 | 0.00370 | 5.46E-08 |

## Appendix B: Changes in Calculated $k_{eff}$ Using Different ENDF Versions

Historically, the LANL NCS division has used ENDF/B-V and ENDF/B-VI nuclear data libraries as part of their validation. The question of how $k_{eff}$ results change for transitioning to ENDF/B-VII.1 is addressed in this appendix. Figures B.1 and B.2 show the change in $k_{eff}$ for the various problems in the historical NCS validation suite. The change is determined by ENDF/B-VII.1 $k_{eff}$ minus ENDF/B-V or ENDF/B-VI $k_{eff}$. The units are pcm, where 1 pcm equals 0.00001. The x-axis is the benchmark case, which is broken down by benchmark series (e.g., HEU-MET-FAST), and the specific cases are alphabetical and are listed in Ref. 8. The historical NCS validation suite has benchmarks covering a broader range of fissionable material, form, spectra, etc. than the set of benchmarks considered in the body of this validation, which consists of more benchmarks in the PMF and MMF series than are in the historical NCS validation suite.

To aggregate the results, the discrepancy defined as the mean absolute value of the number of standard deviations (including benchmark and calculation) of disagreement of calculation to benchmark is given for each data library in Table B.I. The results show a marked improvement on average by migrating from ENDF/B-V or ENDF/B-VI to ENDF/B-VII, with ENDF/B-VII.1 being superior to ENDF/B-VII.0. This validates the decision for migrating to a more modern data library.

**Table B.I. Evolution of Mean Discrepancy for $k_{eff}$ Benchmarks Using Different Data Libraries**

| Nuclear Data Library | Discrepancy (#σ) |
|---|---|
| ENDF/B-V (~1980s) | 2.11 |
| ENDF/B-VI (~1990s) | 2.11 |
| ENDF/B-VII.0 (2006) | 1.54 |
| ENDF/B-VII.1 (2011) | 1.43 |

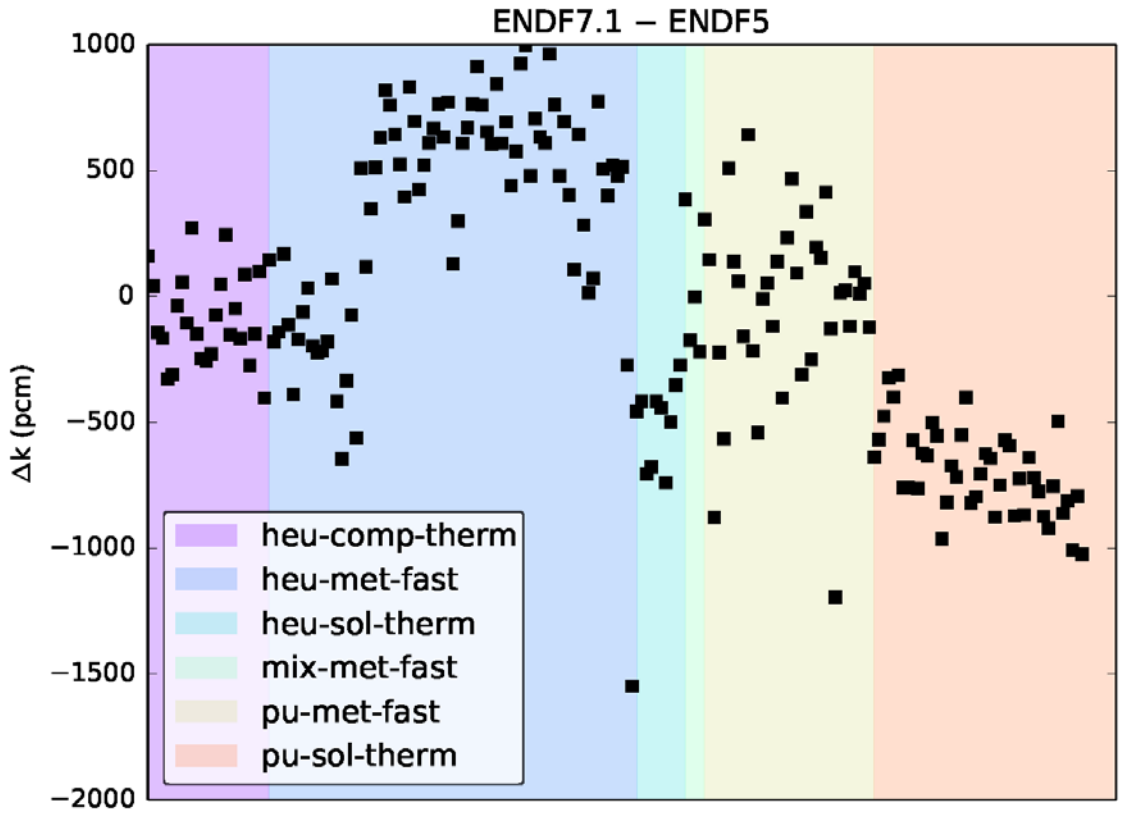


**Fig. B.1: Change in $k_{eff}$ for NCS validation benchmarks from changing nuclear data library from ENDF/B-V to ENDF/B-VII.1.**

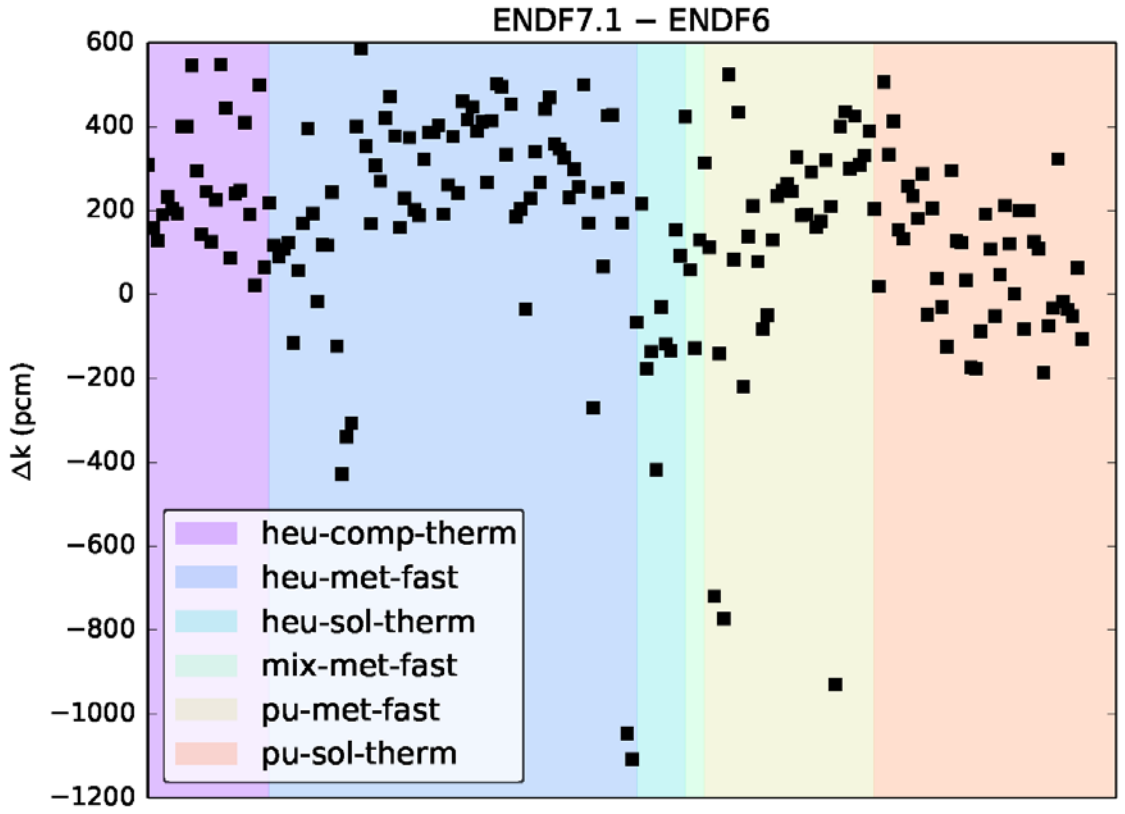


**Fig. B.2: Change in $k_{eff}$ for NCS validation benchmarks from changing nuclear data library from ENDF/B-VI to ENDF/B-VII.1.**

**Appendix C: ANS-8.24 Compliance Matrix**

| ANS 8.24-2007 | Validation Report |
|---|---|
| 4.1<br>Verification of the computer code system shall be completed prior to validation. Correct installation and operation of the computer code system should be documented. | Sec. 2 |
| 4.2<br>The computer code system to be validated shall be placed under an appropriate configuration control program. Any change to the computer code system shall be evaluated to determine its effect on the validation. | Sec. 2 |
| 5.1<br>Appropriate system or process parameters that correlate the experiments to the system or process under consideration shall be identified. | This validation is for predominately fast-spectrum plutonium metal, thermal-spectrum plutonium solution, and plutonium oxide systems with a range of spectra. |
| 5.2<br>Normal and credible abnormal conditions for the system or process shall be identified when determining the appropriate parameters and their range of values. | Identification of normal and credible abnormal conditions is conducted as part of the criticality safety evaluation process. The analyst performing the evaluation is responsible for identifying the normal and credible abnormal conditions. If an analyst chooses to use MCNP to analyze these conditions, he/she is responsible for developing models that are bounding of these conditions. If an analyst chooses to reference existing MCNP calculations, he/she is responsible for assuring the existing calculations are bounding of these conditions. |
| 5.3<br>Experiments shall be reviewed for completeness and accuracy of information prior to use as benchmarks. | The benchmarks are from the ICSBEP Handbook, which has its own review process and is widely used in the criticality safety community. |
| 5.4<br>Selected benchmarks should encompass the appropriate parameter values spanning the range of normal and credible abnormal conditions anticipated for the system or process to which the validation will be applied. | Each analyst is required to develop models that bound the normal and credible abnormal conditions, if MCNP is used. This may be a single model, or multiple models, depending on the complexity of the scenario and experience of the analyst. If this validation document is used, the analyst must develop models within the described AOA, and/or explain any extrapolation outside of the AOA, and apply additional margin if deemed appropriate. |
| 5.5<br>Benchmarks selected should be consistent with the modeling capabilities of the calculational method. | All the benchmark models used in this validation are within the modeling capabilities of MCNP6.1 with ENDF/B-VII.1 cross sections. |
| 5.6<br>To minimize systematic error, benchmarks should be drawn from multiple, independent experimental series and sources. | Sec. 3 |
| 5.7<br>The calculational methods and analysis techniques (e.g., albedos, variance reduction, cross-section processing) used to analyze the set of benchmarks shall be the same as those used to analyze the system or process to which the validation is applied. | The validation report describes the calculational method used to perform the validation. When relying on this validation report, MCNP must be used in accordance with the methods described in this report. |

| | |
|---|---|
| 5.8<br>Modeling of benchmarks shall be the responsibility of individuals experienced in the use of the calculational method. | All analysts using MCNP in the production of criticality safety evaluations have demonstrated proficiency with MCNP as documented in the NCS Analyst Qualification. |
| 5.9<br>Benchmark models prepared by organizations other than the one performing the validation should be evaluated to confirm the appropriateness of the models for the intended use. | Benchmark models were taken from the ICSBEP Handbook or prepared by Skip Khaler or Russ Mosteller. All of these have been independently reviewed for consistency. |
| 6.1.1<br>The method of determining bias and bias uncertainty should be consistent with the quantity and quality of the benchmarks used (e.g., normality, distributions). The selected method should be consistent with the intended use of the bias and the bias uncertainty (e.g., extrapolation or wide interpolation). | Sec. 5 |
| 6.1.2<br>If a positive bias is used in the determination of the calculational margin, its use shall be justified based on an understanding of the cause(s) of such a bias. | Sec. 5 |
| 6.1.3<br>The determination of bias uncertainty should contain allowances for uncertainties in benchmark physical properties and measurement techniques; uncertainties due to limitations in the geometric, material, or neutronic representations (e.g., cross sections) used in a calculational model; and statistical and convergence uncertainties. | Sec. 5 |
| 6.1.4<br>Individual elements (e.g., bias and bias uncertainty) of the calculational margin need not be computed separately. Methods may be used that combine the elements into the calculational margin. | Sec. 5 |
| 6.1.5<br>While statistical methods are typically used in the determination of the calculational margin, nonstatistical methods may be used where appropriate. | Sec. 5 |
| 6.2.1<br>Trends that arise from comparison of the calculated values with benchmark data may be considered. | No trending analysis was performed to compare calculated and benchmark data for Pu metals and solutions. Trending on EALF is performed for Pu oxides; the USL is a piecewise function. |
| 6.2.2<br>Parameters chosen for trending shall be based on the characteristics of the system or process under consideration. | Sec. 3.3 |
| 6.2.3<br>Trends in data used for extrapolation or for wide interpolation (e.g., gaps between groups of data) should be based on an understanding of the causes of such trends. | The trend in USL for Pu oxides on EALF arises from the neutron spectra of the benchmarks and their relative availability and bias with certain spectral ranges. |
| 6.3.1<br>Data may be weighted to account for benchmark uncertainties or other indications of benchmark | Sec. 5 |

| | |
|---|---|
| quality (e.g., degree of characterization or degree of applicability). | |
| 6.3.2<br>Rejection of data outliers shall be based on the inconsistency of the data with known physical behavior or on established statistical rejection methods. | Sec. 3.1 |
| 6.4<br>A margin of subcriticality shall be applied that is sufficiently large to ensure that calculated conditions will actually be subcritical. The selection of a margin of subcriticality should take into account the sensitivity of the system or process to variations in fissile form, geometry, or other physical characteristics. A single margin might not be appropriate over the entire validation applicability. | Sec. 6 |
| 7.1<br>The validation applicability shall be established based on the benchmark applicability and may be extended to allow for extrapolation and wide interpolation of the data. | Secs. 3.2, 4 |
| 7.2<br>The validation applicability should not be so large that a subset of the data with a high degree of similarity to the system or process would produce an upper subcritical limit that is lower than that determined for the entire set. This criterion is recommended to ensure that a subset of data that is closely related to the system or process is not non-conservatively masked by benchmarks that do not match the system as well. | Sec. 3.2 |
| 7.3<br>An upper subcritical limit shall be established based on the calculational margin and the margin of subcriticality. | The USL determines the value of $k_{eff}$ where the analyst can treat the calculated $k_{eff}$ as being subcritical. Sec. 7 gives the specific numbers. |
| 8.1<br>The validation activity shall be documented with sufficient detail to allow for independent technical review. | Report fulfills this requirement. |
| 8.1.1<br>The computer code system being validated shall be described. | Sec. 2 |
| 8.1.2<br>A justification for the selection of the benchmarks used in conducting the validation shall be presented along with identification of the data sources through appropriate references. The benchmark applicability shall be documented. | Sec. 3 |
| 8.1.3<br>The methods and calculations supporting the determination of the bias and bias uncertainty, the calculational margin, and the validation applicability shall be documented. If used, the trending analysis and its technical bases shall be | Sec. 5 |

| | |
|---|---|
| documented. | |
| 8.1.4<br>The validation applicability shall be documented including the justification for any extrapolations or any wide interpolations beyond the bounds of the benchmark applicability. Differences between the validation applicability and the system or process parameters shall be discussed and justified. Limitations of the validation (e.g., gaps in the data, correlated data points, missing or limited data) shall be described. | Sec. 4 |
| 8.1.5<br>The margin of subcriticality and its basis shall be documented. | Sec. 5.1 for code and data. AOA margin is defined by the analyst and shall be documented with the presentation of the calculations. |
| 8.1.6<br>The upper subcritical limit and the methods used to establish it shall be documented. | Report fulfills this requirement. |
| 8.2<br>An independent technical review of the validation shall be performed. The independent technical review should include, but is not limited to, the following:<br>(1) a review of the benchmark applicability;<br>(2) a review of the input files and output files to ensure accurate modeling and adequate convergence;<br>(3) a review of the methodology, and its use, for determining bias, bias uncertainty, and margins;<br>(4) concurrence with the validation applicability. | Red Team review has been performed. The reviewers included representatives from LANL and externally. The reviewers were Forrest Brown (LANL), Mark Chadwick (LANL), Mark Mitchell (LANL), Jerry McKamy (NNSA), and Jim Felty (Sigma Science, Inc.). |